CHALMERS UNIVERSITY OF TECHNOLOGY
Gothenburg, Sweden
www.chalmers.se

PHD THESIS

Most of the light absorbed by a plant is used for photosynthesis, but part of it is reemitted. Some of the reemission is light in the red and far-red regions, which is called chlorophyll fluorescence (ChlF). Normally, this cannot be detected by the naked eye, but it can be detected by optical sensors and used for plant diagnosis.

There is an ongoing change in greenhouses and indoor growing facilities, from the use of traditional high pressure sodium lamps, to light emitting diodes (LEDs). This enables tuning and optimization of both light intensity and light spectrum, which opens for an energy saving potential not possible otherwise. Such controllable lamps can also be used to generate light excitations, which cause changes in the plants' ChlF that depend on the state of the plant. We have conducted such experiments on different plant species, to evaluate if and how ChlF, measured on canopy level, can be used as a biological feedback signal for spectrum optimization, stress detection, and for light intensity optimization.

Our experimental results indicate that feedback of the steady-state ChlF signal can be used for estimation of relative efficiencies of different LED colors for plant growth. This can be used for spectrum calibration to minimize energy consumption if the efficiencies vary over time. Furthermore, we found that the dynamics in the ChlF signal can be used for classification of healthy or stressed plants, for abiotic stress factors (drought, salt, and heat) and possibly also for biotically stress (root infection Pythium investigated). Finally, the amplitude of the ChlF signal, caused by light pulses with a high frequency and a low intensity, was found to have a concave shape with respect to light intensity, with the maximum corresponding to what can be regarded as an optimal light intensity. We suggest the use of an extremum seeking controller to force the light intensity level to this point.

CHALMERS
UNIVERSITY OF TECHNOLOGY

LINNÉA AHLMAN • Chlorophyll fluorescence as a biological feedback signal • 2021

Chlorophyll fluorescence as a biological feedback signal

for optimized plant growth conditions and stress diagnosis

LINNÉA AHLMAN

DEPARTMENT OF ELECTRICAL ENGINEERING
CHALMERS UNIVERSITY OF TECHNOLOGY
Gothenburg, Sweden 2021
www.chalmers.se

THESIS FOR THE DEGREE OF DOCTOR OF PHILOSOPHY

Chlorophyll fluorescence as a biological feedback signal

Linnéa Ahlman

Department of Electrical Engineering
Chalmers University of Technology
Gothenburg, Sweden, 2021

Chlorophyll fluorescence as a biological feedback signal

Linnéa Ahlman
ISBN 978-91-7905-561-5

Doktorsavhandlingar vid Chalmers tekniska högskola
Ny serie nr 5028
ISSN 0346-718X

Department of Electrical Engineering
Division of Systems and Control
Chalmers University of Technology
SE-412 96 Gothenburg, Sweden
Phone: +46 (0)31 772 1000
www.chalmers.se

This thesis has been prepared using LaTeX
Printed by Chalmers digitaltryck
Gothenburg, Sweden, 2021

To my beloved

Abstract

The use of light emitting diodes (LEDs) instead of traditional high pressure sodium lamps, in greenhouses and indoor growing facilities, enables tuning and optimization of both light intensity and light spectrum. This opens for an energy saving potential not possible otherwise. Furthermore, such controllable lamps can be used to generate low intensity light excitations, which cause changes in the plants' chlorophyll fluorescence (ChlF). Analysis of these changes can then be used for plant diagnosis. We have conducted such experiments on plants to evaluate if and how proximal sensed ChlF, measured on canopy level, can be used as a biological feedback signal for spectrum optimization, stress detection, and for light intensity optimization.

We found that steady-state ChlF have a strong correlation with short term photosynthesis and can be used for estimation of relative efficiency of different LED colors with respect to each other. We did not find significant changes in the relative efficiencies when light intensity or spectrum was changed, as was initially hypothesized. However, the method can still be applicable for spectrum calibration, as the efficiencies of different LED colors vary individually as the diodes degrade with time and they also vary to different degree depending on the operating temperature.

Experiments on abiotically stressed plants (drought, salt, and heat) showed that variations in the dynamics of the ChlF signal can be used to classify plants as healthy or unhealthy. Experiments with the root infection *Pythium ultimum* indicated that severe infection is detectable. This is promising as it by its nature is hard to detect without harvesting. More research is needed though, to statistically verify if this, and other biotic stress factors can be detected, and if so, how severe the infection must be.

Fast ChlF gain, defined as the amplitude of the ChlF signal caused by light pulses with a high frequency and a low intensity, was found to have a concave shape with respect to light intensity. Furthermore, the light intensity corresponding to the maximum of the fast ChlF gain coincide with the light level where the photosynthetic rate starts to saturate, which in some sense can be regarded as an optimal light level for efficient growth. Hence, we suggest the use of an extremum seeking controller to force the light intensity level to this point and demonstrates how this works in a simulation study.

Keywords: Fluorescence gain, dynamics, LED, classification, ESC, light spectrum, greenhouse lighting control, indoor farming, basil, cucumber, lemon balm, lettuce, strawberries, abiotic stress, biotic stress, *Pythium ultimum*, powdery mildew *Podosphaera aphanis*.

Acknowledgments

It literally required blood, sweat, and tears. Now, when approaching the end of this PhD journey it looks like it was worth it! First of all, I would like to thank my supervisor/examiner/boss (and unofficial therapist), Prof. Torsten Wik. Thank you for your support, encourage, and the will of sharing your deep knowledge.

I would also like to thank my former colleague Anna-Maria Carstensen, who paved the way in this interdisciplinary area, making my way much smoother. Thank you Daniel Bånkestad for the rewarding collaboration throughout the years. Finally, I want to thank all present and former colleagues at the department, for all interesting, deep, superficial, and fun conversations in the lunchroom.

When I started as a PhD student, I was newly married. Since then, all the work summarized in this thesis was done, but not only that. Furthermost, we have had our three adorable kids, and we have survived some intense and sleepless years when the twins were babies. Above all, we did that and everything else, as a team. I look forward to celebrate our ten–year wedding anniversary next year. Marcus, thank you for your patience, I love you!

Linnéa Ahlman
Sävedalen, 2021

List of publications

This thesis is based on the following publications:

[A] **Linnéa Ahlman**, Daniel Bånkestad, Torsten Wik, "Using chlorophyll *a* fluorescence gains to optimize LED light spectrum for short term photosynthesis". *Computers and Electronics in Agriculture*, 2017.

[B] **Linnéa Ahlman**, Daniel Bånkestad, Torsten Wik, "LED spectrum optimisation using steady-state fluorescence gains". *Acta Horticulturae*, 2016.

[C] **Linnéa Ahlman**, Daniel Bånkestad, Torsten Wik, "Relation between changes in photosynthetic rate and changes in canopy level chlorophyll fluorescence generated by light excitation of different LED colours in various background light". *Remote sensing*, 2019.

[D] **Linnéa Ahlman**, Daniel Bånkestad, Sammar Khalil, Karl-Johan Bergstrand, Torsten Wik, "Stress detection using proximal sensing of chlorophyll fluorescence on canopy level". *AgriEngineering*, 2021.

[E] **Linnéa Ahlman**, Daniel Bånkestad, Torsten Wik, "Tracking optimal plant illumination using proximal sensed chlorophyll fluorescence gain". *Manuscript*, 2021.

Contents

Part I

Introductory chapters

CHAPTER 1

Introduction

Indoor farming enables production of fresh vegetables in urban areas, which is expected to be increasingly important as the world's urban population is growing. In such regions, vertical farms, or top roof gardens, can be efficient ways of utilizing the area and producing food close to customers. Huge amounts of resources are brought into urban areas, and huge amounts of waste are produced. However, much of the waste can be a resource for urban farming, such as wastewater, heat, food and garden waste, CO_2-enriched air from offices and factories etc [1].

Another advantage with indoor farming is the possibility of having a high level of control. This opens for optimization of growth conditions to maximize yield. It is also less, or not at all, affected by weather conditions, neither seasonal variations nor occasional extreme weather conditions, thus paving the way for a stable and predictable food production.

Productive dense indoor farming though, requires efficient artificial light sources. The lamps traditionally used in greenhouses, i.e., high pressure sodium (HPS) lamps, are not well suited for this purpose. They produce a lot of radiant heat and, hence, close distance between lamps and plants is not possible. Furthermore, they have a fixed spectrum and are not well suited for frequent turning on and off, meaning that tuning of spectrum or intensity is not applicable. However, the rapid development of light emitting diodes (LEDs) has led to the possibility of both proximal distance between lamps and

plants, and control of both spectrum and intensity. Hence, the LED lighting opens for a more efficient lighting economy since spectrum and intensity can be optimized for maximal yield and minimal energy consumption.

1.1 Aims & Objectives

The experiments conducted in the work behind this thesis aims at contributing to the work of finding optimal growth conditions for greenhouses or indoor farming. More specifically, our approach has been to use the chlorophyll fluorescence, ChlF, emitted from the plants as a response to deliberate changes in the light intensity they receive, as a biological feedback for improved farming and resource economy.

The general setup has been to use commercial greenhouse LED-lamps to, not only supply growth light, but also to generate the deliberate superimposed light excitations, and then measure the variations in ChlF, from above, on canopy level. The work can be divided into three different research areas: **Spectrum optimization**, **Stress detection** and **Intensity optimization**.

In the **Spectrum optimization**, the main aim was to evaluate the possibility of using fluorescence gains as a biological feedback for spectrum optimization of plant growth. This was investigated, by experiments presented in Paper A, B, and C, to answer the questions:

- Can remotely measured steady-state fluorescence be a sufficiently good measure of photosynthetic rate for this purpose?
- Does the magnitude of the fluorescence gains, caused by light excitations of different colors, change relative to each other when the illumination intensity and/or spectrum are changed and, further, do they depend on plant species?

The work in the other two areas were part of a prestudy for a sensor development project, with the goal of developing a cheap and relatively simple fluorescence sensor as a monitoring tool to be used in greenhouses.

In the **Stress detection** work we investigated the possibility of extracting plant health information in the fluorescence signal, and the results are presented in Paper D. We then tried to answer the question:

- Can different abiotic as well as biotic stress factors be detected from the dynamics of the remotely sensed chlorophyll fluorescence signal generated by low intensity excitations?

Finally, in the **Intensity optimization** work we investigate a new method to find the optimal light intensity online. From previous experiments we

had measurements showing that there is a peak in the fluorescence gain as a function of light intensity. Based on this we investigated:

- Does the light intensity that corresponds to a peak in the fluorescence gain also corresponds to the, in some sense, optimal growth light intensity?
- How should a controller that controls the light towards this point be implemented?

The answer to the first question is investigated by experiments and then, in simulation, we show how an extremum seeking controller can be effectively used for the proposed control task. The results are summarized in Paper E.

1.2 Thesis outline

The first part of this thesis has the purpose of introducing the reader to the areas covered to facilitate the reading of the appended papers. In the next chapter some background knowledge regarding photobiology, growth lighting and extremum seeking control is given, and in Chapter 3 the three research areas are introduced. Further on, in Chapter 4 the included papers are summarized and Chapter 5 gives concluding remarks and indicates future directions of research. Finally, the five papers are appended as a second part of this thesis.

CHAPTER 2

Preliminaries

2.1 Photobiology

Measuring light

The spectrum visible for the human eye is within 380 to 750 nm, but the sensitivity to various wavelengths differs a lot (Figure 2.1). We are most sensitive to green/yellow light and gradually less sensitive for decreasing wavelengths into the blue area and increasing wavelengths into the red area. When considering how bright a light is to a human, this must be taken into consideration. This is indeed the case when measuring luminous flux, in lumen (lm), which is the radiant flux weighted according to the human eye's sensitivity to various wavelengths. However, the luminous flux is not a relevant quantity for plants. Instead, it is mainly the number of photons (per area and time) that is of interest.

The photosynthetically active radiation (PAR) is the flux of photons with wavelengths 400–700 nm, since that is the light that mostly contributes to the photosynthesis. Even though the photons within this region contribute to slightly different degrees, all of them are equally weighted when calculating the photosynthetic photon flux density (PPFD) having the unit $\mu\text{mol}\,\text{m}^{-2}\,\text{s}^{-1}$. Moreover, in addition to measuring light in lumen or PPFD, the energy flux, having the unit $\text{W}\,\text{m}^{-2}\,\text{s}^{-1}$, is of interest when regarding the lighting with

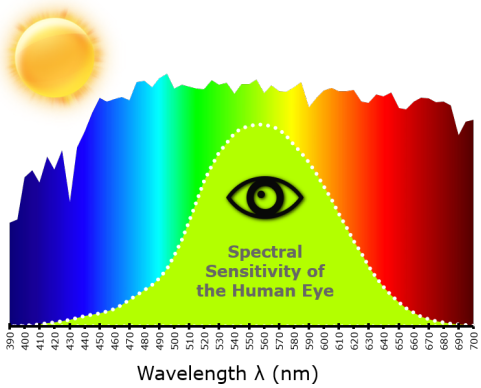

Figure 2.1: Rough illustration of human eye's sensitivity to various wavelengths [2].

respect to the electricity consumed. The energy flux within the PAR wavelengths is

$$\text{Energy flux } = \text{PPFD } \times \int_{400}^{700} E(\lambda)d\lambda \times N_A, \tag{2.1}$$

where N_A is Avogadro's constant, i.e., numbers (of photons) per mole, and $E(\lambda)$ is the energy of one photon having wavelength λ, which is given by

$$E(\lambda) = \frac{hc}{\lambda}, \tag{2.2}$$

where h is Planck's constant and c is the speed of light. Since the energy is inversely proportional to the wavelength, a photon of higher wavelength than another, has less energy, which means that it will cost less energy to produce that one, assuming equal electric efficiency.

Ambient light

The amount of ambient light that reaches the earth varies a lot over the year and with location. Light data collected in Sweden (from SMHI [3], latitude 58.58, longitude 16.15) once every hour during 2016 is presented in Figure 2.2(a), and a closer look into March 2016 is seen in (b) to illustrate the variability over a month. The maximum intensity was detected in June, with almost 1700 µmol $\mathrm{m}^{-2}\,\mathrm{s}^{-1}$, while the maximum intensity in December was seldom above 200 µmol $\mathrm{m}^{-2}\,\mathrm{s}^{-1}$. Figure 2.3 shows the PAR collected in Spain, in September 2018. This data set is collected with a sample rate of 2 seconds. It shows that the light intensity variations can be large, even within second

scale. This is most pronounced with a clear sky, when mostly direct light is measured, whereas a cloudy day the light is diffuse and hence the variations are much smaller.

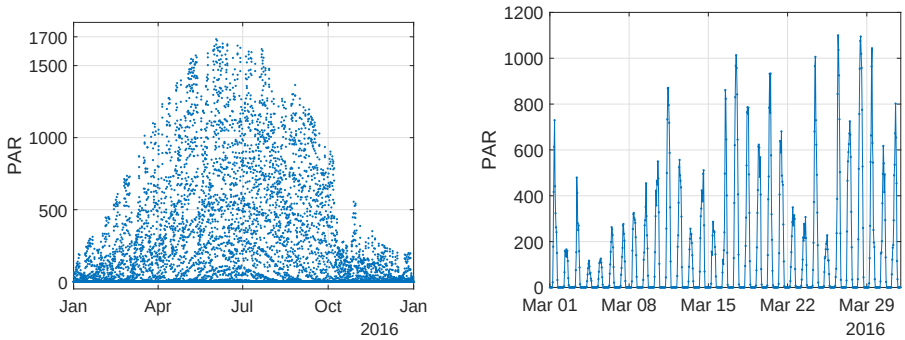

(a) Light profile 2016.

(b) Light profile in March 2016.

Figure 2.2: Ambient light collected in Sweden 2016 [3]. Data collected with a sample time of 1 h.

The total amount of light that a plant receives within one day is referred to as the daily light integral (DLI) and is usually expressed as moles of light (within PAR) per square meter and day. Figure 2.4 shows the mean value of DLI each month in Sweden 2016. Let us assume that we have a closed environment with a lamp emitting 300 µmol $\mathrm{m}^{-2}\,\mathrm{s}^{-1}$ for 12 h/day. That would equal

$$300\ \mu\mathrm{mol}\,\mathrm{m}^{-2}\,\mathrm{s}^{-1} \times 12\ \mathrm{h/day} \times 3600\ \mathrm{s/h}\ \times 10^{-6}/\mu = \mathrm{DLI}\ 13\ \mathrm{mol}\,\mathrm{m}^{-2}\,\mathrm{day}^{-1}.$$

If further assuming that 60–70% of the ambient light is transmitted through the roof of a greenhouse, an ambient DLI of about 20 mol $\mathrm{m}^{-2}\,\mathrm{day}^{-1}$ is needed to get the same amount of light as in the indoor example. In 2016, 57% of all days did not reach that and if excluding the summer months (May-August), 82% of the days did not reach that amount of light. This means that for a large part of the year it is required to have supplemental light to ensure a high growth rate.

Photosynthesis

The photosynthesis is the process where light energy is transformed into chemical energy, primarily stored as carbohydrates in the plant. The phenomena is described in many text books, for example by Lawlor [4], Björn [5], and Durner [6]. Besides light energy, carbon dioxide and water are consumed to

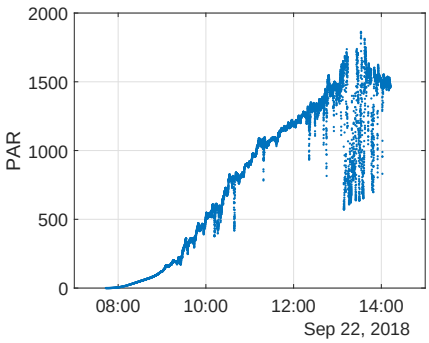

Figure 2.3: Ambient light data collected in September in Spain, with a sample time of 2 s. Courtesy of D. Bånkestad.

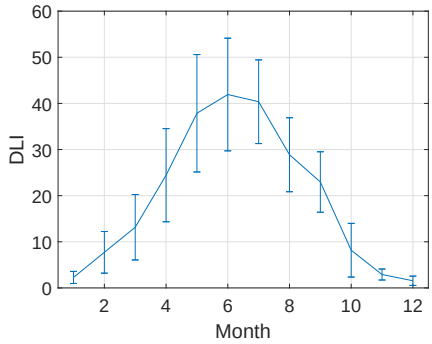

Figure 2.4: The daily light integral (DLI) each month (± std) in Sweden 2016 [3].

form carbohydrates and oxygen, roughly according to

$$6\,CO_2 + 6\,H_2O \xrightarrow{\text{light}} C_6H_{12}O_6 + 6\,O_2. \tag{2.3}$$

The photosynthesis takes place in the plant cell, within an organelle called chloroplast. The chloroplast is filled with a liquid, the stroma, and contains stacks of thylakoid membranes. In these membranes the chlorophyll and the carotenoid pigments are found. These are the pigments that absorb the light energy in the first part of the photosynthesis, called the light reaction.

In the light reaction, light photons are absorbed by the chlorophyll and carotenoid molecules, which become excited. The energy absorbed by the carotenoid is transferred to the chlorophyll molecules. The carotenoid is also vital for protecting the reaction centers from photodamage [7]. The energy of the excited chlorophyll molecules is passed to other molecules within the thylakoid, through the reaction centers called photosystem I (PSI) and II (PSII). They are connected in series and can be regarded as "electron pumps" powered by light photons [5]. The energy is eventually used to synthesize ATP and NADPH (adenosine triphosphate and nicotinamide adenine dinucleotide phosphate), where the energy is temporarily stored until it is used in the next step, the dark reaction. In the formation of ATP and NADPH, electrons are removed from PSII. These are replaced by hydrogen ions which are formed from the oxidation of water,

$$2\,H_2O \rightarrow O_2 + 4\,H^+ + 4\,e^-. \tag{2.4}$$

The oxygen produced in this step diffuses out of the chloroplast and eventually exits the leaf to the air.

The dark reaction takes place in the liquid part of the chloroplast, the stroma. It both occurs in the dark and in the light, and the driving force for the reactions is the energy from ATP and NADPH. A series of reactions ends up in the Calvin cycle, where CO_2 is reduced to carbohydrates, as a biologically stable storage of the energy initially harvested from the sun.

Limiting factors

Figure 2.5 shows a schematic picture of a light response curve, i.e., the rate of photosynthesis for increasing levels of light intensity. Initially, light is the limiting factor for photosynthesis and, hence, the rate of photosynthesis increases linearly with increasing light intensity. Then it enters a region where the increase is not as steep and the light response curve starts to saturate and, finally, in the region of highest light intensity the rate has saturated. To determine the optimal illumination level is complex, being a question of illumination cost and revenue of produce, but in terms of high photosynthesis and a high light use efficiency the intermediate region probably encloses the optimum.

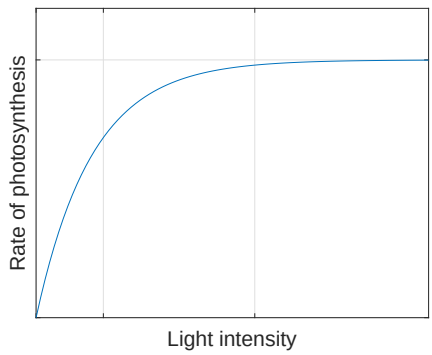

Figure 2.5: A typical light response curve.

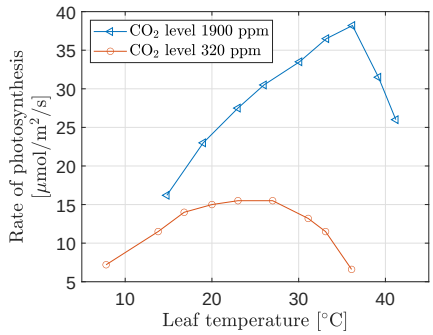

Figure 2.6: The rate of photosynthesis at saturating light (PPFD 1600-2000 $\mu mol\, m^{-2}\, s^{-1}$). Redrawn from data by Jurik *et al.* [8].

When light is not the primary limiting factor for photosynthesis, it could for example be the CO_2 concentration or the water availability that is limiting (cf. Eq. 2.3). In a ventilated greenhouse, the CO_2 concentration will be close

to the ambient concentration, approximately 400 ppm. However, since CO_2 is utilized by plants during the days, the CO_2 level may drop to 150-200 ppm in sealed greenhouses in daytime [9], [10]. If the CO_2 level drops below 100 ppm the CO_2 uptake and hence growth will be completely prohibited [10]. For most crops the saturation point is reached at about 1,000-1,300 ppm under ideal circumstances. Higher levels have little additional positive effects and very much higher would hinder plant growth [10]. Hence, to increase growth, CO_2 supplementation or enrichment can be used, for example by rerouting flue gases from a boiler, which is effective if there is need for heating as well. It is important though, to make sure having complete combustion avoiding impurities that are harmful to plants and to humans working there [9]. Another alternative is liquid CO_2, stored in pressurized tanks that is vaporized through vaporizer units [10].

Moreover, the temperature also affects the growth rate. Higher temperature enhance growth, up to a certain limit. Figure 2.6 shows the rate of photosynthesis for different temperatures, measured on bigtooth aspen leaves, in saturating light (1,600-2,000 $\mu mol\, m^{-2}\, s^{-1}$), for two different CO_2 levels in the air (experiments by Jurik *et al.* [8]). At the low CO_2 level (close to ambient condition at the time of the experiment), the temperature optimum was 25 °C, while for the high CO_2 level it had shifted to 37 °C.

Light quality

On atom level the energy absorption (and emission) is quantized, as electrons excites from the ground state to a higher excited state. It is the chlorophyll a and b, and to some extent carotenoid pigments, that absorbs the light for photosynthesis. Figure 2.7 shows the absorption spectra for dissolved chlorophyll a and b, they have one peak in the blue region and one in the red. Figures like this one is probably one reason of the common myth that blue and red light is always to prefer in indoor farming. On molecular level and in vivo, where pigments are tightly packed into protein complex, the absorption occurs instead from a broader spectrum of wavelengths. This is due to vibrational energy and more closely spaced molecular orbitals from which electronic transitions occur [11].

In two large pioneering studies in the 70's [13], [14], the action spectra of leaves were calculated for a large set of species (22 and 33, respectively) i.e., relative CO_2 uptake rate per incident photons, for different wavelengths in intervals of 25 nm. Figure 2.8 shows an example for two of the species (the two ones differing the most from the mean). McCree [13] concluded that the curves had similar shape for all species tested, i.e., one peak in red

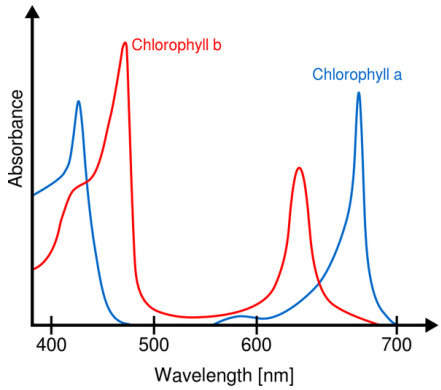

Figure 2.7: Absorption spectrum for Chlorophyll *a* and *b*, in solvent. Picture from [12].

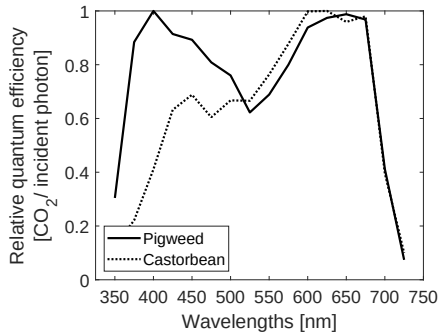

Figure 2.8: Normalised action spectra for incident quanta for Pigweed and Castorbean. Redrawn from data by McCree [13].

and another one in blue, nevertheless there are species dependent differences. Note also that the values in the green region are significantly higher than the absorption spectrum for chlorophyll. When evaluating the growth rate in vivo the action spectrum will vary further due to increased complexity. For example, in vivo green light significantly contributes to photosynthesis and biomass accumulation, especially in the inner and lower leaf layers of the canopy due to the transmission through the first layers [15].

The McCree action spectra apply only to the use of narrow wavelength span. The combined effect of different wavelengths, however, is not necessarily the sum of the quantum efficiency of individual wavelengths. One example of this is the enhancement obtained when combining light of wavelengths below 680 nm with light of wavelengths above 680 nm (far-red light). This is called the *Emerson effect* [16], which is due to the simultaneous excitation of the two interconnected photosystems operating in series.

The quality of the light also affects other aspects of growth. For example, UV-light (280-400 nm) inhibits cell elongation and can cause sunburn while far-red (700-750 nm) stimulates cell elongation, influence flowering and germination (Table 8.1 in [6]). Different plant species are more, or less, sensitive to light quality. For a review of many studies on this topic, see Paradiso and Proietti [15], Ouzounis *et al.* [17], and Olle and Viršile [18].

Chlorophyll *a* fluorescence

Chlorophyll fluorescence is the emission of photons when excited molecules return to a lower energy level [11]. Most emission at normal temperatures derives from chlorophyll a, thereby the term *chlorophyll a fluorescence* [4]. In solution, chlorophyll *a* emits almost one third of the absorbed light as fluorescence, while in vivo the amount is less than a few percent. The fluorescence is emitted in the near infrared region, having peak wavelengths around 685 nm and 740 nm. Figure 2.9 shows an example of (a) an incident light spectrum using four different diode colors and (b) the corresponding reflection and the fluorescent light. In the experiments conducted within this thesis, the fluorescence signal is derived from the second peak, illustrated by the red colored area in the figure.

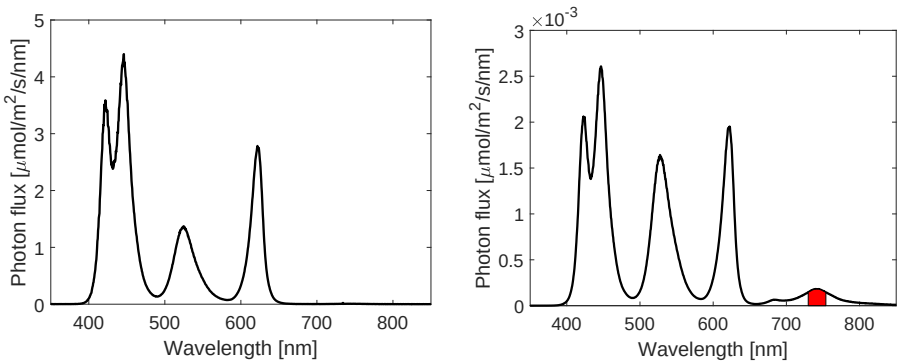

Figure 2.9: Left—Incident light spectrum using four diode colours. Right—Reflected and fluorescent light. The fluorescence signal used in the experiment in this thesis is derived from the 740 nm-peak.

The probability of a photon being reemitted as fluorescence competes with the probability of photochemistry and heat re-emission. Hence, fluorescence emission indirectly contains information about the quantum efficiency of photochemistry and heat dissipation [19]. This close relationship, between chlorophyll fluorescence and photosynthesis, has made fluorescence measurements an indispensable tool in studying photosynthesis in a wide range of applications, all the way from measurements on-leaf to remotely, from satellites [11], [19].

2.2 Growth lighting

In this section we give a brief overview of different lighting options that are common for greenhouse and indoor farming.

High intensity discharge lights

In a high intensity discharge (HID) lamp, an electric current is flowing through a gas mixture [6]. The gas becomes excited by the electrical energy and emits photons. The spectral distribution of the light is mainly determined by the gases involved and the pressure within the lamp [5].

High pressure sodium (HPS) lamps and metal halide (MH) are two of the most common types of HIDs. Both types are used indoor in growth rooms as well as in greenhouses. They can deliver high light intensities (500–1,500 $\mu mol\, m^{-2}\, s^{-1}$) and they have a long life-time, about 30,000 h for HPS and 15,000 h for MH [6]. HPS has for long been the most commonly used type of lamp for greenhouses, due to a high photosynthetic photon flux density, PPFD, per unit electricity. In Table 2.1 the spectral distribution of the lamps are presented. Compared to sunlight, HPS has a low light flux in UV, blue and far red while a high light flux in the green waveband. In addition, HPS emits a substantial part of the photons at higher wavelengths, outside the PAR or visible light region, hence, not enhancing the photosynthesis. This is radiant heat, which heats up the plants. To avoid burning of the plants, the distance between plants and HPS lamps cannot be too short.

Note that all high-pressure lamps should be handled carefully, due to the potential risk of explosion.

Table 2.1: Spectral comparison of common horticultural light sources (adapted from [20]). The illumination is normalised to 100 $\mu mol\, m^{-2}\, s^{-1}$ within PAR (400–700 nm).

Light		Sunlight	HPS	MH	Cool White
UV–B	(250–350)	2.9	0.2	0.7	0.03
UV–A	(350–400)	6.2	0.5	6.7	1.1
Blue	(400–500)	29.2	6.5	20.4	24.8
Green	(500–600)	35.2	56.6	55.5	52.6
Red	(600–700)	35.6	36.9	24.1	22.6
Far–red	(700–750)	17.0	4.0	4.0	1.4

Fluorescent lights

Fluorescent lights are not as intense as HID lights and they have a shorter life-time, typically 5,000–10,000 h. The lamp life-time is also affected by the number of times they are turned on, making them unsuitable for frequent turning on and off. The standard choice for greenhouse growers is cool white fluorescent bulbs. They have an acceptable spectral distribution (Table 2.1) and also the greatest PPFD compared to other fluorescent bulbs. Traditionally they have been extensively used where low light intensity is favorable, for examples for starting seedlings or for simulating spring conditions [6].

Light emitting diodes

Light emitting diodes, LEDs, are solid-state light emitting devices. Thereby they can instantly be turned on or off, without requiring warm-up time [21]. Advanced LED lamps combine diodes that generate different wavelengths (from broad-band light to narrow-spectrum), into an array with light peaks at several wavelengths [6]. As each diode can be dimmable individually, either by current or by pulse width modulation (PWM), the spectrum can be varied, making LED lamps suited for control of spectrum as well as intensity.

The efficacy, µmol per energy input, of individual diodes varies a lot but generally red and blue LEDs have the highest efficacy, while green diodes have efficacies in the order of 1/2 or 1/4 relatively the most efficient ones [22], [23]. The efficacy has gradually increased over time and now there are commercial LEDs (with combined colors) currently providing 3.4 $\mu mol\,J^{-1}$ [24]. The theoretically maximal efficacy, with efficiency 100% W/W, is 3.34 and 5.85 $\mu mol\,J^{-1}$, for wavelengths 400 and 700 nm, respectively. With current techniques it is estimated that the efficacy of combined red and blue LEDs can reach 4.1 $\mu mol\,J^{-1}$ [25].

LEDs do not burn out like a bulb. The most commonly used life-time metric for LEDs is instead the time when the maximum intensity has been reduced by 30%, which occurs after about 50,000 h [26]. Another difference in comparison with bulbs is that LEDs do not radiate heat directly. However, they do produce heat that must be removed to ensure maximal performance and life-time. This can be done by conduction through a liquid cooling device, or through natural or forced convection, in the latter case by using a fan [6]. Furthermore, the fact that LEDs do not radiate heat directly, opens for the ability to place the lamps in close proximity to the plant tissue. This opens up for intermediate lighting or dense vertical farming, with an increased production per land area.

Choice of light source

During the last two decades it has been debated if and how much the economy in greenhouses can be improved by replacing the traditional HPS lamps by LEDs. The main arguments have been that the efficiency of LEDs is higher, but on the other hand the investment cost is higher, as well as the need of supplemental heating. The total economy balance is affected by many factors and the conclusion can differ depending on initial assumptions. Furthermore, ongoing development of the lamps also change the prerequisites.

In a study from 2014, Nelson and Bugbee [23] concluded that the energy efficacy, i.e., produced µmol per energy input, at that time was about the same, 1.7 $\mu mol\,J^{-1}$, for the most efficient (1000 W) HPS and LED fixture, but lower installation cost for HPS resulted in favour of that type. However, the angle of the radiation from the lamps also differs. If taking into account that light emitted above a certain angle does not hit the plant and is wasted radiation, the conclusion could differ.

In a more recent study, Katzin *et al.* [27] compared the currently most efficient HPS and LED lamps (efficacy 1.8 and 3 $\mu mol\,J^{-1}$, respectively). The comparison was done with simulations using GreenLight (an open source greenhouse model), in order to evaluate multiple inputs. They concluded that LEDs did reduce the energy demand for lighting, but increased the demand for heating as LEDs produce less heat. Thus, depending on ambient conditions the conclusion differ, but on average 10–25% of the total energy used could be saved.

A major advantage with LEDs is the ability to be in close proximity to the plant and to customize the spectrum. The controllability of the LEDs implies that large savings can also be made by applying abiotic feedforward control of, e.g., ambient PAR. There are also large potential savings to be made by biological feedback, which is the topic behind the investigations presented in this thesis. Given the development in recent years it is likely that LED will be the standard choice in a relatively near future.

2.3 Extremum seeking control

A control task where the goal is to track a maximum (or a minimum) of an objective function belongs to the class of extremum seeking control (ESC) [28], [29]. This can be done without the need of a model of the plant, in contrast to for example model predictive control (MPC), where an objective function is minimized subject to a given plant model. Furthermore, ESC has the ability of adapting to a (slowly) varying optimum, is performed in real time, and is

based on the feedback from output measurements.

ESC was developed in the 1920's [30], initially for optimization of static plants, but it was also applied on dynamical plants. During the 1950's and 60's the method was spread in a wider community. Several novel methods for ESC were published and the development of computer technology enhanced the interest for ESC [31]. Another breakthrough came in 2000, with the work of Krstić and Wang [32]. They widened the applicability of ESC, as they proved a stable, stationary solution (of the classic perturbation-based ESC, see next section) in the local neighborhood of the steady-state optimum, for a much wider class of non-linear dynamical systems.

The ESC problem can be stated as follows: Consider a nonlinear, dynamical system described by

$$\begin{aligned} \dot{x} &= f(x, u) \\ y &= h(x), \end{aligned} \tag{2.5}$$

where $x \in \mathbb{R}^n$ is the vector of state variables, $u \in \mathbb{R}$ is the input, or control signal, and $y \in \mathbb{R}$ is the output. Assume that Eq. 2.5 is open-loop stable and that the steady-states are parameterized by the input through a function $l : \mathbb{R} \to \mathbb{R}^n$, such that

$$f(x, u) = 0 \text{ if and only if } x = l(u). \tag{2.6}$$

The equilibrium is assumed to be locally exponentially stable. Hence, the system can be stabilized without modeling knowledge of neither $f(x, u)$ nor $l(u)$. The goal for the controller is to maximize[1] the objective function

$$J(u) = h \circ l(u), \tag{2.7}$$

which corresponds to the steady-state input-output map. All functions, i.e., f, h, l, and J, are assumed to be sufficiently smooth for all necessary derivatives to exist and $J(u)$ is assumed to have a concave shape with no local extrema.

Sinusoid perturbation ESC

The most traditional extremum seeking scheme is presented in Figure 2.10 [30]. A sinusoid perturbation signal is added (modulated) to the nominal input, $\hat{u}$, in order to evaluate where on the objective function curve (Eq. 2.7) the current input corresponds to. Note that the perturbation frequency must

[1] We consider maximization here, but the method can equally well be applied to minimization.

be slow in comparison with the plant dynamics, since the objective function is the steady-state input-output map. If u is on either side of the optimum, u^*, the perturbation will create a periodic response of the output, that is either in phase or out of phase with the perturbation, i.e.,

$$\text{in phase for } u < u^*$$
$$\text{out of phase for } u > u^*,$$

which is illustrated in Figure 2.11. To extract the gradient information from the output, the signal is first sent through a high pass filter, $F_H(s)$, to remove the DC component, followed by multiplication (demodulation) with the original perturbation. To get rid of higher order harmonics a low pass filter, $F_L(s)$, is used. Hence, the signal is now positive if the output and the perturbation signals are in phase and negative otherwise. Finally, the integrator integrates the error and forces u to the optimal value.

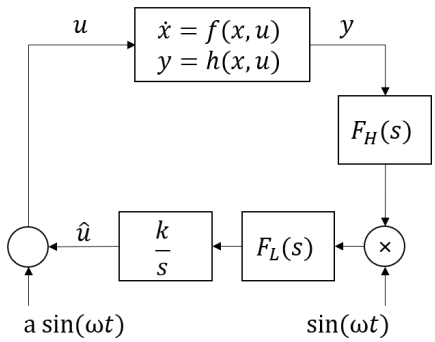

Figure 2.10: ESC scheme for a sinusoid perturbation signal.

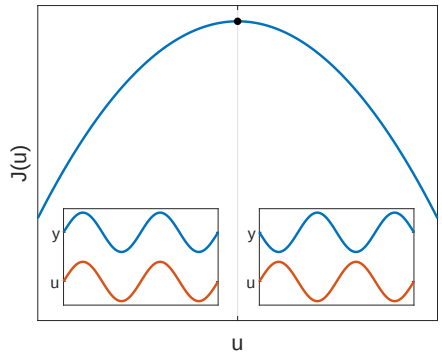

Figure 2.11: The objective function, $J(u)$, is concave with a maximum at $u = u^*$.

The amplitude of the sinusoid perturbation, a, needs to be large enough to cause measurable changes in the output but still as small as possible since it, of course, causes system oscillations. As mentioned, the period of the perturbation, $sin(\omega t)$, needs to be slow relative to the dynamics of the plant, and the cut off frequencies of the filters must be smaller than ω, since the high pass filter should pass the variations in the sinusoid, and for the low pass filter it is only the DC component that is of interest. Characteristic when applying ESC to dynamical systems is that the control becomes slow because of the required time scale separation. Trying to speed up the system can lead to instability.

Constant stepping ESC

A more trivial method to estimate the direction of the slope of the objective function (Eq. 2.7) is the constant stepping method [31]. The control scheme is presented in Figure 2.12. The control signal, u, is held constant for Δt time units and then the output is measured and stored. The control signal is then shifted Δu, and the output is measured again. If moving uphill of $J(u)$, towards the maximum, the current output is larger than the stored one. If so, one continues to change the control signal in the same direction, or else, one changes sign of Δu and change the control signal correspondingly. In such a control loop, there are only two design parameters, Δt and Δu.

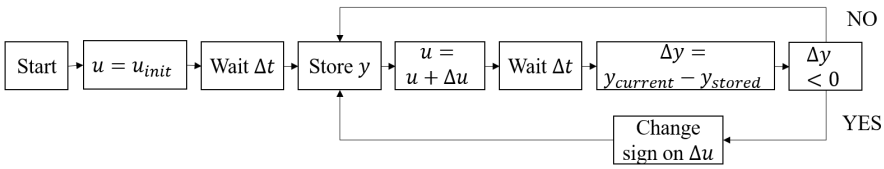

Figure 2.12: Control scheme for the stepping method.

CHAPTER 3

Research areas

3.1 Light spectrum optimization

If growth efficiency of plants varies over time and with the exposed light spectrum, there is a potential to use automatic control methods for online optimization of light spectrum. In order to maximize plant growth for a given, constant illumination power, P_{tot} (Figure 3.1), a measure of growth rate is needed. We have therefore studied the potential of using steady-state chlorophyll *a* fluorescence at 740 nm, F740, for that purpose. The advantage is that the fluorescence response is fast, remotely measured on canopy level and non-destructive to the plants. Therefore, fluorescence is indeed a promising candidate to be used as a biological feedback in a closed loop aiming at finding optimal spectra for maximized plant growth.

The fraction of absorbed light that is used for photosynthesis, re-emitted as heat, or re-emitted as fluorescent light will vary, for example as a function of plant status and illumination intensity. This has been studied both on leaf level [33] and on canopy level [34]. For example, the *relative* level of fluorescence is negatively correlated with photosynthesis (i.e., desirable plant growth) at low light intensities, while it is positively correlated at high light intensities and under stress [35], [36]. For healthy plants exposed to light with only small variations in intensity, a reasonable assumption is that the photosynthetic rate and the *total* fluorescence are positively correlated. A

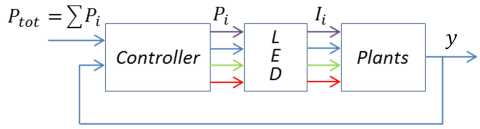

Figure 3.1: To find an optimal spectrum, i.e., how to distribute the power P_{tot} among the different diode groups by feedback control, one needs to find a quantity of plant growth that can be measured remotely and online. Within this thesis we investigate if steady-state chlorophyll *a* fluorescence at 740 nm, F740, can be a candidate measure y. P_i is the power to each LED group, and I_i is the corresponding intensity of the emitted light.

strong such correlation was also found in the experiments presented in Paper A and Paper C. Under such an assumption, the maximum photosynthetic rate for a predefined total power, P_{tot}, corresponds to the spectrum that maximizes the fluorescence, F740.

Now, assume that N different LED colors are available. Then F740 depends on all the LED sources, i.e.,

$$F740 = f(P_1, ..., P_i, ..., P_N), \tag{3.1}$$

where P_i is the electrical power applied to the i:th group (color) of LEDs and f is a scalar function. For a predefined total power P_{tot} we may write

$$P_N = P_{tot} - \sum_{i=1}^{N-1} P_i. \tag{3.2}$$

As our assumed optimization goal is to maximize F740, the gradient of F740 should be zero with respect to all sources, assuming that a (global) maximum exists. Differentiating Eq. 3.1 w.r.t. P_i, and using Eq. 3.2, give

$$\frac{dF740}{dP_i} = \frac{\partial f}{\partial P_i} + \frac{\partial f}{\partial P_N}\frac{\partial P_N}{\partial P_i} \tag{3.3a}$$

$$= \frac{\partial f}{\partial P_i} - \frac{\partial f}{\partial P_N} = 0 \quad \text{for all } i. \tag{3.3b}$$

The last equality implies that the *fluorescence gains*, defined as $\partial F740/\partial P_i$ (i.e., $\partial f/\partial P_i$), should optimally be equal for all LED groups. As we are only interested in how the fluorescence gains relate to each other, the actual relation between growth and F740 need not be known, as long as they are positively correlated to each other. The control task then fits to a combination

of extremum seeking control (see [37] and references therein) to track the fluorescence gains, and self optimizing control [38] to aim for equal gains [39]. In principle, when not being at the optimum, the controller would increase the power to the LEDs with the highest gain and reduce the power to the one(s) with the lowest gain.

Accordingly, our hypothesis is that with the setup presented above, the controller will adjust the spectrum towards the one that maximizes the short term photosynthesis. When implementing the suggested controller, one could include limitations on for example B:G:R:FR ratios, in order to ensure good morphology. It should be noted though, that the optimal spectrum in the long run might differ from the one that maximizes the photosynthesis in the short term. For example, initially applying a spectrum that stimulates leaf expansion, rather than photosynthesis, can lead to better light interception and thereby higher biomass in the long run.

3.2 Stress detection

If plants are subjected to inhibitory environmentally stress, the growth efficiency is reduced. These stressors can be categorized as abiotic or biotic. Light, drought, and salinity stress belongs to abiotic stress factors while insects and pathogens, such as fungi and bacteria, belong to biotic stress factors. If the stressors are detected at an early stage their negative impact can be minimized by removing plants or apply early treatment. Standard methods for stress detection are often destructive or disruptive [40], hence, not an option for on-line detection. Different optical sensors have been investigated; hyperspectral images, mulitcolor fluorescence images and fluorescence spectra. However, sensor-based phenotyping is still at an early stage of development and not yet commonly applied in field [41], [42].

We have conducted experiments in order to evaluate if the dynamics in the fluorescence response to weak light excitations can be used as features in a machine learning context, to evaluate if plants are stressed or not. The fluorescence has the advantage that it can potentially react on environmental changes prior to when the changes are visible to the human eye. Further strengths with our method is that the measurements are done on-line, remotely on canopy level, and that the plant neither needs to be dark adapted nor exposed to saturating light. Instead, market available greenhouse LED lamps are used to excite the fluorescence signal and a photodiode with a bandpass optical filter could be applicable for the detection. With this relatively cheap setup it could be economically justifiable to distribute sensors over a large

greenhouse.

Features from the fluorescence signal that potentially could discriminate between stressed and healthy plants can be extracted in many ways. The alternative used here is to treat the excitation light as the input signal, u, and the fluorescence as the output, y, and from experimental time-series data use system identification to create a dynamic model of the system. Features could then be extracted both from the time and frequency domain. In previous work on light stress, frequency domain characteristics were shown to correlate with level of stress [43]. Here, we focus on features in the time-domain. Further on, other growth parameters could be included in a classification algorithm; such as plant age or development status, temperature, relative humidity etc. With a large set of annotated data, a classification algorithm can then potentially be tuned to diagnose whether the plants are healthy or not.

3.3 Light intensity optimization

If there is a real time, non-destructive way of biologically measuring the photosynthetic efficiency on canopy level at the current light intensity, one could potentially optimize the light intensity for minimized power consumption and maximized growth. Many parameters can potentially affect the optimal light illumination, such as development status of the crop, time of the day, abiotical or biotical stress factors, or other environmental factors.

An infrared gas analyzer can be used to measure the instant photosynthetic rate, in terms of carbon dioxide uptake per leaf area and time. This is done by measurements of carbon dioxide, oxygen, and vapor, in a controlled air flow, throw the leaf cuvette that enclose a part of a leaf. In Figure 3.2 two examples are shown, one with an built in light source (a) and one with a clear window (b) letting the ambient light hit the leaf. Such instruments are not suitable for the feedback task, being too expensive and not aggregating over canopy illuminated by the lamp, but valuable as a reference instrument in research.

We have investigated if the chlorophyll fluorescence, ChlF, can be a candidate signal to be used for the purpose of online light intensity optimization. More specifically, the fast ChlF gain, calculated as the amplitude of the ChlF caused by (1 Hz) pulses in the incident light. Hence, the ChlF gain is used as an estimate of the derivative of the absolute ChlF w.r.t. incident light.

If the plant use the light equally, independently of the intensity level, the relation between incident light and ChlF would be constant, in other words a constant derivative or gain. However, that is not the case. For high light intensities saturation occurs and the efficiency from incident light to photo-

Figure 3.2: An infrared gas analyser, for measuring the photosynthetic rate in terms of CO_2 uptake per m^2 leaf area and s. Mounted with a leaf cuvette combined with a light source (left), and a clear leaf cuvette allowing the ambient light reaching the leaf (right).

synthesis decreases. This has also been detected in the ChlF, that for high light intensities the ChlF gain decreases.

Figure 3.3(a) shows the light response curves, i.e., photosynthetic rate for stepwise increased light intensity, measured with an IRGA on sunflower leaves. For high light intensities the photosynthesis saturates, and the efficiency between light illumination and growth decreases. To determine the level of illumination that optimally balances energy cost and photosynthetic rate is complex. However, aiming for a high photosynthetic rate, and a high efficiency from incident light to photosynthesis, then the light level where the photosynthetic rate starts to saturate is optimal.

Figure 3.3(b) shows the normalized ChlF gain, measured with a spectrometer on canopy level. These measurements were done simultaneously with the light response curves in (a). The ChlF gains have a concave shape, and the peak coincides with the light intensity where the light response curve starts to saturate.

We propose to use the ChlF gain as a feedback signal, y, in a control loop to control the light intensity level, u, towards the point that maximizes the objective function $J(u) = y$, i.e.,

$$\max_u J(u). \tag{3.4}$$

For a concave objective function, $J(u)$, without local extrema, this can be achieved using an extremum seeking controller.

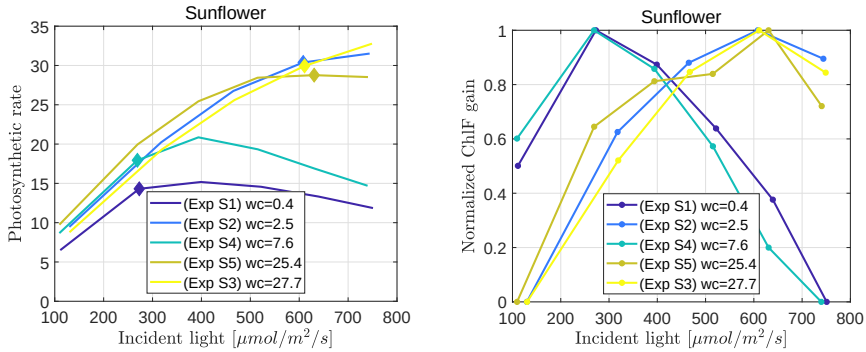

(a) Sunflower, photosynthesis.

(b) Sunflower, fluorescence gain.

Figure 3.3: Experiments on Sunflower. (a) Photosynthetic rate versus incident light. (b) Normalized ChlF gain versus incident light. The filled diamonds indicates the light level where the ChlF gain has its maximum.

Ongoing experiments

The implementation of an extremum seeking control strategy in physical experiments is ongoing. This is beyond the scope for this thesis, but we will briefly present some of the challenges and ways towards a working solution. The experiments presented in this section are done on lettuce.

The first challenge encountered was that the experimental ChlF gain response behaved differently depending on light history, and more specifically, whether the light is increasing or decreasing. The phenomenon of trajectories that depend on direction can be described by hysteresis [44] or direction dependent dynamics [45].

Figure 3.4(a) shows the ChlF gain as a function of lamp input for two different experiments on lettuce. In both cases the experiments started at low intensity, stepwise increasing the intensity and then decreasing it sometime after a maximal ChlF gain had been observed. For these experiments the fluorescence gain was higher when the light was increasing than when it was decreasing.

In the first set (blue stars) the intensity increased with lamp setting $\Delta u = 10$ every $\Delta t = 20$ sec (approximately corresponding to a rate of 13 $\mu mol\, m^{-2}\, s^{-1}$/min) and in the second run (red circles) the step size was larger (lamp setting 100) and was held for 10 min (hence a rate of about 4.3 $\mu mol\, m^{-2}\, s^{-1}$/min). Both of the two settings capture a maximum at approximately the same intensity when increasing the light, but none of them found it again when decreasing the light.

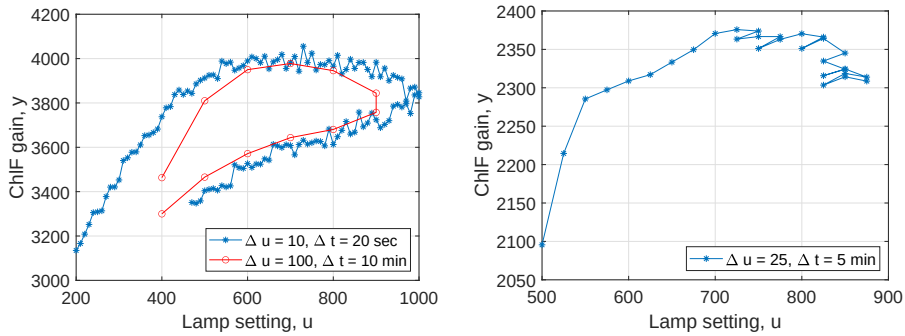

(a) Manually changed lamp settings (b) Controller changed lamp settings

Figure 3.4: Experiments on lettuce. ChlF gain as a function of incident light intensity. (a) Manually increased and then decreased the light intensity. (b) A controller increased the light intensity.

If implementing the control strategy suggested in Paper E, without taking this phenomenon into consideration, the intensity will drift towards higher values. One example of this is presented in Figure 3.4(b), where a controller has changed the light in steps of lamp intensity 25 (10 μmol m^{-2} s^{-1}) every 5 minutes. The intensity starts at 500 and increases stepwise. So does also the ChlF gain, until the intensity input is 750. Then the ChlF gain decreases slightly for the first time and, hence, the controller changes direction and decreases the intensity for the next step. However, when decreasing the intensity, the response becomes lower compared to when moving in the positive direction. Hence, the controller decides to increase the light intensity again. This process is repeated such that a decrease is followed by one to three increasing steps. As a consequence, this leads to a successive increase in light intensity and an overall decrease in ChlF gain, contrary to the purpose of the extremum seeking scheme.

Another thing that complicates the task, is that the peak in the ChlF gain is not always very sharp, in the sense that the peak can be followed by almost a plateau. One way of handle that is to change the objective function, $J(u)$, for example, by multiplication with a straight line

$$J(u) = y \cdot (-k \cdot u + m), \tag{3.5}$$

where y is the ChlF gain, u is the light intensity and k and m are tunable scalars. Figure 3.5 shows how the objective function changes when multiplying with different lines (constant k and m for each line, highest k-value represented in the blue line, stepwise decreasing to $k = 0$ for the orange line).

This is also a way of pushing the location of the maximum in a certain direction (black diamonds point out the maximal value for each objective function). Tuning the line thus gives the grower means to speed up or slow down the growth while still having an adaption to the plants state.

A new sensor is under development. The detection is done with a lock-in amplifier, which can detect very small AC signals, i.e., the fluorescence, in the presence of large broad spectrum noise, e.g., the reflectance in all wavelengths, including the fluorescence region. Compared to the current setup with the spectrometer, this setup will be must faster (kHz range instead of Hz) and the generated excitation intensity will be even lower. The ChlF gain is now measured as the amplitude of the light (in the 740 nm-region), at the frequency used for the excitation lamp. Hence, we expect that we more or less measure the same thing, i.e., the increase in fluorescence given a small excitation signal, at the current background light.

Figure 3.6 shows the ChlF gain calculated with the spectrometer (blue line) and the new sensor (red line) simultaneously. The light is stepwise increased from 225 to 475 $\mu mol\,m^{-2}\,s^{-1}$ ($\Delta u = 10\ \mu mol\,m^{-2}\,s^{-1}$, $\Delta t = 4$ min). Both sensors detect a peak approximately at the same light intensity. However, the new sensor detects a faster decreasing ChlF gain when passing the maximum, which is beneficial from a control perspective. Another advantage with the new instrument is that it is much faster than the spectrometer and, hence, able to detect a more stable signal even in the presence of disturbances. This opens for the possibility of using the sensor in ambient light conditions.

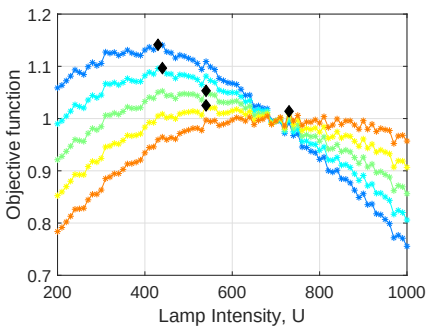

Figure 3.5: Objective function, when multiplied ChlF gain with different linear functions according to Eq. 3.5.

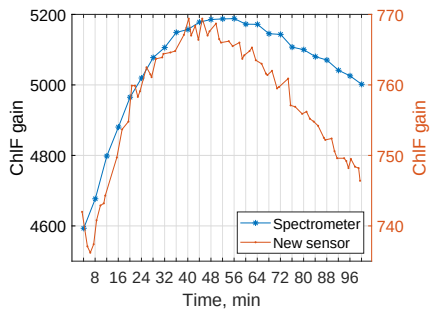

Figure 3.6: ChlF gain measured with a spectrometer (blue line) and the new fluorescence sensor. Stepwise increase of light intensity from 225 to 475 $\mu mol\,m^{-2}\,s^{-1}$.

CHAPTER 4

Summary of included papers

This chapter provides a summary of the included papers.

4.1 Paper A

Linnéa Ahlman, Daniel Bånkestad, Torsten Wik
Using chlorophyll *a* fluorescence gains to optimize LED light spectrum for short term photosynthesis
Computers and Electronics in Agriculture,
vol. 142, pp. 224–234, 2017.

A series of experiments were conducted on basil plants in order to examine whether remotely sensed steady-state chlorophyll *a* fluorescence at 740 nm, F740, can be used as a control parameter in a feedback loop, aiming at adjusting the incident light spectrum for maximal plant growth. A second goal was to investigate if the derivatives of the chlorophyll fluorescence w.r.t. applied powers (fluorescence gains) change relative to each other for different light intensities and spectra. Using one LED group at a time, a high correlation between steady-state chlorophyll *a* fluorescence at 740 nm, remotely measured at canopy level, and photosynthetic rate, PN, measured on leaf, was found. This indicates that F740 can be used as a relative measure of PN, at least for the spectra and (low) light intensities being investigated. For different operating points, having a wide variety of spectra and intensity levels,

the fluorescence gains when changing each of the different LED groups were compared. The relative order of the gains was remarkably consistent. With respect to incident photons the gain was highest for red light followed by blue and lowest for green light. Investigating with respect to applied powers, the efficiency of the individual diodes is a dominant factor.

4.2 Paper B

Linnéa Ahlman, Daniel Bånkestad, Torsten Wik
LED spectrum optimisation using steady-state fluorescence gains
Acta Horticulturae,
vol. 1134, pp. 367-374, 2016.

Two different methods for calculating the fluorescence gain were compared, to evaluate if the time of the process could be reduced. Six different plant species were included in the investigation; besides basil, which was used in Paper A, tomato, cucumber, dill and two types of lettuce were also included. One LED group was used at a time, and the light was either held constant for 9 min at each light level (in order to reach steady-state fluorescence), or slowly ramped from a low to a higher level. The fluorescence gains, $dF740/dq$ ($\Delta F740/\Delta q$), were calculated for the two methods and for all LED groups. Differences in the mutual relation of the fluorescence gains are observed for different plant species, even though the similarities are more pronounced. The largest difference between the species were the relative difference between LED 400 and LED 530. Cucumber got the lowest gain for LED 400 and the lettuces and dill got the lowest gain for LED 530. For the second method, the ramp experiments, the experiments were conducted on four of the plant species. The two methods essentially gave the same relative gains, but ramping tends to slightly overestimate the output from the blue LEDs.

4.3 Paper C

Linnéa Ahlman, Daniel Bånkestad, Torsten Wik
Relation between changes in photosynthetic rate and changes in canopy level chlorophyll fluorescence generated by light excitation of different LED colours in various background light
Remote sensing,
vol. 11, no. 4:343, 2019.

As our previous results indicated that red LEDs were most efficient per

quanta, we wanted to evaluate the mutual relation of the fluorescence gains when the proportion of red light in the background spectrum increases. This was done by experiments on cucumber and lettuce. Spectra from 50% up to 100% red light were evaluated at intensity levels ranging from 160 to 1000 µmol m^{-2} s^{-1}. An additional aim was to evaluate the correlation between fluorescence and photosynthesis at various background light levels. At each light level an excitation was added sequentially by each of the six LEDs that were included in the investigation. The relative efficiency of the different LED colors in terms of the fluorescence gains are in agreement with the action spectrum (i.e., the photosynthetic rate as a function of wavelengths) for cucumber and lettuce, found by McCree [13]. The mutual relation between the fluorescence gains corresponding to the different LED colors did not change significantly with background light quality, but it was found to be species dependent. Furthermore, the relative size of the gains did change due to light quantity, but only up to the level where the photosynthesis light curve saturates. This opens for using the mutual relation of the fluorescence gains to find the light level where the photosynthesis saturates.

4.4 Paper D

Linnéa Ahlman, Daniel Bånkestad, Sammar Khalil, Karl-Johan Bergstrand, Torsten Wik
Stress detection using proximal sensing of chlorophyll fluorescence on canopy level
AgriEngineering,
vol. 3, pp. 648–668, 2021.

In this research, we scanned over several abiotic and biotic stress factors (and several plant species) to evaluate the possibility of stress detection using proximal sensed chlorophyll fluorescence, on canopy level. Blue diodes from a growth light LED lamp was used to excite the fluorescence response. It was found that the abiotic stress (salt, drought and heat) can successfully be detected by evaluating the dynamics of the fluorescence response, while biotic stress (root infection *Pythium ultimum* and leaf infection Powdery mildew *Podosphaera aphanis*) were harder to detect. However, the results indicate that for a severe (biotic) infection the stress is detectable. More experiments are needed to determine the critical level of infection required to be detectable, and then decide whether it is an acceptable limitation or not. For the root infection case, the disease is hard to visually detect and, hence, it is still an interesting option. Powdery mildew on the other hand does not affect the

whole plant at start, but spreads point-wise. Due to that nature, it will likely be more efficient to have a sensor with higher spatial resolution as it is desired to detect the mildew already at a stage when it is only visible on very small spots on single leaves.

4.5 Paper E

Linnéa Ahlman, Daniel Bånkestad, Torsten Wik
Tracking optimal plant illumination using proximal sensed chlorophyll fluorescence gain
Manuscript,
2021.

In previous research (Paper A) we noticed that the steady-state ChlF gain on canopy level, measured as change in fluorescence intensity when a weak excitation light is turned on or off, depended on the background light intensity with a peak occurring close to the expected production light intensity. This was further investigated in two master theses within our research group, who also found a peak in the fast ChlF gain on canopy level, measured as variations in ChlF caused by a weak excitation lamp, pulsing with a frequency of 1 Hz. In this work, we measured the fast ChlF gain on sunflower, lettuce, and basil. Simultaneously, we measured the photosynthetic rate, on leaf level, with an infrared gas analyzer. The results show that the light intensity level corresponding to the peak in the ChlF gain, coincides with the light intensity where the photosynthetic rate starts to saturate. This is assumed to be an optimal light illumination level, with a high light use efficiency and a high photosynthesis level. We then propose using an extremum seeking controller for automatically adjusting the light intensity, towards the point where the fast ChlF gain is maximized. In a simulation study we show how this is effectively done.

CHAPTER 5

Concluding remarks and future directions

Extensive experimental work was conducted for the **Spectrum optimization** research (Paper A, B and C). The main conclusions were:

- Steady-state ChlF has a strong correlation with short term photosynthetic rate and is, hence, a candidate signal for estimation of the same.
- The magnitude of the steady-state ChlF gains for different LED colors, does not change substantially relative to each other, when the illumination intensity or the spectrum are changed.

Hence, even though steady-state ChlF is a good candidate of a biological feedback signal to be used in a spectrum optimization loop, the results show that there is no reason for online spectrum control to track the plants as the variations are very small in the short term. However, various plant species have different preferences and the efficacy of the diodes can change significantly over time due to aging but also as a function of operating temperature. To save energy, LED lamp producers are using passive cooling instead of fans in some cases. As a result the operating temperature of the LEDs, which has immediate effects on their efficiency, will vary much more. There is therefore a possibility to use the proposed technique to calibrate the lamp for the current conditions and the specific plant species used, and to suggest the currently most energy efficient spectrum. To ensure good morphologic status of the plants, limitations on the spectrum needs to be included though.

As part of a sensor development project two different research areas were investigated, **Stress detection** (Paper D) and **Intensity optimization** (Paper E). For the first area we concluded:

- The investigated abiotic stress factors (drought, salt, and by mistake, heat) can be detected by comparing the dynamics of the ChlF signal.

- More research is needed to determine if biotic stress (root infection *Pythium ultimum* or leaf infection powdery mildew *Podosphaera aphanis*) can be detected, and if so, how severe the infection must be.

Our experimental setup was too small to draw statistically significant conclusions, but the results indicated that severe infection can be detected. We suggest more research on the root infection *Pythium*, since it by its nature, is hard to detect visually and affects more of less the whole plant. If detectable, one needs to find the limit of infection needed to be detected, and from that decide if it is an acceptable limit or not.

The leaf infection powdery mildew spreads in spots. Because of that, the degree of infection varies over the leaf, and between leaves, and averaging over a larger area (canopy area covered by the sensor) gives a low value even for high infection in spots. Hence, for future research we suggest a detection method with a higher spatial resolution.

We have taken one step in that direction, by using a consumer DSLR camera (Canon EOS 6D Mark II) that we modified by removing the built-in IR-filter and adding a high pass filter. The goal is to evaluate if this device can be used as a fluorescence sensor with higher spatial resolution. Time series of photos were collected from the powdery mildew setup and the analysis is ongoing work. The hypothesis is that spots highly infected with powdery mildew can be detected by this camera.

For the **Intensity optimization** research, experiments were carried out where the fast ChlF gain and the photosynthetic rate were measured simultaneously and we could conclude that:

- Light intensity level where the fast ChlF gain is maximized seemed to be within the region where the light response curve has started to saturate, which is a good light level in terms of high photosynthetic rate and a high efficiency from incident light to photosynthesis.

- An extremum seeking controller can effectively, without exact knowledge of the complex biophysics between incident light and ChlF, control the light towards the point of maximal fast ChlF gain.

Based on the experimental data, a model of the ChlF as a function of incident light was built and then a simulation study illustrated how the extremum seeking controller can be used to control the light. However, later measurements on lettuce showed that there is a hysteresis-like behavior of the fluorescence gain measurements, meaning that the output differs depending on the direction of the change in the light.

This is an interesting path to follow in future research, adapting the design of the controller to handle the hysteresis, and evaluating the results during a whole growth cycle. Natural extensions are to see how the optimum is affected by different stress factors; making the control potentially useful also for diagnosis.

References

[1] T. Kozai and G. Niu, "Chapter 2 - role of the plant factory with artificial lighting (pfal) in urban areas", in *Plant Factory (Second Edition)*, T. Kozai, G. Niu, and M. Takagaki, Eds., Second Edition, Academic Press, 2020, pp. 7–34.

[2] (2020). The language of light radiant vision systems - spectral sensitivity of human eye png, [Online]. Available: `https://www.pngaaa.com/detail/2248270`.

[3] SMHI. (2021). Extracting strång data. T. Carlund, Ed. Data produced with support from the Swedish Radiation Protection Authority and the Swedish Environmental Agency., [Online]. Available: `http://strang.smhi.se/extraction/`.

[4] D. W. Lawlor, *Photosynthesis*, Third, B. S. P. Limited, Ed. Garland Science, 2001.

[5] L. O. Björn, *Photobiology, The Science of Life and Light*, Second, Springer, Ed. 2002.

[6] E. F. Durner, *Principles of Horticultural Physiology*. CABI Publishing, 2013.

[7] A. Vershinin, "Biological functions of carotenoids - diversity and evolution", *BioFactors*, vol. 10, pp. 99–104, 2-3 1999.

[8] T. W. Jurik, J. A. Weber, and D. M. Gates, "Short-term effects of co2 on gas exchange of leaves of bigtooth aspen (populus grandidentata) in the field", *Plant Physiology*, vol. 75, no. 4, pp. 1022–1026, 1984.

[9] M. Poudel and B. Dunn, "Greenhouse carbon dioxide supplementation", Oklahoma State University, Tech. Rep., 2017.

[10] T. Goldammer, "Carbon dioxide in greenhouses", in *Greenhouse Management A Guide to Operations and Technology*. Apex Publishers, 2019.

[11] A. Porcar-Castell, E. Tyystjarvi, J. Atherton, C. van der Tol, J. Flexas, E. E. Pfundel, J. Moreno, C. Frankenberg, and J. A. Berry, "Linking chlorophyll a fluorescence to photosynthesis for remote sensing applications: Mechanisms and challenges", *Journal of Experimental Botany*, vol. 65, no. 15, pp. 4065–4095, 2014.

[12] D. Pugliesi. (2012). Chlorophyll ab spectra-en.svg, [Online]. Available: `https://commons.wikimedia.org/wiki/File:Chlorophyll_ab_spectra-en.svg`.

[13] K. J. McCree, "Action spectrum, absorptance and quantum yield of photosynthesis in crop plants", *Agricultural Meteorology*, vol. 9, pp. 191–216, 1972.

[14] K. Inada, "Action spectra for photosynthesis in higher plants", *Plant and Cell Physiology*, vol. 17, no. 2, pp. 355–365, 1976.

[15] R. Paradiso and S. Proietti, "Light-quality manipulation to control plant growth and photomorphogenesis in greenhouse horticulture: The state of the art and the opportunities of modern led systems", *Journal of Plant Growth Regulation*, pp. 1435–8107, 2021.

[16] R. Emerson, "Dependence of yield of photosynthesis in long-wave red on wavelength and intensity of supplementary light", *Science (American Association for the Advancement of Science)*, vol. 125, p. 746, 3251 1957.

[17] T. Ouzounis, E. Rosenqvist, and C.-O. Ottosen, "Spectral effects of artificial light on plant physiology and secondary metabolism: A review", *HortScience*, vol. 50, no. 8, pp. 1128–1135, 2015.

[18] M. Olle and A. Viršile, "The effects of light-emitting diode lighting on greenhouse plant growth and quality", *Agricultural and Food Science*, vol. 22, no. 2, 2013.

[19] E. H. Murchie and T. Lawson, "Chlorophyll fluorescence analysis: a guide to good practice and understanding some new applications.", *Journal of experimental botany*, vol. 64, no. 13, pp. 3983–3998, 2013.

[20] G. Deitzer, "Spectral comparisons of sunlight and different lamps", in *International lighting in controlled environments workshop*, T. Tibbitts, Ed., University of Wisconsin -Madison, 1994, pp. 197–199.

[21] R. C. Morrow, "Led lighting in horticulture led lighting in horticulture", *HortScience*, vol. 43, no. 7, pp. 1947–1950, 2008.

[22] L. Ahlman, D. Bånkestad, and T. Wik, "Using chlorophyll a fluorescence gains to optimize led light spectrum for short term photosynthesis", *Computers and Electronics in Agriculture*, vol. 142, no. Part A, pp. 224–234, 2017.

[23] J. A. Nelson and B. Bugbee, "Economic analysis of greenhouse lighting: Light emitting diodes vs. high intensity discharge fixtures", *PLOS ONE*, vol. 9, no. 6, pp. 1–10, 2014.

[24] (2021). Horticultural lighting qualified products list 2021, The DesignLights Consortium, [Online]. Available: `https://www.designlights.org/horticultural-lighting/` (visited on 06/29/2021).

[25] P. Kusuma, P. M. Pattison, and B. Bugbee, "From physics to fixtures to food: Current and potential led efficacy", *Horticulture Research*, 56th ser., vol. 7, pp. 2052–7276, 2020.

[26] C. M. Bourget, "An introduction to light-emitting diodes", *HortScience*, vol. 43, no. 7, pp. 1944–1946, 2008.

[27] D. Katzin, L. F. Marcelis, and S. van Mourik, "Energy savings in greenhouses by transition from high-pressure sodium to led lighting", *Applied Energy*, vol. 281, p. 116 019, 2021.

[28] K. B. Ariyur and M. Krstić, "Siso scheme and linear analysis", in *Real-Time Optimization by Extremum-Seeking Control*. John Wiley & Sons, Ltd, 2003, ch. 1, pp. 1–20.

[29] O. Trollberg, "On real-time optimization using extremum seeking control and economic model predictive control", PhD thesis, Kungliga Tekniska högskolan, 2017.

[30] M. Leblanc, "Sur l'électrification des chemins de fer au moyen de courants alternatifs de fréquence élevée", *Revue générale de l'électricité*, vol. 12, no. 8, pp. 275–277, 1922.

[31] J. Sternby, *A Review of Extremum Control*, English, ser. Technical Reports TFRT-7161. Department of Automatic Control, Lund Institute of Technology (LTH), 1979.

[32] M. Krstić and H.-H. Wang, "Stability of extremum seeking feedback for general nonlinear dynamic systems", *Automatica*, vol. 36, no. 4, pp. 595–601, 2000.

[33] J. Flexas, J. M. Escalona, S. Evain, J. Gulías, I. Moya, C. B. Osmond, and H. Medrano, "Steady-state chlorophyll fluorescence (Fs) measurements as a tool to follow variations of net CO_2 assimilation and stomatal conductance during water-stress in C_3 plants", *Physiologia Plantarum*, vol. 114, pp. 231–240, 2002.

[34] L. Guanter, Y. Zhang, M. Jung, J. Joiner, M. Voigt, J. A. Berry, C. Frankenberg, A. R. Huete, P. Zarco-Tejada, J.-E. Lee, M. S. Moran, G. Ponce-Campos, C. Beer, G. Camps-Valls, N. Buchmann, D. Gianelle, K. Klumpp, A. Cescatti, J. M. Baker, and T. J. Griffis, "Reply to magnani et al.: Linking large-scale chlorophyll fluorescence observations with cropland gross primary production", *Proceedings of the National Academy of Sciences*, vol. 111, no. 25, E2511, 2014.

[35] K. Maxwell and G. N. Johnson, "Chlorophyll fluorescence - a practical guide", *Journal of Experimental Botany*, vol. 51, no. 345, pp. 659–668, 2000.

[36] C. van der Tol, W. Verhoef, and A. Rosema, "A model for chlorophyll fluorescence and photosynthesis at leaf scale", *Agricultural and Forest Meteorology*, vol. 149, no. 1, pp. 96–105, 2009.

[37] O. Trollberg, B. Carlsson, and E. W. Jacobsen, "Extremum seeking control of the canon process - existence of multiple stationary solutions", *Journal of Process Control*, vol. 24, no. 2, pp. 348–356, 2014.

[38] S. Skogestad, "Self-optimizing control: The missing link between steady-state optimization and control", *Computers and Chemical Engineering*, vol. 24, pp. 569–575, 2000.

[39] T. Wik, A. Carstensen, and T. Pocock, *Spectrum optimization for artificial illumination*, WO Patent App. PCT/EP2013/069,820, 2014.

[40] S. Sankaran, A. Mishra, R. Ehsani, and C. Davis, "A review of advanced techniques for detecting plant diseases", *Computers and Electronics in Agriculture*, vol. 72, no. 1, pp. 1–13, 2010.

[41] I. Simko, R. J. Hayes, and R. T. Furbank, "Non-destructive phenotyping of lettuce plants in early stages of development with optical sensors", English, *Frontiers in Plant Science*, vol. 7, 2019.

[42] A. Galieni, N. D'Ascenzo, F. Stagnari, G. Pagnani, Q. Xie, and M. Pisante, "Past and future of plant stress detection: An overview from remote sensing to positron emission tomography", *Frontiers in Plant Science*, vol. 11, p. 1975, 2021.

[43] A.-M. Carstensen, T. Pocock, D. Bånkestad, and T. Wik, "Remote detection of light tolerance in basil through frequency and transient analysis of light induced fluorescence", *Computers and Electronics in Agriculture*, vol. 127, pp. 289–301, 2016.

[44] M. Hedegärd, "Estimation of torque in heavy duty vehicles with focus on sensor hysteresis", Ny serie: 4152, PhD thesis, Chalmers tekniska högskola, 2016.

[45] A. H. Tan, "Direction-dependent systems – a survey", *Automatica*, vol. 45, pp. 2729–2743, 12 2009.

Part II

Papers

PAPER A

Using chlorophyll *a* fluorescence gains to optimize LED light spectrum for short term photosynthesis

Linnéa Ahlman, Daniel Bånkestad, Torsten Wik

Computers and Electronics in Agriculture,
vol. 142, pp. 224–234, 2017

The layout has been revised.

Abstract

When changing from the traditional high pressure sodium (HPS) lamps to light emitting diode (LED) lamps there is a quite unexplored energy saving potential in the fact that they are far better suited for control, since both spectrum and light intensity can be adjusted. This work aims at finding a way to automatically adjust the spectrum of a LED lamp, equipped with several different types of LEDs, to maximize plant growth by feedback of a remote online measure correlated with growth. A series of experiments were conducted on basil plants in order to examine whether remotely sensed steady-state chlorophyll fluorescence (F740) can be used for this purpose, and if its derivatives (fluorescence gains) w.r.t. applied powers change relative to each other for different light intensities and spectra. A strong correlation between F740 and photosynthetic rate was indeed found. However, the order (w.r.t. LED type) of the fluorescence gains was only moderately affected by the light intensities and spectra investigated. The gain was highest w.r.t. red light (630 nm), though, when taking the electrical efficiencies of individual LED types into consideration, blue LEDs (450 nm) were equally, or even more efficient than the red ones. An online controller to regulate optimal spectrum for basil appears to be unnecessary. However, the fluorescence gains could be used to adapt to changes in the efficiencies when crops and operating conditions change, or when the diodes degrade. The method also shows promise as a tool to find optimal light intensity levels as well as identifying plant stress.

1 Introduction

Modern greenhouses having lighting systems are large consumers of electricity. In Europe alone, the power consumption from greenhouse lamps is estimated to be 100–200 TWh per year (combining information from Eurostat [1], Christensen and Larsson [2], Persson [3], and Stenberg [4]). High pressure sodium (HPS) lamps are still dominating and the illumination is in general controlled manually by simply switching the lamps on and off. Changing to light emitting diodes (LEDs) entails an energy saving potential [5], due to higher electrical

efficiency of many LEDs compared to HPS lamps. Ongoing research aiming at using LEDs for irradiance control to avoid light inhibition [6], to regulate electron transport rate [7] and to match time of harvest to demand [8] may decrease the illumination cost per produced plant even further. Yet another possibility to reduce the energy use might be to optimise the spectrum by changing the power split to diodes of different colours. The energy optimal split could potentially depend on a number of factors, such as plant species, required characteristics of the plant, available LED groups and their electrical efficiency.

In the seventies two large studies were conducted [9], [10] in order to determine the photosynthetic efficiency of photons of different wavelengths using monochromatic light. McCree [9] used leaves of 22 different species of crop plants and measured the action spectra, i.e. the CO_2 uptake rate for incident irradiance, and also the absorbance, for each wavelength (intervals of 25 nm). He concluded that the curves had similar shape for all species tested, which was later confirmed by Inada [10] who did experiments on leaves from 33 different species. The concluded similarity, however, should not be interpreted as "equal", now that we have the possibility to modify the spectrum quite freely with advanced LED lamps. Figure 1 shows normalized action spectra for incident quanta, derived from the experimental data given by McCree [9]. The two species selected, Pigweed (*Amaranthus edulis* Speg) and Castorbean (*Ricinus communis* L.), were the ones that deviated the most from the mean. These results clearly indicate that the most efficient light spectrum, in terms of CO_2 uptake rate, differs between different crops. The photosynthetic rate in a light combining sources that have different wavelengths may not necessarily equal the sum of the individual sources' photosynthetic rates. One example is the enhancement obtained when combining light of shorter wavelength (less than 680 nm; such as red light) with light of longer wavelength (greater than 680 nm; such as far-red light), the so called "Emerson effect" [11], which is related to the excitation of the two photosystems. Further, the results likely differ if investigated at leaf level or at canopy level [12].

Many studies have been conducted that investigates the spectral effect on plant growth, commonly by comparing the impact that various light sources, and in particular their blue:green:red-ratio, has on the manually measured growth of a few plant species during their life cycles, e.g. Ouzounis *et al.* [13], Cope *et al.* [14], Massa *et al.* [15], Kim *et al.* [16], and Dougher and Bugbee [17]. There are also studies on using LEDs as supplement to sunlight in greenhouses [18], [19]. However, to the best of our knowledge there are no studies reported on automatically finding the best spectrum based on a remote measure.

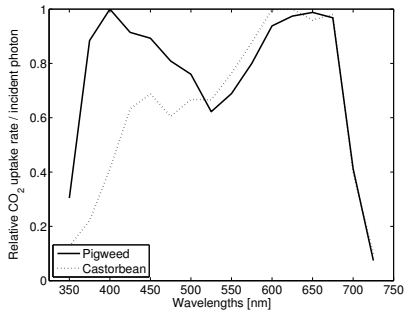

Figure 1: Normalized action spectra for incident quanta for Pigweed and Castorbean. Derived from experimental data given by McCree [9].

The present work aims at finding a way to automatically optimize the spectrum based on a remote measure of growth. Figure 2 illustrates the idea, where the task is to distribute a predefined input electrical power, P_{tot}, on the available diodes so as to maximize the plant performance, y. Having a plant performance measure that can be measured remotely, a feedback controller could be sought that automatically adjusts the power towards the optimal spectrum.

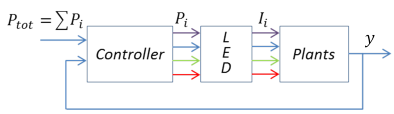

Figure 2: In order to find an optimal spectrum, i.e. how to distribute the power P_{tot} among the different diode groups by feedback control, one needs to find a parameter of plant growth that could be measured remotely and online. In this study we investigate if chlorophyll fluorescence F740 could be a candidate measure y.

The light energy absorbed by the leaf is either used to drive the photosynthesis, dissipated as heat or re-emitted as fluorescence [20], [21]. In the conducted experiments the photosynthetic rate, measured by an infrared gas analyser, is used as the reference of the "plant performance" to be maximized and steady-state chlorophyll fluorescence is the candidate signal to be used in the feedback loop, since it is remotely measurable and non-destructive. The fluorescence signal originates from chlorophyll *a* in photosystems I and II and is an emission of absorbed light energy with peak wavelengths around 685 and 740 nm [22]. The fluorescence peak at 740 nm (F740) tends to give the strongest signal because the 685 nm peak (F685) is to a larger extent

reabsorbed by chlorophyll *a* [23], [24]. In the analysis in this study only measurements of F740 are shown, since they correlated better with the photosynthetic rate than F685, and is not disturbed by light from the LEDs in the lamp having a peak at 660 nm.

A number of studies in the same research area, lighting control in horticulture by biological feedback, have also used chlorophyll flurescence as control signal, but in different ways. Carstensen *et al.* [6] presents a novel method for probing photosynthetic status based on analysis of the dynamic chlorophyll fluorescence response to an excitation light. Detection of the chlorophyll fluorescence signal is made remotely on canopy level. Iersel *et al.* [7] use PAM fluorometry on leaf level to measure quantum yield of photosystem II (Φ_{PSII}) and demonstrates that it can be used for controlling electron transport rate (ETR). Bånkestad and Wik [8] evaluates the performance of an active proximal remote sensing system, measuring the ratio of red to far-red fluorescence (F685/F740), for the assessment of growth and biomass. In contrast, the present study explores the information in steady-state chlorophyll fluorescence F740 and how it relates to photosynthesis. Clearly, the properties of the chlorophyll fluorescence signal (intensity, spectrum, and dynamics) *in vivo* are controlled by many physical and physiological factors, making it attractive for biological sensing, but also challenging to interpret. The complexity of the signal increase with increasing scale, and more research is needed to expand the knowledge gained from leaf level measurements to canopy level and beyond [21]. This study addresses that particular challenge.

The relation between the amount of absorbed light, the amount of fluorescent light and the photosynthetic rate has been studied on both leaf level [25] and canopy level [26] and is dependent on plant health. For example, the *fraction* of fluorescence and photosynthesis is negatively correlated at low light intensity while it is positively correlated at high light intensity and stress [20], [27]. However, the *absolute* quantities of both fluorescence and photosynthesis are expected to increase with an increased incident light intensity, though the photosynthetic rate will eventually saturate (c.f. Figure 4). With the hypothesis, that there is a positive correlation, not necessarily linear, between (the absolute quantity of) photosynthetic rate and steady-state fluorescence (under the conditions of interest here, i.e. well-irrigated and fertilized crops under moderate light conditions) the maximum photosynthetic rate for a predefined total power, P_{tot}, corresponds to the spectrum that maximises F740.

Assume that N different types of LEDs are avaliable. Then F740 depends on all the LED sources, i.e.

$$F740 = f(P_1, ..., P_N) \tag{A.1}$$

where P_i is the electrical power applied to the i:th group of LEDs. For a predefined total power P_{tot} we may write

$$P_N = P_{tot} - \sum_{i=1}^{N-1} P_i \tag{A.2}$$

Since the optimal spectrum is to maximise F740, the gradient of F740 should be zero with respect to all sources. Inserting (A.2) into (A.1) and differentiating gives

$$\begin{aligned} \frac{dF740}{dP_i} &= \frac{\partial f}{\partial P_i} + \frac{\partial f}{\partial P_N}\frac{\partial P_N}{\partial P_i} \\ &= \frac{\partial f}{\partial P_i} - \frac{\partial f}{\partial P_N} = 0 \quad \text{for all } i \end{aligned} \tag{A.3}$$

The last equality implies that the *fluorescence gains*, defined as $\partial F740/\partial P_i$ (i.e. $\partial f/\partial P_i$), should be equal for all LED groups i. Since we are only interested in how the fluorescence gains relate to each other, the actual relation between growth and F740 need not to be known. All that matters is that they are positively correlated to each other. The control task then fits to a combination of extremum seeking control (see Trollberg *et al.* [28] and references therein) to track the fluorescence gains, and self optimizing control [29] to aim for equal gains [30]. In principle, when not being at optimum, the controller would increase the power to the LEDs with the highest gain and reduce the power to the one(s) with the lowest gain. Motivated by this, a series of experiments manipulating the power to four different LED groups ranging from 420 nm to 630 nm were conducted on basil in order to investigate the following:

- Is remotely measured F740 a sufficiently good measure of photosynthetic rate?
- Do the magnitudes of the fluorescence gains ($\partial F740/\partial P_i$) change relative to each other when the light intensity is changed?
- Do the magnitudes of the fluorescence gains ($\partial F740/\partial P_i$) change relative to each other when the spectrum is changed?

2 Materials and methods

Three different sets of experiments were conducted on basil plants:

(A) No background light
Stepwise increasing one LED group at a time.

(B) Background light with blue to red (B:R) ratio 3:1 and 1:3
Four intensity levels for each of the two spectra. Ramping one LED group at a time through each operating point.

(C) High intensity background light
Randomly changing one LED group at a time as a step change away from the operating point.

All experiments were carried out in a Styrofoam box ($w \times d \times h = 0.7 \times 0.7 \times 0.9$ m) with two LED lamps placed above (see Figure 3. The light was detected by two spectrometers, one facing the lamps and one facing the plants. In the following, the conditions, instruments and setups are described in more detail.

2.1 Plants

Two trays with basil pots were placed in the box during the experiments. Fully grown commercially produced basil plants were used in experiment *(A)* and *(C)*, whilst in experiment *(B)* two different sets of plants grown in the lab were used. The first one was basil *Ocimum basilicum* 'Nufar' grown in $250\,\mu mol\,m^{-2}\,s^{-1}$ for six weeks. The second set was basil *Ocimum basilicum* 'Genovese' grown in $160\,\mu mol\,m^{-2}\,s^{-1}$ for four weeks.

2.2 Lamps

Two L4AS1 LED lamps (Heliospectra, Sweden), placed 0.9 m above the plants, were used as the only light source during the experiments.

The lamps contain diode groups having different peak wavelengths, of which we used 420, 450, 530, 630 and 660 nm. Table 1 shows relative (to LED 450) electrical efficiencies of the individual diode groups, both in terms of radiant flux and photon flux. In the cases when LED 660 was used, it was held at a constant level since it overlaps with the fluorescence peak at 685 nm which initially was a candidate signal to investigate. The diodes are optically mounted in the lamp to provide a homogenous light at plant level. Due to heat generation from the lamp, the temperature in the box increased with light intensity. For light intensities lower than $500\,\mu mol\,m^{-2}\,s^{-1}$ the temperature were in the range 25–28 °C, for incident light around $1000\,\mu mol\,m^{-2}\,s^{-1}$ the temperature was about 30 °C, and for the one set with incident light just above $2250\,\mu mol\,m^{-2}\,s^{-1}$ (see Table 4) the temperature reached 36 °C. This increase in temperature under high light needs to be considered when analysing the effect of incident light on photosynthesis.

Table 1: Relative electrical efficiencies of the individual LED groups in the L4AS1 lamp model (Heliospectra, Sweden) used in the study, as characterized by SP Technical Research Institute of Sweden.

LED group	Rel. radiant eff. (W/W)	Rel. photon eff. (µmol/J)
420	0.69	0.65
450	1.00	1.00
530	0.37	0.44
630	0.59	0.82

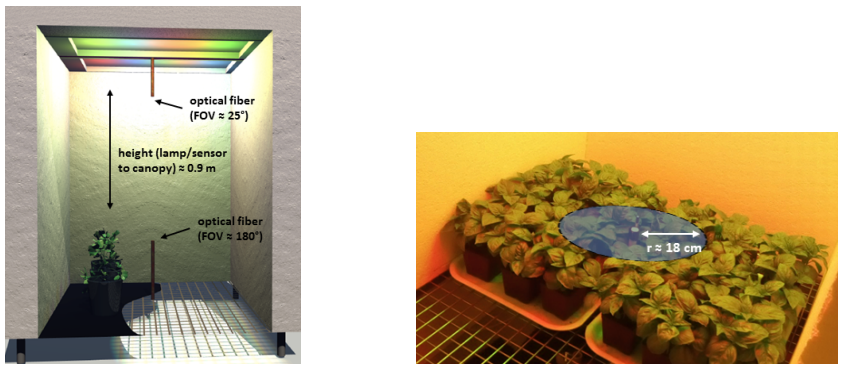

(a) (b)

Figure 3: (a) Styrofoam box (measurement unit) equipped with two lamps and two optical fibers for measuring incident light and canopy fluorescence; (b) two full trays of basil were placed in the unit for measurements, and the area viewed by the sensor had a radius of approximately 18 cm (the area in the image is for illustration).

2.3 Spectrometers

The incident light from the LED lamp was detected at canopy level by a Maya 2000 Pro Spectrometer (Ocean Optics, Dunedin, FL, USA) equipped with a 50 µm optical fiber and a cosine diffuser giving a field of view of 180 °. The reflected and fluoresced light were also detected by another Maya 2000 Pro Spectrometer, but equipped with a 600 µm optical fiber with a field of view of about 25 ° in order to only measure green area. The fiber was placed between the two lamps, facing the plants. The fluorescence signal F740 was determined by integration over the wavelength interval 735–745 nm.

2.4 Infrared gas analyser

An infrared gas analyser, IRGA TPS-2 (PP systems, Haverhill, MA, USA) was used to determine the photosynthetic rate, in terms of CO_2 uptake per m^2 leaf area and s. The calculations are based on measurements of CO_2, O_2 and H_2O in a controlled air flow over a leaf sealed in a chamber, the leaf cuvette. The cuvette has a window which makes it possible to use the ambient light as light source (as in our case), but it is also possible to directly connect the leaf cuvette to the lamp (red and white LEDs) provided with the equipment. Figure 4 shows photosynthetic light response curves of basil leaves from commercially produced plants. Three sample leaves and the IRGA's own light source were used in the measurement.

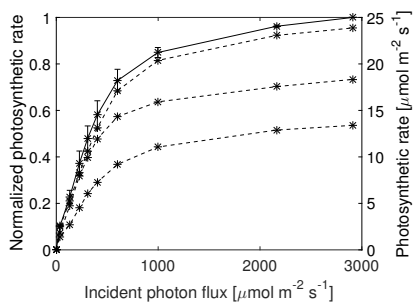

Figure 4: Photosynthetic light response curves of basil leaves showing CO_2 uptake as a function of incident light (PAR). The dotted lines (right axis) show data from the three samples and the solid line (left axis) is the corresponding average of normalized data. The bars indicates ±1 standard deviation.

2.5 Experimental setup

As mentioned, three different setups were used in the experiments. In the first one, *(A)*, the photosynthetic rate and fluorescence were measured and compared when using one LED group at a time as the only light source. In the latter two, *(B)* and *(C)*, the deviation of the fluorescence was recorded while changing one LED group at a time around an operating point (background spectrum).

Experiment (A) The plants were exposed to light from one LED group at a time. LEDs with maximum intensity at 420, 450, 530 and 630 nm were used. The experiments were repeated four times, twice starting with the LED group of lowest wavelength and continued in the order of increasing wavelength, and twice in the opposite order. Ten light intensity steps were used for each LED, and the light was held constant for 12–15 min at each level in order to reach a steady state (see Figure 5a). Both fluorescence and photosynthetic rate were measured throughout the experiments.

Experiment (B) Two spectra were chosen, one predominantly red (regR) having B:R ratio 1:3, and one predominantly blue (regB) having a B:R-ratio 3:1, see Table 2. Four different intensity levels of each spectrum were used, thus 8 operating points in total. LEDs with maximum intensity at 420, 450, 530 and 630 nm were used and only one group of diodes was changed at a time. For regR an additional LED group was used, 660 nm, in order to reach the B:R-ratio 1:3, but it was held constant throughout each experiment.

Table 2: Light intensities at the operating points in *Experiment (B)* measured during the experiments. PAR: 400–700 nm ($\mu mol\, m^{-2}\, s^{-1}$), blue: 400–500 nm, green: 500–600 nm, red: 600–700 nm.

Light regime	PAR	B:R	% Green
regR *i*	130	1:2.9	10
regR *ii*	195	1:2.7	10
regR *iii*	260	1:2.9	10
regR *iv*	540	1:2.9	10
regB *i*	195	3.1:1	18
regB *ii*	225	3.1:1	18
regB *iii*	270	3.1:1	18
regB *iv*	315	3.1:1	34*

*In order to increase total PAR in regB *iv* the green light (530 nm) had to be increased, since the blue LEDs had reached maximum capacity.

Two sets of experiments were performed with slightly different setups, summarized in Table 3. One setup started with 15 minutes of dark adaption in

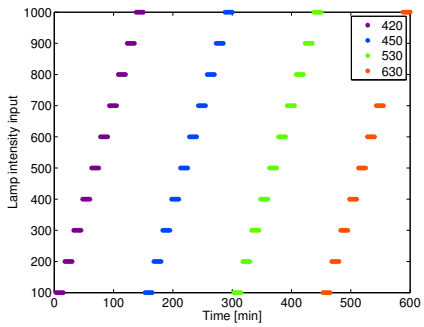

(a) Lamp input *Experiment (A)*.

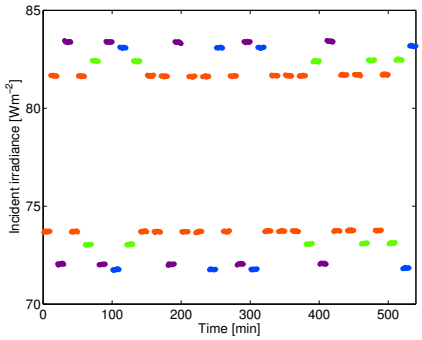

(b) Measured incident irradiance *Experiment (C)*.

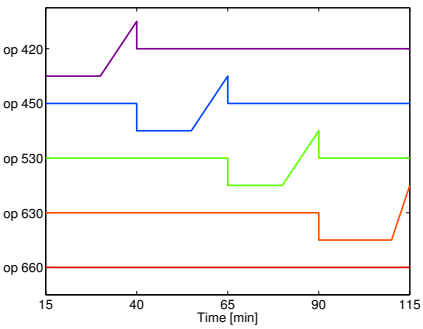

(c) Schematic changes for each LED, *Experiment (B)* 1st set.

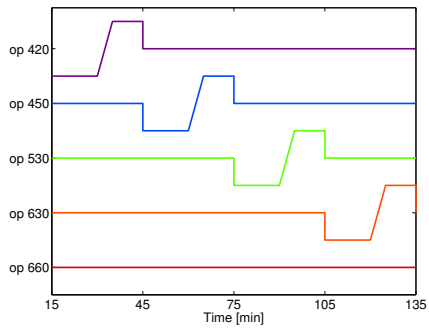

(d) Schematic changes for each LED, *Experiment (B)* 2nd set.

Figure 5: Lamp settings for the different experiments. (a) *Experiment (A)* Each LED steps from minimum to maximum lamp intensity in 10 steps. Lamp intensity input on the y axis refers to the setting in the lamp software. Second and fourth experiment had this setup, first and third experiment reversed the order of the LEDs. (b) *Experiment (C)* Total incident irradiance for one operating point. The color indicates which diode group that deviate from the operating point. (c) *Experiment (B)*, 1st set. Schematic changes for each LED around its operating point. Constant light in 15 min before the 10 min ramp. Twice starting with LED 420 and increasing ramps (as in the figure) and once in reversed order starting with LED 630 and decreasing ramps. (d) *Experiment (B)*, 2nd set. Schematic changes for each LED around its operating point. Constant light in 15 min, 5 min ramp, constant light 10 min. Once starting with LED 420 and increasing ramps (as in the figure) and once in reversed order starting with LED 630 and decreasing ramps.

order to get a reference value for the IRGA. Thereafter one LED group at a time was changed from its value at the operating point. Figure 5c depicts the schematic change of each LED group in the first set; starting with 15 minutes of constant light slightly lower than the operating point for the current LED group, followed by a 10 minutes ramp through the operating point. This scheme continued for each LED group in the order of increasing wavelength, directly one after another. The experiments were repeated three times at each operating point, of which one was in the reversed direction, i.e., starting with the LED group of highest wavelength (630) and with a decreasing ramp.

For the second setup the plateau level was held for 15 minutes, the ramp lasted 5 minutes, and the final value was held constant for 10 minutes (see Figure 5d). Each experiment was repeated twice, one with increasing light (starting with LED 420) and one with decreasing light (starting with LED 630).

Table 3: The conditions for the 1st and 2nd set of *Experiment (B)*.

	1st set	2nd set
Background light	regR *i, ii, iii* regB *i, iii*	regR *iii, iv* regB *ii,iv*
Setup	plateau, ramp	plateau, ramp, plateau
	15, 10 (min)	15, 5, 10 (min)
Replicates	3; up, down, up	2; up, down
Plant age	6 weeks	4 weeks
Growth light	250 µmol m^{-2} s^{-1}	160 µmol m^{-2} s^{-1}

Experiment (C) The motive for this set was to see how the fluorescence gains were affected as the light intensities increased, and to introduce some randomness regarding the sequence of which LED group that was changed. The operating points used in this set of experiments have been divided into two groups; predominating red light (5 spectra) and predominating blue light (three spectra), although the B:R-ratio varied more here than in *Experiment (B)*. Total PAR, B:R-ratio and the percentage of green light for the eight operating points used are shown in Table 4.

Randomly, one LED group at a time was deviated from the operating point. First by lowering the light and then by increasing it (the total intensity step was approximately 40 µmol m^{-2} s^{-1}) and at each level it was held constant for 10–15 minutes. An example is shown in Figure 5b, for that particular operating point LED 630 was changed 12 times, LED 530 and 420 5 times each and LED 450 4 times.

Table 4: Light intensities at the operating points in *Experiment (C)* measured during the experiments. PAR: 400–700 nm (µmol m^{-2} s^{-1}), blue: 400–500 nm, green: 500–600 nm, red: 600–700 nm.

Light regime	PAR	B:R	% Green
regR *v*	320	1:3.1	10.2
regR *vi*	377	1:3.5	10.3
regR *vii*	895	1:2.7	10.6
regR *viii*	1134	1:8.3	6.4
regR *ix*	2276	1:2.5	10.1
regB *v*	243	2.7:1	20.0
regB *vi*	654	8.5:1	10.2
regB *vii*	955	3.5:1	23.6

3 Results and Discussion

For the interpretation of the results it is important to keep in mind that for the intended use of the results (the method described in Introduction) it is only the *relative* quantities of each LED group compared to the others, within each experiment, that is important. This is also the strength of the approach since the method essentially becomes insensitive to environmental conditions and canopy structure.

3.1 *(A)* No background light

Both photosynthetic rate and fluorescence have an almost linear relationship with light intensity, at low to moderate light levels. Figure 6 shows the relative fluorescence (F740) for all experiments versus the mean values of the relative photosynthetic rate (PN). Each dot is coloured according to which LED group that was used. There is a strong correlation ($R^2 = 0.982$ for a first order curve fit and $R^2 = 0.996$ for a second order curve fit) between photosynthetic rate, measured on leaf level, and fluorescence at 740 nm, measured on canopy level, for the investigated light intensities (0–350 µmol m^{-2} s^{-1}). This is remarkable considering the complexity of the two de-excitation pathways and that measurements on canopy level are convoluted by e.g. canopy structure. It is, at least partly, explained by the dominance of absorbed light on both fluxes [26], [31].

At the highest light intensities (250–350 µmol m^{-2} s^{-1}), where only red light is used, F740 increases somewhat faster than PN does, indicating a higher fluorescence emission efficiency relative to photosynthesis. This relative change is expected, the yield of photosynthesis decreases whilst the yield of fluores-

cence increases with increasing irradiance under low to moderate light levels [20], [27], and it is also expected to be this small due to small variations in yields and the dominant effect of absorbed light [31]. The data was obtained under light limiting conditions (c.f. Figure 4) and therefore it is not possible to determine what happens with the relationship at light saturation.

The experiment was repeated four times. Figure 7 shows the mean values ± 1 standard deviation of (a) PN and (b) F740 versus incident photon flux. The standard deviation is smaller in the fluorescence data, which is one of the potential benefits of canopy level measurements, having an averaging effect, as compared to leaf level measurements. No difference could be observed as an effect of the order of the LED groups.

By using a second order curve fit the derivatives for each LED group have been calculated. Figure 8 shows the derivative of (a) PN and (b) F740 versus incident photon flux. The derivatives are very similar in between LED groups and do not change much with light intensity, but there are indeed some small variations. As mentioned, based on the literature [20], [27] we expect a small increase and small decrease in the yields/derivatives of fluorescence and photosynthesis, respectively, with light intensity. This was also observed, with the exception of LED450 and LED530 exhibiting a small increase in photosynthetic yield that we are unable to explain, but which may possibly be related to acclimation [32], [33].

At the lowest light intensities the derivative is highest when changing LED 630, followed by 420, 450 and then 530, for both PN and F740. The data suggests that these relations change relative to each other, as light intensity increases. Assuming that the quantities are additive, Figure 8a (photosynthetic yield) indicates that up to about $150\,\mu\mathrm{mol\,m^{-2}\,s^{-1}}$ it is most efficient to provide light from LED 630 and thereafter one should increase the light from LED 450. The lines in Figure 8b (fluorescence gain) also intersect, but not at the exactly same light intensities. The conclusion when looking at the latter figure is that the most efficient light to use is LED 630 up to about $100\,\mu\mathrm{mol\,m^{-2}\,s^{-1}}$ and then use LED 420. Even though the conclusion slightly differs when using the leaf level photosynthetic yield and when using the canopy level fluorescence gain, both methods capture the fact that, at low light levels, LED 630 is the most efficient, followed by 420, 450 and 530. As a comparison one can calculate relative photosynthetic efficiency of the different LEDs based on McCree's data [9] by multiplying McCree's action spectrum of photosynthesis per incident quanta (average of all 22 species) with the spectrum of each LED normalized to the same photon flux. This operation yields the same order of LED efficiencies (i.e. LED 630 is most efficient, followed by 420, 450 and 530; data and calculations not shown).

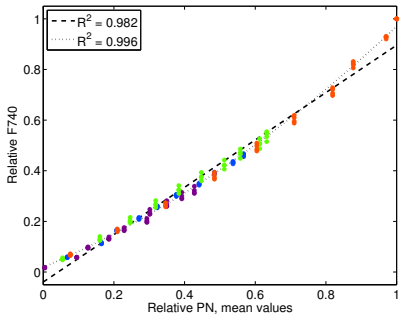

Figure 6: Relative fluorescence, F740, versus mean relative photosynthetic rate, PN. Dashed line shows a first order curve fit ($R^2 = 0.982$) and the dotted line shows a second order curve fit ($R^2 = 0.996$). Each data point is coloured according to which LED group that was used.

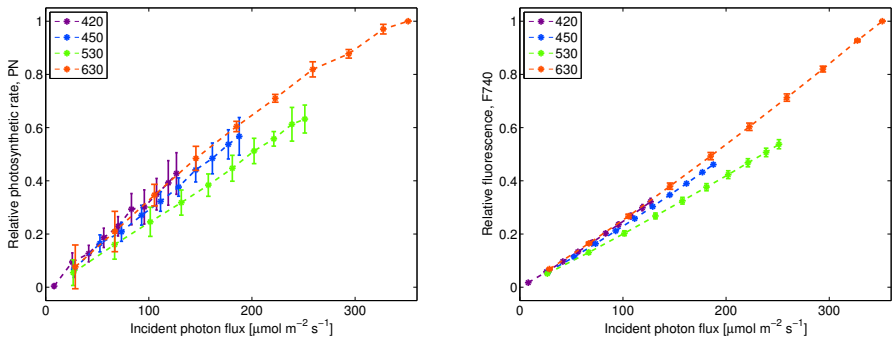

(a) Relative photosynthetic rate, PN, vs. incident photon flux.

(b) Relative fluorescence, F740, vs. incident photon flux.

Figure 7: Results from *Experiment (A)*, i.e. using one LED group at a time. The experiment was repeated four times, the bars indicates ±1 standard deviation.

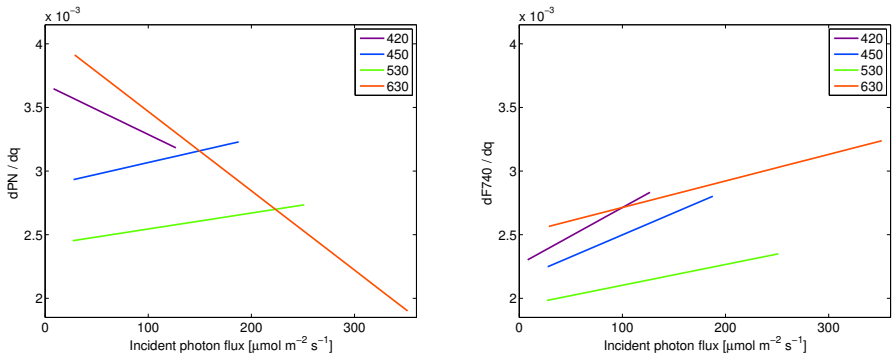

(a) dPN/dI vs. incident photon flux.

(b) Fluorescence gains vs. incident photon flux.

Figure 8: Derivatives for second order curve fits to data in Figure 7.

All the analysis above was made with respect to the incident photon flux. One conclusion is that the (short term) photosynthetic rate for a given photon flux ($\mu\text{mol}\,\text{m}^{-2}\,\text{s}^{-1}$) does not differ much depending on which LED group that is used, i.e. the light spectrum. If comparing photosynthetic rate versus incident irradiance (Wm^{-2}) instead, which would be of interest when aiming at finding the light spectrum , with a certain energy content, that maximizes the photosynthetic rate, the lines differentiate more (see Figure 9a). In such case it is most efficient to use red diodes since light energy is inversely proportional to wavelength ($E = hc/\lambda$, where h is the Planck constant, c is the speed of light and λ is the wavelength).

Another factor to take into consideration is the electrical efficiencies of the diodes in the LED lamp (see Table 1). Figure 9b shows that the applied electrical power (for a particular photosynthetic rate) is lowest using LED 450 or 630 and highest using LED 530. Clearly, the relative order of the photosynthetic efficiencies of the LEDs are dominated by their electrical efficiencies. Note that the analysis are based on electrical efficiencies of this particular lamp; the relation is likely to be somewhat different in other LED lamps depending on LED specifications, electronics, temperature (cooling) and optics.

3.2 *(B)* Background light with B:R-ratio 3:1 and 1:3

The potential effects of different spectra were compared, using spectra with blue to red (B:R) ratio 1:3 and 3:1 (see Table 2), and four different intensity levels for each spectrum. At each operating point one LED group was changed at a time and the fluorescence gains (see Table 5 for abbreviations) were

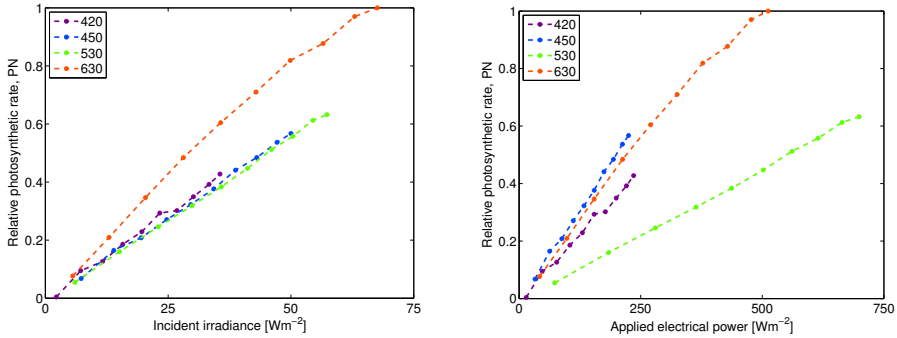

Figure 9: Relative photosynthetic rate vs. (a) incident irradiance and (b) applied electrical power, in *Experiment (A)*. Per incident irradiance (a) LED 630 has the highest fluorescence gain while for applied electrical power (b) LED 450 and 630 are about equal, due to a high electrical efficiency of LED 450.

recorded.

Table 5: Abbreviations of the fluorescence gains w.r.t. different quantities.

Derivative of F740 w.r.t.	Abbr.
Applied Electrical Power	$\partial F740/\partial P_i$
Irradiance	$\partial F740/\partial I_i$
Photon Flux	$\partial F740/\partial q_i$

The fluorescence gains when changing individual LED groups at each operating point are shown in Figure 10, i.e. the derivative of F740 with respect to incident photon flux ($\partial F740/\partial q_i$), incident irradiance ($\partial F740/\partial I_i$) and applied electrical power ($\partial F740/\partial P_i$).

The fluorescence gains were lower for blue intense background light (compare left and right columns in Figures 10), probably partly due to lower absolute fluorescence values (see Figure 11), which might be related to less absorption of blue intense background light as well as less canopy penetration causing less reabsorption of F685.

The derivatives relative to each other, when changing different LEDs, do not differ substantially as a consequence of neither the light intensity nor the light spectrum. It is interpreted as, independently of the operating point (in the interval investigated) the same actions are needed to approach the optimal spectrum. Per incident photon flux, $\partial F740/\partial I_i$ is highest for LED 630 (red) and lowest for LED 530 (green) (see Figure 10 a,b). This is in line with the

result and conclusion from experiment *A*, i.e. changing cultivar and adding background light did not change the order of the derivatives. However, in this data there is one operating point above $500\,\mu mol\,m^{-2}\,s^{-1}$(see Figure 10 a), for which there is no significant difference in $\partial F740/\partial I_i$ when changing LED 420, 450 or 530.

If taken into consideration that energy content is dependent on wavelength (see Figure 10 c,d), LED 630 gives rise to a significantly higher fluorescence gain, while the other three diode groups have lower and similar gains. In the third row of plots the efficiencies of the different diode groups are taken into consideration. Same as in experiment *A*, fluorescence gain is highest (and about equal) for LED 630 and 450 (red and blue) and lowest for LED 530 (green).

3.3 *(C)* High intensity background light

These experiments were conducted as a complement to *Experiment (B)* to investigate possible differences as the light intensity was further increased. The results are combined with the data from *Experiment (B)*. To be able to compare different sets of experiments normalization is needed since the level of the fluorescence (and consequently also its derivative) depends on the amount of biomass, the distance to the spectrometer etc. Figure 11 shows the level of fluorescence for *Experiment (B)* and *(C)* where the three lowest light intensity levels from *Experiment (C)*, having the same magnitude as in *Experiment (B)*, have been used for normalization. As a result, all F740 values for *Experiment (C)* were multiplied by a factor (2.13) in order to get in the same region as in *Experiment (B)*.

In Figure 12 the fluorescence gains versus incident photon flux for this experiment, together with the data from *Experiment (B)*, are shown. The gains do not continue to increase for the highest light intensities. We also note that the gain remains highest for LED 630. For light intensities lower than $500\,\mu mol\,m^{-2}\,s^{-1}$ LED 530 generates the lowest gain but for higher light intensities LED 530 has increased relative to the others and there is no significant difference in the fluorescence gains for LED 420, 450 and 530.

The data set includes light intensities expected to saturate photosynthesis. Based on light response curves on leaf level (see Figure 4), the plants move from light limitation to light saturation at around $800\,\mu mol\,m^{-2}\,s^{-1}$, which indeed coincides with the transition from increasing to decreasing fluorescence gains. This relationship has been reported by others [31] and is included in models of leaf chlorophyll fluorescence [27], [34]. The decline in fluorescence emission efficiency has been correlated with an increase in non-photochemical

Predominantly red background light *Predominantly blue background light*

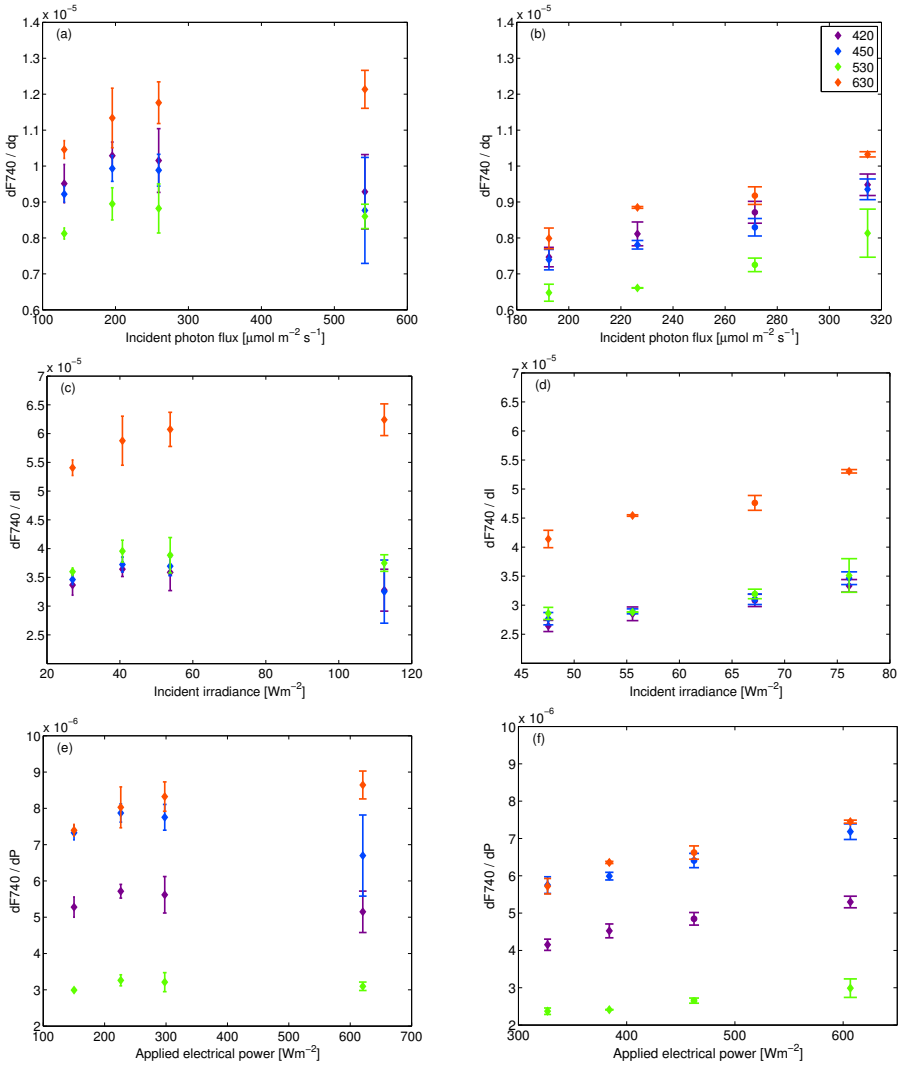

Figure 10: Fluorescence gains in *Experiment (B)*. Left column: Predominantly red background light (B:R 1:3). Right column: Predominantly blue background light (B:R 3:1). (a,b) $\partial F740/dq_i$ vs. incident photon flux q, (c,d) $\partial F740/dI_i$ vs. incident irradiance I and (e,f) $\partial F740/dP_i$ vs. applied electrical power P. The bars indicates ± 1 standard deviation.

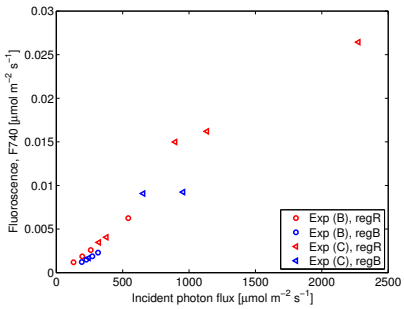

Figure 11: F740 vs incident photon flux at the operating points in *Experiment (B)* (circles) and *Experiment (C)* (triangles). The colour indicates whether predominantly red or blue background light have been used.

Predominantly red background light

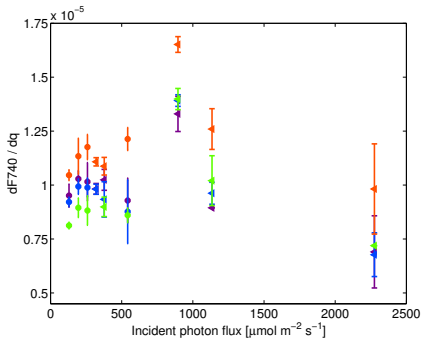

(a) *Experiment (B)*, circles, 4 operating points and *Experiment (C)*, triangles, 5 operating points.

Predominantly blue background light

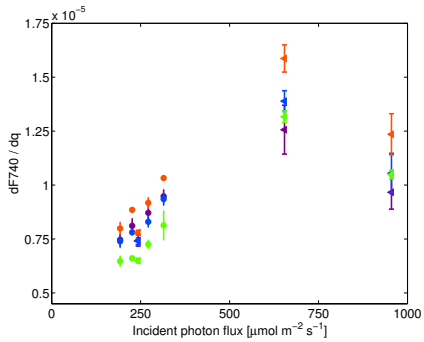

(b) *Experiment (B)*, circles, 4 operating points and *Experiment (C)*, triangles, 3 operating points.

Figure 12: The fluorescence gains vs. incident photon flux, for (a) predominately red background light and (b) predominately blue background light. The same information as in Figure 10a,b (i.e. the circles which are from *Experiment (B)*) with added information from *Experiment (C)*, i.e. the triangles. The bars indicates ±1 standard deviation.

quenching (NPQ), often attributed to reactions of the xantophyll cycle [35], [36]. However, the exact mechanisms of NPQ is still an area of active research. In simple and general terms, under low light most of the absorbed light energy is dissipated through photochemical quenching and with increasing irradiance the yield of photosynthesis decreases while the yield of fluorescence increases [20], [27]. Moving to high irradiance levels dissipation of excess energy through NPQ kicks in and the yields of the other two de-excitation pathways decrease. Further on, the peak in fluorescence yield seems to correlate with light saturation of photosynthesis [31]. Our data suggests that this is indeed the case also on canopy level. A weakness in our measurements, however, is that the temperature in the unit increased significantly at the highest irradiance levels and heat stress has been shown to decrease fluorescence yield, as well as photosynthetic yield [37]. Thus, it is not possible to disentangle the effect of high light and high temperature on fluorescence yield at the highest irradiance levels, but it is likely to be synergistic [36]. Zeaxanthin formation in the xantophyll cycle (de-epoxidation), which increases NPQ and has been linked to both light saturation and high temperature [38], is probably one of the mechanisms involved. Interestingly, the fluorescence at high irradiances are affected by other stressors as well, most commonly by a decline in fluorescence yield [37]. Also, the irradiance at which the peak in fluorescence yield occurs decreases with increasing stress [25], [27]. As such, measurements of the fluorescence gain parameter, as described in this paper, can potentially be used to derive the light saturation point and/or identify plant stress on canopy level.

4 Conclusions and Future work

In this study we have investigated the possibility of using remotely sensed fluorescence (gain) as a feedback signal for energy optimizing the spectrum of a LED lamp w.r.t. short term photosynthetic rate in basil.

With experiments using one LED group at a time (*Experiment (A)*) we have shown that for the considered light intensities (0–350 µmol m^{-2} s^{-1}) there is a strong and nearly linear correlation between steady-state fluorescence around 740 nm, F740, and photosynthetic rate, PN, for basil plants (see Figure 6). This indicates that F740 can be used as a relative measure of PN for the investigated light intensities. More experiments are needed to characterize the relationship in more detail, including photosynthesis measurements on canopy level, light saturating conditions as well as different levels and types of plant stress.

For a given incident photon flux, the short term photosynthetic rate was

not very sensitive to which LED group that was used. But some variations were indeed noted and the relative gains did change somewhat as the intensities varied (see Figures 7 and 8). For a given incident irradiance (W/m^2) though, the differences were more significant. LED 630 (having the longest wavelength) is the most efficient, since an energy quanta contains more photons the longer the wavelength. When including the efficiencies of the different diodes in the analysis, which is the relevant quantity for minimizing the energy consumption, LED 450 and 630 were found to be equally efficient in driving photosynthesis (see Figure 9).

Experiments with different background light show that the fluorescence gains $\partial F740/\partial P_i$ are not substantially affected by neither the background spectra considered (B:R ratio 1:3 and 3:1) nor the light intensity. The only significant shift noted, was when the total incident light exceeded 500 $\mu mol\, m^{-2}\, s^{-1}$. The fluorescence gain, $\partial F740/\partial q$, for green LEDs (530 nm) was then slightly increased relative to the others, resulting in similar gains for LED 420, 450 and 530, though still lower than for LED 630 (see Figure 12).

These experiments suggest that the fluorescence gains could be used to find optimal spectrum in terms of maximizing photosynthetic rate for a given applied electrical power; but since the relation between the fluorescence gains seems to be rather static with respect to light intensity and spectrum (see Figure 10e and f) an online controller might be unnecessary for optimizing the power split to the different diodes. Note, however, that this conclusion is based on, and limited to, measurements of short term changes in photosynthesis on leaf level (and fluorescence on canopy level) of healthy basil plants grown under low to moderate light intensities. It could be interesting to investigate other operating conditions in future work. Under the studied conditions the controller would increase LED 450 and 630 until they saturate. If higher light intensity is needed it would provide light from LED 420 and only turn on LED 530 if all the others were already saturated. This indicates that specified bounds of the spectrum to ensure healthy and morphologically well developed plants need to be determined beforehand. Instead of having an online controller, it should be possible to use this method for calibrating the spectrum to different plant species and to identify if and how the efficiencies of the diodes change relative to each other over time, or as a function of different operating conditions.

Data from the high intensity background light experiment show that there is a transition from increasing to decreasing fluorescence gains around the light saturation point of photosynthesis, and with support from the literature we speculate that the method can potentially also be used for finding the optimal light level as well as identify stress on canopy level. However, the applicability

of the method for this purpose needs to be investigated further; it was not an objective in this study.

References

[1] Eurostat. (2015). Crops under glass: Number of farms and areas by agricultural size of farm (uaa) and size of crops under glass area. Retrieved: 2015/04/24, Eurostat, [Online]. Available: `http://ec.europa.eu/`.

[2] I. Christensen and G. Larsson, "Energianvändning i trädgårdsnäringen", Grön Kompetens, Tech. Rep. Jordbruksverket Jo 2009/1596, 2010.

[3] J. Persson, "Energianvändning i växthus 2011. tomat, gurka och prydnadsväxter", Jordbruksverket, Tech. Rep. Statistikrapport 2012:05, 2012.

[4] C. Stenberg, "Trädgårdsproduktion 2011, korrigerad version", Jordbruksverket, Tech. Rep. JO 33 SM 1201, 2012.

[5] D. Singh, C. Basu, M. Meinhardt-Wollweber, and B. Roth, "Leds for energy efficient greenhouse lighting", *Renewable & Sustainable Energy Reviews*, vol. 49, pp. 139–147, 2015, Singh, Devesh Basu, Chandrajit Meinhardt-Wollweber, Merve Roth, Bernhard.

[6] A.-M. Carstensen, T. Pocock, D. Bånkestad, and T. Wik, "Remote detection of light tolerance in basil through frequency and transient analysis of light induced fluorescence", *Computers and Electronics in Agriculture*, vol. 127, pp. 289–301, 2016.

[7] M. W. van Iersel, G. Weaver, M. T. Martin, R. S. Ferrarezi, E. Mattos, and M. Haidekker, "A chlorophyll fluorescence-based biofeedback system to control photosynthetic lighting in controlled environment agriculture", *Journal of the American Society for Horticultural Science*, vol. 141, no. 2, pp. 169–176, 2016.

[8] D. Bånkestad and T. Wik, "Growth tracking of basil by proximal remote sensing of chlorophyll fluorescence in growth chamber and greenhouse environments", *Computers and Electronics in Agriculture*, vol. 128, pp. 77–86, 2016.

[9] K. J. McCree, "Action spectrum, absorptance and quantum yield of photosynthesis in crop plants", *Agricultural Meteorology*, vol. 9, pp. 191–216, 1972.

[10] K. Inada, "Action spectra for photosynthesis in higher plants", *Plant and Cell Physiology*, vol. 17, no. 2, pp. 355–365, 1976.

[11] R. Emerson, “Dependence of yield of photosynthesis in long-wave red on wavelength and intensity of supplementary light”, *Science (American Association for the Advancement of Science)*, vol. 125, p. 746, 3251 1957.

[12] R. Paradiso, E. Meinen, J. F. H. Snel, P. De Visser, W. Van Ieperen, S. W. Hogewoning, and L. F. M. Marcelis, “Spectral dependence of photosynthesis and light absorptance in single leaves and canopy in rose”, *Scientia Horticulturae*, vol. 127, no. 4, pp. 548–554, 2011.

[13] T. Ouzounis, X. Frette, C. O. Ottosen, and E. Rosenqvist, “Spectral effects of leds on chlorophyll fluorescence and pigmentation in phalaenopsis "vivien’ and "purple star’”, *Physiologia Plantarum*, vol. 154, no. 2, pp. 314–327, 2015, Ouzounis, Theoharis Frette, Xavier Ottosen, Carl-Otto Rosenqvist, Eva 1399-3054.

[14] K. R. Cope, M. C. Snowden, and B. Bugbee, “Photobiological interactions of blue light and photosynthetic photon flux: Effects of monochromatic and broad-spectrum light sources”, *Photochemistry and Photobiology*, vol. 90, no. 3, pp. 574–584, 2014.

[15] G. D. Massa, H.-H. Kim, R. M. Wheeler, and C. A. Mitchell, “Plant productivity in response to led lighting”, *HortScience*, vol. 43, no. 7, pp. 1951–1956, 2008.

[16] H.-H. Kim, G. D. Goins, R. M. Wheeler, and J. C. Sager, “Green-light supplementation for enhanced lettuce growth under red- and blue-light-emitting diodes”, *HortScience*, vol. 39, no. 7, pp. 1617–1622, 2004.

[17] T. A. O. Dougher and B. Bugbee, “Differences in the response of wheat, soybean and lettuce to reduced blue radiation”, *Photochemistry and Photobiology*, vol. 73, no. 2, pp. 199–207, 2001.

[18] R. Hernandez and C. Kubota, “Tomato seedling growth and morphological responses to supplemental led lighting red:blue ratios under varied daily solar light integrals”, *Acta Horticulturae*, vol. 956, pp. 187–194, 2012.

[19] ——, “Growth and morphological response of cucumber seedlings to supplemental red and blue photon flux ratios under varied solar daily light integrals”, *Scientia Horticulturae*, vol. 173, pp. 92–99, 2014.

[20] K. Maxwell and G. N. Johnson, “Chlorophyll fluorescence - a practical guide”, *Journal of Experimental Botany*, vol. 51, no. 345, pp. 659–668, 2000.

[21] A. Porcar-Castell, E. Tyystjarvi, J. Atherton, C. van der Tol, J. Flexas, E. E. Pfundel, J. Moreno, C. Frankenberg, and J. A. Berry, "Linking chlorophyll a fluorescence to photosynthesis for remote sensing applications: Mechanisms and challenges", *Journal of Experimental Botany*, vol. 65, no. 15, pp. 4065–4095, 2014.

[22] G. C. Papageorgiou and Govindjee, Eds., *Chlorophyll a Fluorescence A Signature of Photosynthesis*. Springer, 2004, vol. 19.

[23] A. A. Gitelson, C. Buschmann, and H. K. Lichtenthaler, "Leaf chlorophyll fluorescence corrected for re-absorption by means of absorption and reflectance measurements", *Journal of Plant Physiology*, vol. 152, no. 2-3, pp. 283–296, 1998.

[24] C. Buschmann, "Variability and application of the chlorophyll fluorescence emission ratio red/far-red of leaves", English, *Photosynthesis Research*, vol. 92, no. 2, pp. 261–271, 2007.

[25] J. Flexas, J. M. Escalona, S. Evain, J. Gulías, I. Moya, C. B. Osmond, and H. Medrano, "Steady-state chlorophyll fluorescence (Fs) measurements as a tool to follow variations of net CO_2 assimilation and stomatal conductance during water-stress in C_3 plants", *Physiologia Plantarum*, vol. 114, pp. 231–240, 2002.

[26] L. Guanter, Y. Zhang, M. Jung, J. Joiner, M. Voigt, J. A. Berry, C. Frankenberg, A. R. Huete, P. Zarco-Tejada, J.-E. Lee, M. S. Moran, G. Ponce-Campos, C. Beer, G. Camps-Valls, N. Buchmann, D. Gianelle, K. Klumpp, A. Cescatti, J. M. Baker, and T. J. Griffis, "Reply to magnani et al.: Linking large-scale chlorophyll fluorescence observations with cropland gross primary production", *Proceedings of the National Academy of Sciences*, vol. 111, no. 25, E2511, 2014.

[27] C. van der Tol, W. Verhoef, and A. Rosema, "A model for chlorophyll fluorescence and photosynthesis at leaf scale", *Agricultural and Forest Meteorology*, vol. 149, no. 1, pp. 96–105, 2009.

[28] O. Trollberg, B. Carlsson, and E. W. Jacobsen, "Extremum seeking control of the canon process - existence of multiple stationary solutions", *Journal of Process Control*, vol. 24, no. 2, pp. 348–356, 2014.

[29] S. Skogestad, "Self-optimizing control: The missing link between steady-state optimization and control", *Computers and Chemical Engineering*, vol. 24, pp. 569–575, 2000.

[30] T. Wik, A. Carstensen, and T. Pocock, *Spectrum optimization for artificial illumination*, WO Patent App. PCT/EP2013/069,820, 2014.

[31] C. Van Der Tol, J. A. Berry, P. K. E. Campbell, and U. Rascher, "Models of fluorescence and photosynthesis for interpreting measurements of solar-induced chlorophyll fluorescence", vol. 119, no. 12, pp. 2312–2327, 2014.

[32] S. Eberhard, G. Finazzi, and F.-A. Wollman, *The dynamics of photosynthesis*, 2008.

[33] R. G. Walters, "Towards an understanding of photosynthetic acclimation", *Journal of Experimental Botany*, vol. 56, no. 411, pp. 435–447, 2005.

[34] N. Vilfan, C. van der Tol, O. Muller, U. Rascher, and W. Verhoef, "Fluspect-b: A model for leaf fluorescence, reflectance and transmittance spectra", vol. 186, pp. 596–615, 2016.

[35] B. Demmig-Adams and W. W. Adams, "Photoprotection and other responses of plants to high light stress", *Annu. Rev. Plant. Physiol. Plant. Mol. Biol.*, vol. 43, no. 1, pp. 599–626, 1992.

[36] A. Rosema, J. F. H. Snel, H. Zahn, W. F. Buurmeijer, and L. W. A. Van Hove, "The relation between laser-induced chlorophyll fluorescence and photosynthesis", *Remote Sensing of Environment*, vol. 65, no. 2, pp. 143–154, 1998.

[37] A. Ač, Z. Malenovský, J. Olejníčková, A. Gallé, U. Rascher, and G. Mohammed, "Meta-analysis assessing potential of steady-state chlorophyll fluorescence for remote sensing detection of plant water, temperature and nitrogen stress", *Remote Sensing of Environment*, vol. 168, pp. 420–436, 2015.

[38] A. M. Gilmore and H. Y. Yamamoto, "Dark induction of zeaxanthin-dependent nonphotochemical fluorescence quenching mediated by atp.", *Proceedings of the National Academy of Sciences of the United States of America*, vol. 89, no. 5, pp. 1899–1903, 1992.

PAPER B

LED spectrum optimisation using steady-state fluorescence gains

Linnéa Ahlman, Daniel Bånkestad, Torsten Wik

Acta Horticulturae,
vol. 1134, pp. 367-374, 2016

The layout has been revised.

Abstract

The use of light emitting diodes (LEDs) in greenhouses entails the possibility to control the light in a better way, since both spectrum and light intensity can be adjusted. We aim at developing a method to automatically find the optimal spectrum in terms of energy consumption and plant growth. Previous work shows that chlorophyll fluorescence (ChlF) at 740 nm strongly correlates with the photosynthetic rate (carbon dioxide uptake rate) and that the net efficiency of a LED group therefore is coupled to the fluorescence gain w.r.t. energy consumption, i.e. the slope of a curve depicting steady-state ChlF versus applied power to the LED group. In the present work we compare the fluorescence gains for six different LED types (wavelength peaks from 400 to 660 nm) and six different species: tomato, cucumber, basil, lettuce (two species) and dill. We also compare two different kinds of experiments: steady-state experiment, waiting for the fluorescence to reach a steady state at a few incident light intensities, and ramp experiment, where the light intensity is increased slowly. The ramp experiment gives essentially the same information as the steady-state experiment, but was found to slightly overestimating the gains of the blue LEDs. Being aware of this, it should be possible to initially use the faster (ramp) method in order to find the right light composition, possibly using steady-state experiments for a fewer LEDs in order to tune the lamp. The relative order of the fluorescence gains among the tested LED groups is similar, but not identical, for all species tested. LED 660 has the highest fluorescence gain per incident photon, and LED 400 and/or LED 530 has the lowest. However, the important quantity is in fact the fluorescence gain per applied electrical power. If the individual electrical efficiencies of the LEDs change the most efficient power split on the different LEDs might change.
Keywords: optimal light spectrum, light emitting diode (LED), fluorescence gain, chlorophyll fluorescence, photosynthesis, greenhouse illumination

1 Introduction

The illumination in greenhouses is dominated by high pressure sodium (HPS) lamps that are generally controlled manually by on/off control. Changing to light emitting diodes (LEDs) entails an energy saving potential [1], due to higher electrical efficiency of many LEDs compared to HPS lamps. Combining different LEDs, also enables control of the spectral distribution of the light, which could potentially reduce the energy further. Many studies have been conducted that investigates the spectral effect on plant growth, commonly by comparing the impact that various light sources, and in particular their ratio among blue, green, and red light, have on the growth of different plant species during their life cycles, e.g., [2]–[6]. There are also a few studies on the use of LEDs as supplement to sunlight in greenhouses [7], [8].

The energy optimal split of the applied power on the different LED colours could possibly depend on a number of factors, such as plant species, required characteristics of the plant, available LED groups and their electrical efficiency. The aim of the work presented here is to automatically find the optimal spectrum based on a remote measure of growth. The idea is that for the specific crop being cultivated, bounds on the ratios of different colours (for example between blue, green and red wavelengths) have been specified to guarantee morphologically healthy and high producing plants. However, within these bounds we aim to use the power split that maximizes the growth for a given applied electrical power P_{tot} (Figure 1). In order to do so, a measure of the growth rate on canopy level is needed. Here, we have focused on finding an indirect proxy marker for photosynthesis by measuring chlorophyll fluorescence (ChlF).

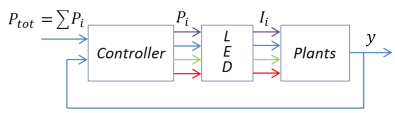

Figure 1: A schematic picture of our aim; developing a method too automatically find the energy optimal split of the applied power P_{tot} among the available LED groups. The fluorescence gain (i.e. the slope of a curve depicting steady-state ChlF versus applied power) is the candidate signal (y) to be used in the feedback loop.

In a previous study on basil [9] the potential of using top-of-canopy steady-state ChlF at 740 nm as a measure of growth rate was investigated. Although the relationship between ChlF and photosynthesis is complex in general, and the ChlF signal is convoluted by structure on a canopy level, a strong nearly

linear relationship between steady-state ChlF and photosynthesis (measured as carbon dioxide uptake on leaf-level) was observed on healthy plants subject to a large number of PAR light intensities (Figure 2). This simple relationship may be attributed to the correlation between ChlF and absorbed PAR, which in turn is closely related to photosynthesis in healthy plants, as has been discussed by others [10]. As a consequence of this relation Ahlman *et al.* [9] and Wik *et al.* [11] showed that the (short term) efficiency of one LED group relative to another is directly related to the fluorescence gain, i.e., the slope of a curve depicting steady-state ChlF versus the applied power to the LED group. The intuitive interpretation is that if you want to increase the lamp power you should use the LEDs that increase the steady-state ChlF the most. Conversely, if the lamp power is to be decreased one should decrease the power to the group that decreases the fluorescence the least.

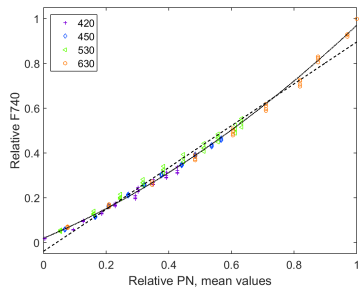

Figure 2: The relative fluorescence at 740 nm (F740) versus the relative photosynthetic rate (PN), i.e., CO_2 uptake rate, measured by an infrared gas analyser on leaf-level. One LED group was used at a time, with light intensities up to 350 µmol m^{-2} s^{-1}. Dashed line shows a first order curve fit ($R^2 = 0.982$) and the solid line shows a second order curve fit ($R^2 = 0.996$). Data from Ahlman *et al.* [9].

In the investigation by Ahlman *et al.* [9] red photons were found to be best in terms of photosynthetic efficiency (mol CO_2/mol incident photons), but after taking the photon efficiencies of the LEDs (ratio of photon flux to electrical power) into account some blue LEDs were equally efficient as the red LEDs. It was also found that the photosynthetic efficiency depended on the light intensity to some extent. Since the photon efficiency changes with temperature and age, remotely sensed ChlF could potentially be used to calibrate a lamp to optimal photosynthetic efficiency (within the ratio-bounds specified for the plant). In order to assess the potential use, a number of different plant species have now been investigated, namely tomato, cucumber, basil, lettuce (two types) and dill.

Using a lamp equipped with multiple LED groups the ChlF gain was measured for six different colours ranging from 400 to 660 nm (peak wavelength). For a calibration to be conducted within reasonable time, a fairly short time can be spent on determining the gain of each LED colour, which means that the steady-state fluorescence can normally only be determined for a few light levels. Since it was found that the gain changes somewhat with intensity, and possibly to the extent that the order of the LEDs in terms of efficiency may change, it is desirable to have more densely gridded information. Therefore, the possibility to use the ChlF when each LED colour is slowly ramped, instead of steady-state ChlF for a few intensities, was also investigated.

The main outcome of this investigation is that the results are similar, but not identical, for all species tested. LED 660 has the highest gain per incident photon and LED 400 and/or LED 530 has the lowest. However, it has to be kept in mind that the relevant quantity is in fact the gain per applied electrical power, which is highest for LED 660 followed by LED 450 and LED420. Using ramp experiment instead of steady-state experiment seems to slightly overestimate the efficiency of blue LEDs (or underestimate red ones).

2 Materials and methods

2.1 Plant species and growth conditions

A number of species were studied, tomato (*Solanum lycopersicum* F1 'Lizzano'), cucumber (*Cucumis sativus* F1 'Max'), basil (*Ocimum basilicum* 'Aroma 2'), two types of lettuce (*Lactuva sativa* 'Black seeded Simpson' and 'Galiano') and dill (*Anethum graveolens* 'Ella'). All plants were grown in a controlled environment (16 h photoperiod and 23/17 $^{\circ}C$ day/night temperatures) at Heliospectra Plant Lab under LED lamps (LX602G, Heliospectra, Sweden), having three diode types; blue (450 nm), red (660 nm) and white (5700 K), and the light intensity at plant level was set to 280 µmol m^{-2} s^{-1} photosynthetic photon flux density (PPFD) for tomato, and 160 µmol m^{-2} s^{-1} for the others. The light spectrum contained approximately 20% blue (400–500 nm), 10% green (500–600 nm) and 70% red (600–700 nm) light. Most of the samples were grown under other, but similar, light in the beginning of their growth cycles.

The experiments were conducted 3–6 weeks after seeding, except for tomatoes which were almost four months old.

2.2 Experimental unit

All experiments were carried out in an experimental unit, 0.5 x 0.7 m, delimited with reflective curtains (silver/white Diamond Diffusion Foil, Easy Grow, UK). Two LED lamps (RX30 Heliospectra, Sweden) were placed above the experimental unit. Six different LED groups were used, having peak wavelengths at about: 400, 420, 450, 530, 620, 660 nm (Figure 3), and relative photon efficiencies (photons per applied electrical energy) of: 0.38, 0.60, 0.66, 0.27, 0.26, and 1.00, respectively, at maximum intensity of the individual LED groups.

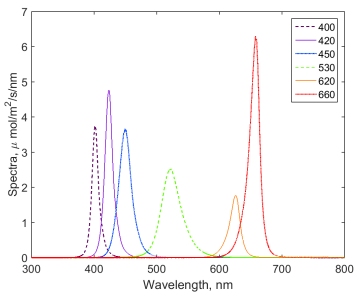

Figure 3: Incident light spectra, using one of the six LED groups at a time. In the analysis the incident light has been integrated from 350 to 700 nm, in order to capture all light.

The light was detected by two spectrometers, (Maya 2000 Pro Spectrometer, Ocean Optics, US), each equipped with a 600 µm optical fibre. One was placed at canopy level, measuring the incident light, and having a cosine diffuser giving a field of view of 180°. The distance from the lamp to the canopy level was approximately 0.5 m, but differed slightly depending on plant size. For the tomato, which was significantly higher than the other plants, the height of the experimental unit was modified to retain the same distance between lamp and canopy. The other spectrometer was placed between the lamps and facing the plants to detect the fluorescence signal. In order to only measure green area, the field of view was delimited to about 25°.

The temperature throughout the experiments was 23 ±1°C (measured in the luminaire), except for when LED 530 was used, the temperature then increased 2 °C due to the lower electrical efficiency of those LEDs.

2.3 Light scheme

During one experiment all six LED groups were used, one at a time, starting with LED 400 and continuing in the order of increasing peak wavelength. Two different kinds of experiments were tested, steady-state experiments and ramp experiments. In the first set of experiments each light level was held for 9 min, in order to reach (close to) steady-state fluorescence. Three light intensity levels (in increasing order; based on the capacity of the specific LED group; shown in Figure 4) were tested for each LED group. The second set of experiments (conducted on all plant species except lettuce 'Galiano' and dill) aimed at investigating if the same information (differences in fluorescence and fluorescence gains between the different LED groups) could be found without awaiting steady-state. The light was then held at a constant low level for 2 min, whereupon the light was slowly increased during 2.5 min, while the fluorescence and the incident light were measured at 25 different light intensity levels in total. The range spanned by the ramp was normally around 80 µmol m^{-2} s^{-1}, but differed depending on the capacities of the LEDs (from 35 µmol m^{-2} s^{-1} for LED 630, to 140 µmol m^{-2} s^{-1} for LED 660; see Figure 4).

2.4 Data processing

In the analysis the incident light, measured in µmol m^{-2} s^{-1}, has been integrated from 350 to 700 nm, in order to capture all light energy, including the LED having peak wavelength at 400 nm (Figure 3). The fluorescence signal, also measured in µmol m^{-2} s^{-1}, is the integral over the peak from 735 to 745 nm.

After one experiment, the plants were moved from the experimental unit in order to make room for the next plant species. The steady-state and ramp experiments for each species were done with a maximum of one day in between.

In order to compare experiments (between species and also experiments on the same species performed on different occasions), the signal needs to be normalized, since the fluorescence signal is sensitive to for example the distance between plant and spectrometer, and to the geometry of the plants. All values in one experiment were therefore normalized with the same factor so that the fluorescence gain for LED 660 equals one for the case when a straight line was fitted by least squares to the data. When a polynomial of degree two was fitted to the data (only for ramp experiments), the fluorescence gains varied with light intensity, and the normalization was done so that the mean value of the fluorescence gain for LED 660 equals one.

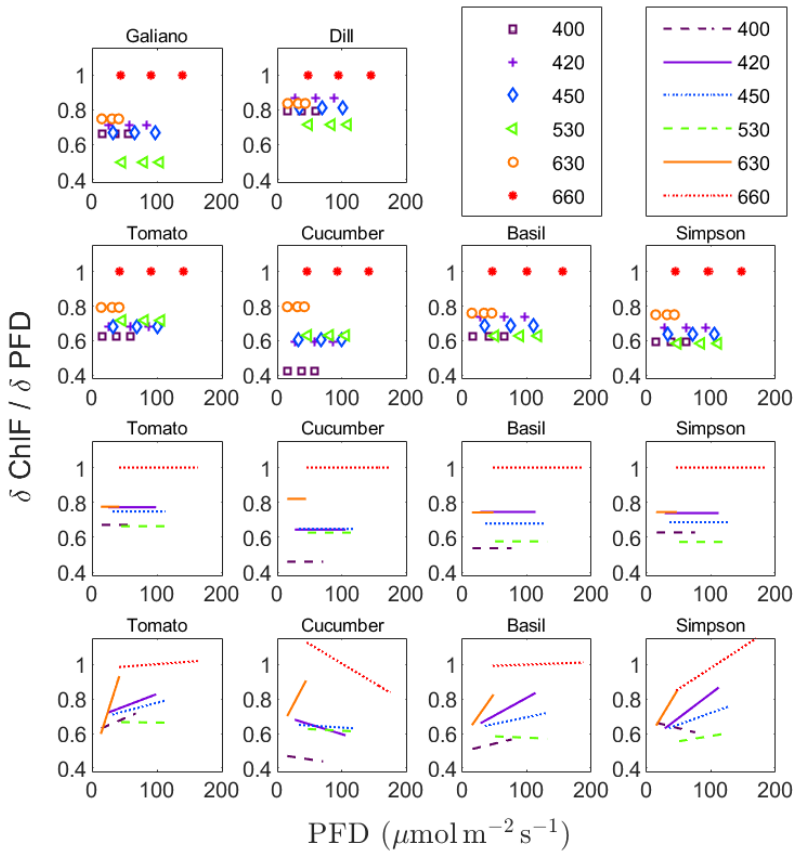

Figure 4: Normalized fluorescence gains w.r.t. PFD, i.e. the slope of steady-state ChlF (photon flux integrated from 735 to 745 nm) to incident PFD, versus incident PFD integrated from 350 to 700 nm. Steady-state experiments are presented in the first two rows. The fluorescence measured for three incident light intensity level for each LED group and the gains are calculated from a line fitted to the data. Results from the ramp experiments are presented in row three and four; first the gain when a first order polynomial is fitted to the data (row 3; $R^2_{adj} > 0.99$) and then when a second order polynomial is fitted to the data (row 4; $R^2_{adj} > 0.99$). Each set is normalized such that the mean value of the fluorescence gain is maximum 1 (always maximum for LED 660).

3 Results and discussion

3.1 Steady-state experiment

For all species tested, LED 660 gives the significantly highest fluorescence gain w.r.t. incident photon flux density (PFD) compared to the others (Figure 4, first and second row). LED 630 gives the second highest gain for all species except for dill, where it is on par with the blue LEDs. Next is LED 420, closely followed by LED 450, and the least efficient of the blue ones is LED 400. For dill and lettuce 'Galiano', LED 530 gives the lowest gain, while for cucumber and tomato LED 530 performs slightly better than all the three blue LEDs. For lettuce 'Simpson' and basil, LED 400 and LED 530 have the same (and the lowest) gain.

This is essentially similar to the spectral effect of CO_2 uptake that McCree measured on small leaf sections of 22 different plant species [12]. One peak was noted in the red light region and a second, normally a bit lower, peak in the blue light region. Depending on species the peak varied, both spectrally and in relative intensity. The distinct difference between the two red diodes (LED 660 and LED 630) observed in our experiments, could, however, not have been predicted by looking at McCree's results.

The largest relative differences in gains are observed for cucumber. After LED 660, LED 630 had the highest significantly gain and LED 400 the lowest. For all other species the five LED gains (LED 660 not counted) are fairly close to each other. This means that per incident photon the differences in output (fluorescence or photosynthetic rate) are small for all species tested. This indicates that differences in photon efficiencies, from applied power to photon flux, are crucial when aiming for the highest photosynthetic rate for a given applied power, which is confirmed in Figure 5 showing that LED 660 followed by LED 450 and LED 420 have the significantly highest gains w.r.t. electrical power.

3.2 Ramp experiment

First order polynomial fit

Measuring the fluorescence and fluorescence gains without awaiting steady-state, (but slowly increase the light intensity, see Figure 4, third row) gives essentially the same results as the steady-state experiments. LED 660 still has the highest fluorescence gains for all species tested (lettuce 'Galiano' and dill were not included in this setup), the other LED gains are lower and closer to each other and LED 400 and/or LED 530 have the lowest gains.

Cucumber is still the species where the differences are most pronounced, with LED 630 higher, and LED 400 lower than the other blue and green ones. An interesting difference, though, between the steady-state experiment and the ramp experiment, is that in the latter one the three blue LEDs seem to be slightly overestimated compared to the others (or the red LEDs are underestimated), resulting in no difference in gains for LED 630 and LED 420 (except for cucumber).

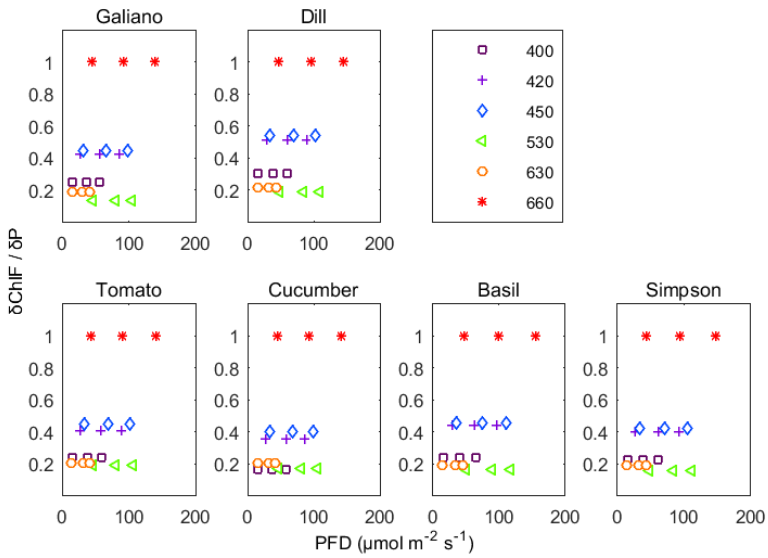

Figure 5: Normalized fluorescence gains w.r.t. applied electrical power as a function of PFD for the steady-state experiments. The fluorescence gains are calculated by multiplying the fluorescence gains w.r.t. PFD (Figure 4) with the photon efficiency of each LED group, respectively. The photon efficiency was measured at maximum intensity of the LED group and is assumed to be constant.

Second order polynomial fit

An advantage with measuring the output at several different light intensities (in the ramp experiments the fluorescence was measured at 25 light intensity levels, compared to three levels for steady-state experiments), is that it allows a fit of a model of higher order. The 4th row in Figure 4 shows the fluorescence gains from the ramp experiments, when a second order polynomial is fitted to the data.

As can be seen, some of the gains intersect with each other. The corresponding intensity levels can be interpreted as levels where the relative efficiency of the LEDs changes order. For example, for tomatoes the gain for LED 420 and LED 630 intersect at approximately $20\,\mu mol\,m^{-2}\,s^{-1}$, indicating that LED 420 may be more efficient than LED 630 below that intensity level. Note that including the specific photon efficiency of each LED group in the analysis will change both the magnitude and the slope of the individual gains such that the levels of intersection also may change (not included here).

Intersection of the fluorescence gains of the three blue LEDs (400, 420 and 450), which are obtained for some of the sets, indicates that even for a predefined blue to red ratio, the optimal power split within the blue LEDs differ depending on the light intensity.

The slope of the gain for LED 630 is significantly higher than for LED 660, indicating that (if the gains can be extrapolated) for high light intensity LED 630 could be more efficient than LED 660. Though, it cannot be precluded that part of the reason for the different shapes, is that the incident light for LED 630 and LED 660 differ significantly, up to about $45\,\mu mol\,m^{-2}\,s^{-1}$ for LED 630, and only above that for LED 660.

4 Conclusion

For all plant species investigated, i.e. tomato (*Lizzano*), cucumber (*F1 'Max'*), basil (*Aroma 2*), lettuce (*Black Seeded Simpsons* and *Galiano*) and dill (*Ella*), the fluorescence gain w.r.t. incident PFD was highest using LED 660. For the other five LEDs (400, 420, 450, 530 and 630) the differences were smaller but LED 400 or LED 530 were always lowest, which is not surprising considering that part of the LED 400 spectrum is outside the normal PAR range and the dip in quantum yield and absorbance in the green waveband [12]. Cucumber is the species having the largest differences in the fluorescence gains. Notice, though, that in terms of overall efficiency the relevant quantity is the fluorescence gain w.r.t. applied electrical power, which was highest for LED 660 followed by LED 450 and LED 420 as these LEDs are the most efficient in the lamp being used. If the electrical efficiency of the individual LEDs changes, due to for example different operating conditions or degradation over time, the result might differ.

Slowly increasing the light intensity and measuring the fluorescence increase (ramp experiment) gives essentially the same relative gains as if awaiting steady-state for a few light intensity levels. One difference noted, though, was that the ramping tends to slightly overestimate the output from the blue

LEDs. Having several measurements allows a fit of a curve of higher order (second order polynomial fit was tested for ramp experiments), giving fluorescence gains that varies with intensity level. The results indicate that depending on light intensity level the optimal power split might vary.

The experimental time differed significantly between the two types of experiments; the ramp experiment took only 1/6 of the time for the steady-state experiment. One needs to be aware of the slight difference in result that did exist, but the time saving would probably justify the use of ramp experiments. Ideally, fast measurements (like ramp experiments) could be used to find an initial approximation of the optimal light at current conditions. Further steady-state experiments could then be used to tune the settings for LEDs having similar gains.

Ongoing research is carried out to investigate if the method and results can be translated to the situation where a combination of LEDs are being used.

5 Acknowledgements

The financial support for this work came from the program Mistra Innovation (within the Swedish Foundation for Strategic Environmental research). The authors are indebted to Julio César and Sina Soukhakian who wrote important parts of the software for the lamps.

References

[1] D. Singh, C. Basu, M. Meinhardt-Wollweber, and B. Roth, “Leds for energy efficient greenhouse lighting”, *Renewable & Sustainable Energy Reviews*, vol. 49, pp. 139–147, 2015, Singh, Devesh Basu, Chandrajit Meinhardt-Wollweber, Merve Roth, Bernhard.

[2] T. Ouzounis, X. Frette, C. O. Ottosen, and E. Rosenqvist, “Spectral effects of leds on chlorophyll fluorescence and pigmentation in phalaenopsis "vivien’ and "purple star’”, *Physiologia Plantarum*, vol. 154, no. 2, pp. 314–327, 2015, Ouzounis, Theoharis Frette, Xavier Ottosen, Carl-Otto Rosenqvist, Eva 1399-3054.

[3] K. R. Cope, M. C. Snowden, and B. Bugbee, “Photobiological interactions of blue light and photosynthetic photon flux: Effects of monochromatic and broad-spectrum light sources”, *Photochemistry and Photobiology*, vol. 90, no. 3, pp. 574–584, 2014.

[4] G. D. Massa, H.-H. Kim, R. M. Wheeler, and C. A. Mitchell, "Plant productivity in response to led lighting", *HortScience*, vol. 43, no. 7, pp. 1951–1956, 2008.

[5] H.-H. Kim, G. D. Goins, R. M. Wheeler, and J. C. Sager, "Green-light supplementation for enhanced lettuce growth under red- and blue-light-emitting diodes", *HortScience*, vol. 39, no. 7, pp. 1617–1622, 2004.

[6] T. A. O. Dougher and B. Bugbee, "Differences in the response of wheat, soybean and lettuce to reduced blue radiation", *Photochemistry and Photobiology*, vol. 73, no. 2, pp. 199–207, 2001.

[7] R. Hernandez and C. Kubota, "Tomato seedling growth and morphological responses to supplemental led lighting red:blue ratios under varied daily solar light integrals", *Acta Horticulturae*, vol. 956, pp. 187–194, 2012.

[8] ——, "Growth and morphological response of cucumber seedlings to supplemental red and blue photon flux ratios under varied solar daily light integrals", *Scientia Horticulturae*, vol. 173, pp. 92–99, 2014.

[9] L. Ahlman, D. Bånkestad, and T. Wik, "Using chlorophyll a fluorescence gains to optimize led light spectrum for short term photosynthesis", *Computers and Electronics in Agriculture*, vol. 142, no. Part A, pp. 224–234, 2017.

[10] L. Guanter, Y. Zhang, M. Jung, and J. Joiner, "Global and time-resolved monitoring of crop photosynthesis with chlorophyll fluorescence", *Proceedings of the National Academy of Sciences*, pp. 1327–1333, 2014.

[11] T. Wik, A. Carstensen, and T. Pocock, *Spectrum optimization for artificial illumination*, WO Patent App. PCT/EP2013/069,820, 2014.

[12] K. J. McCree, "Action spectrum, absorptance and quantum yield of photosynthesis in crop plants", *Agricultural Meteorology*, vol. 9, pp. 191–216, 1972.

PAPER C

Relation between changes in photosynthetic rate and changes in canopy level chlorophyll fluorescence generated by light excitation of different LED colours in various background light

Linnéa Ahlman, Daniel Bånkestad, Torsten Wik

Remote sensing,
vol. 11, no. 4:343, 2019

The layout has been revised.

Abstract

Using light emitting diodes (LEDs) for greenhouse illumination enables the use of automatic control, since both light quality and quantity can be tuned. Potential candidate signals when using biological feedback for light optimisation are steady-state chlorophyll a fluorescence gains at 740 nm, defined as the difference in steady-state fluorescence at 740 nm divided by the difference in incident light quanta caused by (a small) excitation of different LED colours. In this study, experiments were conducted under various background light (quality and quantity) to evaluate if these fluorescence gains change relative to each other. The light regimes investigated were intensities in the range 160–1000 µmol m^{-2} s^{-1}, and a spectral distribution ranging from 50% to 100% red light. No significant changes in the mutual relation of the fluorescence gains for the investigated LED colours (400, 420, 450, 530, 630 and 660 nm), could be observed when the background light quality was changed. However, changes were noticed as function of light quantity. When passing the photosynthesis saturate intensity level, no further changes in the mutual fluorescence gains could be observed.
Keywords: optimal light spectrum; greenhouse illumination; light emitting diode; chlorophyll fluorescence; fluorescence gain; photosynthesis

1 Introduction

Today, greenhouses are to a large extent automated [1]. There is climate control, stepwise movement of the plants from sowing area to the harvesting area, and automated irrigation and fertilisation. Traditionally though, high pressure sodium (HPS) lamps that are only controlled by switching them on or off are used. However, an increasing amount of growers are interested in using light emitting diodes (LEDs) for greenhouse illumination instead. One benefit with such a transition is the enabling of tuning both the light quality (spectrum) and quantity (intensity). The quality and quantity of light affect plant growth in many ways; it affects growth, such as biomass, leaf elongation and chlorophyll concentration, as well as metabolic effects, such as antioxidant potential or vitamin and nitrate concentrations. In general, UV-

light (280–400 nm) inhibits cell elongation and can cause sunburn, blue light (400–520 nm) enhances the photosynthesis, green light (520–610 nm) enhances photosynthesis but is to a larger extent (relative to blue and red) transmitted through, and reflected by, the leaves, red light (610–750 nm) enhances the photosynthesis and impacts the photoperiodism while far-red (750–1000 nm) stimulates cell elongation and influences flowering and germination (Table 8.1 in [2]). For a review of studies on light quality effects on plant growth we refer to Olle and Viršile [3] and Ouzounis *et al.* [4]. However, the question, "what specific spectrum and photon flux density is optimal for maximal productivity?", is still not easy to answer, since it depends on plant species, the ontogenesis stage, surrounding environment and how "maximal productivity" is defined. As an example, Snowden *et al.* [5] measured the sensitivity to blue light for a number of species including cucumber and lettuce. Increasing the amount of blue light did not significantly affect plant growth for lettuce. For cucumber on the other hand, the increased amount of blue light reduced growth (by 22%), but only if the total light intensity was high ($500\,\mu mol\,m^{-2}\,s^{-1}$) and not if it was low ($200\,\mu mol\,m^{-2}\,s^{-1}$).

One possible way of defining optimal light spectrum is the spectrum that increase photosynthesis the most. Already in 1937, Hoover [6] determined the rate of photosynthesis as a function of wavelength of the light (measured on a wheat plant), called the action spectrum, and concluded that there is a peak in red light wavelengths and a secondary one in blue. In the 1970s two large studies were conducted on leaves from 22 and 33 plant species, respectively, with the conclusion that the action spectra were similar (but not identical) for all species tested [7], [8]. However, the early action spectra were conducted on cut leaves illuminated with light with a wavelength span of 25 nm at a time. We propose firstly, that it cannot be ruled out that the results would differ if the measurements are made remotely on a canopy level. Secondly, it cannot be taken for granted that the results are identical in presence of background light. One example of the opposite is the "Emerson effect" [9]. He showed that the photosynthetic rate was higher when illuminating with red and far-red light (wavelengths lower and higher than 680 nm, respectively) in combination, compared to the sum of the photosynthetic rate when illuminate with either red or far-red light. This is due to the two photosystems in plants, which are activated by light of different wavelength.

If the plants have different spectral preferences depending on the current growth environment, one could in theory build a self-optimising controller, to find the optimal light spectrum for the current state, by using feedback control [10]. For such a scenario one needs a non-destructive biological growth signal that can be measured fast, remotely, and preferably without inter-

acting with the plants. We suggest chlorophyll fluorescence to be such a candidate. The main tools used for measuring and analyzing chlorophyll fluorescence are the pulse amplitude modulation fluorometer (PAM) developed by Schreiber [11] and the photosynthetic efficiency plant analyzer (PEA) developed by Strasser *et al.* [12]. The PAM measures the fluorescence response to short duration (micro second) light pulses and discriminates chlorophyll fluorescence induced by the excitation pulse from chlorophyll fluorescence induced by ambient light through synchronous detection. The actual yields of photochemistry and heat dissipation, respectively, are sorted out from the fluorescence signal by the so-called fluorescence quenching analysis [11]. The PEA measures the fluorescence rise during the first second of saturating illumination, and analyzes photosynthesis through inflection points on the resulting fluorescence curve [12]. Both these methods require a precise measurement of the fluorescence from fully dark adapted plants, to compare with the fluorescence at fully saturating light. These requirements limit the use of the methods for remote sensing during day time and imply a restriction of their use to mainly on-leaf measurements.

There are methods developed for remote sensing applications. The best example is the passive solar-induced fluorescence (SIF) methodology, facilitating satellite measurements, based on fluorescence detection within the Fraunhofer lines, the dark lines in the solar spectrum caused by absorption by chemical elements in the Earth's atmosphere [13], [14]. There are ongoing efforts in remote sensing research to quantify relationships between steady-state chlorophyll fluorescence (e.g., using SIF) and photosynthesis [15]. Although promising, the new SIF methodology, as well as other remote sensing methodologies, introduces many scientific questions that remain to be answered. The main questions are related to temporal, spatial and mechanistic up-scaling when going from traditional leaf-level measurements using the PAM-technique [15] to SIF. For example, how do we handle differences in canopy structure and geometry, and what type of information can be derived from the signal when the quantum yield of photochemistry cannot be directly resolved? We are trying to expand that knowledge base, by employing an active proximal remote sensing system, measuring chlorophyll fluorescence on canopy level. The measure we propose, is a relative quantity of how much the fluorescence (in a wavelength span around 740 nm) increases for a certain intensity change. We define the steady-state chlorophyll a fluorescence gain (dF740/dq) as the difference in fluorescence at 740 nm divided by the difference in incident light quanta caused by (a small) excitation of one LED colour. This work is an expansion of earlier research [16], [17], where we proposed the use of the fluorescence gain as an measure of the photosynthetic efficiency increase, to be

used as a feedback signal in a (future) self-optimising controller to find the optimal light spectrum.

The relations between the amount of absorbed light, the amount of fluorescent light and the photosynthetic rate have been studied on both leaf level [18] and canopy level [19], and are dependent on plant health. For example, the fraction of fluorescence and photosynthesis is negatively correlated at low light intensity while it is positively correlated at high light intensity and stress [20]–[22]. However, the absolute quantities of both fluorescence and photosynthesis are expected to increase with an increased incident light intensity, and the absolute values (not to be confused with the fraction) will hence be positively correlated. We have seen that there is indeed a strong correlation between steady-state chlorophyll a fluorescence at 740 nm (F740) and photosynthetic rate (measurements on basil, in absence of background light, [16]), which indicates that the F740 could be a useful remotely measured signal to estimate the photosynthetic efficiency. The maximum photosynthetic rate for a predefined total power corresponds to the spectrum that maximies F740 [10]. It also means that the LED colour that has the highest fluorescence gain, is the one that increases photosynthesis the most (per incident quanta) at the current settings.

In previous experiments we compared the fluorescence gains caused by an excitation of six different LED colours (in the absence of background light), for six different plant species [17], including basil, cucumber, and lettuce. Differences in the mutual relation of the fluorescence gains (caused by the different LED colours) were noticed between different plant species. However, red LEDs caused the highest fluorescence gains per incident quanta for all species tested. Experiments on basil have also been conducted under various background light [16]. In contrast to the working hypothesis, that the mutual relations of the fluorescence gains would vary with various background light, the variation of individual fluorescence gains were minor for the background lights studied. Red LEDs remained the most efficient per quanta for all investigated background light. In this article we present experiments on cucumber and lettuce, conducted in order to answer the following research questions:

- Is there a strong correlation between photosynthetic rate (PN) and steady-state fluorescence (F740) also in the presence of background light?

- Do the mutual fluorescence gains, caused by excitation of different LED colours, change as the background light spectrum approaches only red light at different intensity levels?

2 Materials and Methods

Experiments were conducted on cucumber (*Cucumis sativus* F1 'Max') and lettuce (*Lactuva sativa* 'Black seeded Simpson'), with all settings summarized in Table 1. Two experimental sets are presented, set A and set B, as we wanted to repeat the experiments, initially only performed at background light intensity 160 µmol m^{-2} s^{-1} (set A), also for higher background light intensity levels (200, 350, 500 and 1000 µmol m^{-2} s^{-1}, set B). The slightly different settings in the two setups were a consequence of the available resources at the time.

Table 1: Summary of the experimental conditions.

	Set A	**Set B**				
Growth conditions	160 µmol m^{-2} s^{-1}	195 µmol m^{-2} s^{-1}				
Plant age when experiments start	7 weeks	5 weeks				
Intensity of background light	160 µmol m^{-2} s^{-1}	200, 350, 500, 1000[c] µmol m^{-2} s^{-1}				
Spectra (% red light)	50, 70, 85, 95, 100	50, 70, 85, 95, 100				
LEDs used for excitation (nm)	400, 420, 450, 530, 630, 660	400, 420, 450, 530, 630, 660				
Time at each level	3 min	long setting: 3 min				
		short setting: 20 s				
Repetitions	2 *^{i}	Intensity	200	350	500	1000
		3 min/lev	**c**^{i}**l**	**c**^{i}	**c**^{i}**ccl**	**cc**
		20 s/lev *	**ccll**	**ccll**	**ccll**	**cc**
Infrared gas analyzer (IRGA) settings						
Flow rate	400 µmol/s	300 µmol/s				
CO_2 content	400 ppm	400 ppm				
Temperature	23 °C	21 °C				
Relative humidity	50%	50%				
Irga used (see *i*) during exp.	two machines at each run	one machine at a time, only for cucumber at three different intensity levels				
Light curves	one (increasing intensity)	three (decreasing intensity)				

c = cucumber, **l** = lettuce, [c] = intensity level only for cucumber, *i* = irga used in this setup
* = switching between increased and decreased wavelength order

2.1 Conditions during Plant Growth

Five days after seeding, the plants were placed under LED lamps (LX60, Heliospectra, Sweden) in a plant lab with a photoperiod of 16 h and 23/17 °C day/night temperatures. The photosynthetic photon flux at plant level was approximately 160/195 µmol m^{-2} s^{-1} (set A/set B), with a spectral distribution of 20% blue, 10% green and 70% red light. Due to the different growth light intensities (which were a result of the available resources at the time), the experiments were conducted seven and five weeks after seeding for sets A and B, respectively, to have plants at approximately the same size.

2.2 Experimental Setup

The experiments were performed in a plant lab, in an experimental unit, delimited with reflective curtains (silver/white Diamond Diffusion Foil, Easy Grow, UK) giving a closed, controlled environment. In set A, two RX30 lamps (Heliospectra, Sweden) generated both background light and excitation light. Six different LED colours with peak wavelengths at 400, 420, 450, 530, 630 and 660 nm were used. These were all the available LEDs in the lamp that where assumed not to have any significant overlap with the spectrum of the fluorescence signal in the span 735–745 nm. In set B, the same type of lamp was used for the excitation light, but the background light was generated by two LX (Heliospectra, Sweden) lamps. Three LED groups in the LX60 lamps were used; blue, white, and red. The white LED produce light also in the fluorescence region. However, as the intensity of the white LED remained constant at each background light level and the experiments study variations in fluorescence, this overlap should have no effect. Figure 1 shows the spectrum for each LED colour in the LX lamp and RX lamp, respectively.

2.3 Spectrometer Measurements

To detect the incident light and the reflected/fluorescent light two spectrometers were used, one facing the plants and one facing the lamps. In set A we used two Maya2000 Pro spectrometers (Ocean Optics, USA), each equipped with a 600 µm optical fibre, and in set B one Maya2000 Pro (equipped with a 600 µm optical fibre) and one STS-VIS (Ocean Optics, USA; no fiber needed). The incident light detector (Maya/STS, in set A/B) was placed at the canopy level with a cosine diffuser providing a field of view of 180°. The distance from the canopy level to the lamp was 40–50 cm (depending on plant height). The spectrometer detecting the reflected/fluorescent light (Maya in both sets) was placed on the side of the lamps with a field of view limited to 20° to only

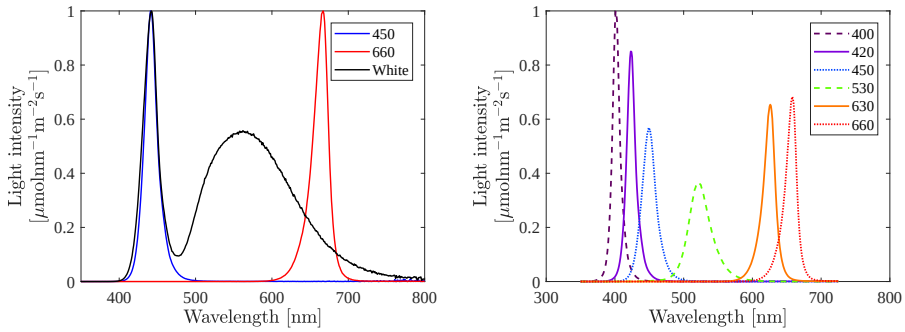

Figure 1: (**a**) Spectrum from the LX lamp for the blue, white and red LEDs, used to generate background light. (**b**) Spectrum from the RX lamp for each of the six LEDs used to generate excitation light.

measure green area.

The input signal in this system is the light intensity reaching the canopy level. The wavelength span for photons that is normally considered important for photosynthesis is 400–700 nm, which is commonly referred to as photosynthetically active radiation (PAR). However, the cutoff wavelength is slightly different for different species [7]. Throughout this article, the photon flux in the range 350–700 nm has been included in the input light intensity, in order to capture all light, including the light from the LEDs having peak wavelength at 400 nm. Furthermore, blue light is defined as photons in the range 350–500 nm, green light in the range 500–600 nm and red light in the range 600–700 nm.

The primary output signal of the system is the fluorescence. The reflected and fluorescent light were measured with a spectrometer covering the whole wavelength span (see Figure 2a). Earlier work did not show satisfactory results when analysing reflected light, and therefore we have focused on analysing the data in the fluorescence band (having a first peak at 685 nm and a second at 740 nm). Furthermore, previous research [16] found a better correlation between photosynthetic rate and the fluorescence at 740 nm, compared to the peak at 685 nm. In addition, LED 660 significantly overlaps with the fluorescence spectrum at 685 nm though it was assumed not to overlap at 740 nm at the time of the experiments (later it was, however, found to have a small overlap affecting the results to some extent, see Section 3.2). However, this motivates our choice of only presenting the fluorescence at 740 nm.

Figure 2b shows the fluorescence spectra for lettuce at background light

$500\,\mu\text{mol}\,\text{m}^{-2}\,\text{s}^{-1}$, and when an excitation step is added with LED 400 and with LED 660. The vertical lines points out the wavelength span 735–745 nm, which is were we have integrated the intensity to get the fluorescence signal, i.e.,

$$F740 = \int_{\lambda=735\,nm}^{745\,nm} \text{Photon flux}\; d\lambda. \tag{C.1}$$

The absolute value of the fluorescence was affected by the chlorophyll content in the canopy but also by the background light level (intensity and spectrum) and the distance between the spectrometer and the plants. Notice that in Figure 2a, the white LED (having one peak at 450 nm and a second one at 560 nm) have a tail in the red and far-red region and hence overlaps with the fluorescence signal. To cope with this, we studied the relative increase in fluorescence, more precisely the increase in fluorescence, caused by one specific LED colour at a time, divided by the increase in incident light caused by that LED. This is referred to as the fluorescence gain, i.e.,

$$\text{Fluorescence gain } = dF740/dq \approx \frac{\Delta F740}{\Delta q} = \frac{F740_{EX} - F740_{BL}}{q_{EX} - q_{BL}}, \tag{C.2}$$

where F740 is the fluorescence signal according to Equation (C.1) at background light (BL) and when additional excitation light (EX) is added, and q is the quantum flux ($\mu\text{mol}\,\text{m}^{-2}\,\text{s}^{-1}$) of the incident light in the wavelength span 350–700 nm.

2.4 Reference Measurements

As a reference measurement an infrared gas analyzer (IRGA, Li-Cor 6400XT, USA) was used (in set A, two IRGA systems were used in parallel) to determine the photosynthetic rate as CO_2 uptake per leaf area and time. The calculations were based on measurements of the carbon dioxide and water content of a controlled air flow over a leaf sealed in a chamber, called the leaf cuvette. The cuvette had a transparent window, allowing measurements to be made under the desired light quality and quantity. The air flow, carbon dioxide content and the leaf temperature were automatically controlled, details are found in Table 1. The plants have been illuminated with the light settings similar to the first light level prior to the experiment in order for the photosynthesis to reach a steady value. However, no dark adaption was done, since we were primarily interested in changes and not absolute values. Four light curves were also performed, one with the same settings as in set A, and three with the same settings as in set B.

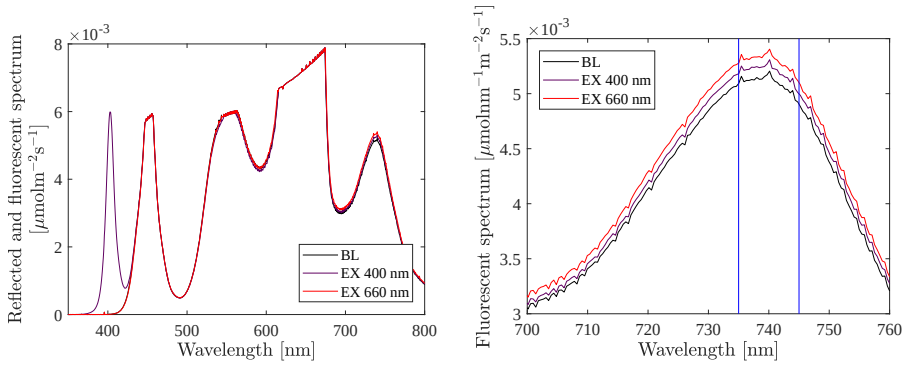

(**a**) Reflected/fluorescent spectra for whole wavelength span

(**b**) Details of the fluorescence region

Figure 2: Reflected/fluorescent spectra for lettuce at background light intensity 500 µmol m^{-2} s^{-1} and spectrum with 85% red light. Three spectra are shown; for background light and with an additional excitation signal with light emitting diode (LED) 400 and LED 660 respectively. Vertical lines in plot (**b**), indicate the region where the spectrum is integrated to get the F740 signal according to Equation (C.1). Notice that the spectrometer is light saturated in wavelengths 630–670 nm, however this is outside the wavelength of interest (i.e., the span 735–745 nm).

Differences in photosynthetic rate between species may be partly attributed to foliar pigment content and composition. Relative chlorophyll and flavonoid content were therefore estimated using Dualex Scientific® (Force-A, France), a leaf-clip optical sensor designed to non-destructively evaluate the content of chlorophyll and epidermal flavonoids [23], [24]. We collected 32 point measurements for the analysis (four measurements on each of four leaves from two plants).

2.5 Data Processing

The spectrometers took a sample every second. A mean value of the 4 or 10 last measurements at each intensity step (that was held for 20 s or 3 min respectively) was used as the measure for that setting. Figure 3 shows the raw data of the incident light and the fluorescence signal as a function of time, and the large dots indicates the mean value of the last points at each step. The fluorescence at background light (BL) level was measured between each excitation (in total 6 or 7 times/BL), and these data were used to identify possible trends in the fluorescence that were not an effect of the excitation light. The integration times (IT) were set in advance. The same IT was used

for all excitations at one specific BL level, but were adjusted when changing BL, to get as strong a signal as possible of the relatively weak fluorescence. As a consequence, a large part of the reflection spectrum became saturated, which can be seen in Figure 2a (in the range 630–670 nm). However, these wavelengths are not included in this analysis.

Under the assumption that the variance is the same for all LEDs used, even though they have different means, the pooled (or combined) variance can be estimated by [25]

$$s_p^2 = \frac{\sum_i \sum_{j=1}^{n_i} (y_j - \bar{y}_i)^2}{\sum_i (n_i - 1)}, \tag{C.3}$$

where $\bar{y}_i$ is the mean value of the fluorescence gain for each LED colour at each intensity level, and n_i is the total number of measurements of that state i ($n_i = 5$ different background spectra times 2–5 repetitions). Further, the standard error of the mean (s_m), can be estimated by

$$s_m = \frac{s_p}{\sqrt{n_i}}. \tag{C.4}$$

The IRGA measurements (on leaf level) had a much higher noise to signal ratio, compared to the fluorescence (canopy level) measurements. The measurement frequency is approximately 3 measures/min, and the mean value of the five last measurements at each light level were used to get an estimate of the photosynthetic rate (PN) at the current light level. The mean value of the photosynthetic rate at the BL level before and after an excitation step was used to determine the PN for the background light level. This was a way of compensating for trends in the data (i.e., for not being at a true steady-state). There has been no dark adaption, since only relative values, i.e., increase in PN due to excitation, were of interest.

2.6 Experimental Light Scheme

The background light intensities (within the PAR region) that were investigated were 160, 200, 350, 500 and 1000 µmol m^{-2} s^{-1} and for each intensity level five different spectra were investigated, having 50, 70, 85, 95 and 100% red light and a constant blue to green ratio, B:G, of 2:1. Figure 4 shows the spectral distribution for spectra having 50% and 85% red light respectively. At each background light (for all combinations of intensity and spectra) an excitation signal (a step of about 20 µmol m^{-2} s^{-1}) was added. This was sequentially done with all six different LEDs that were included in the investigation, i.e., LEDs having peak wavelength at 400, 420, 450, 530, 630 and 660 nm.

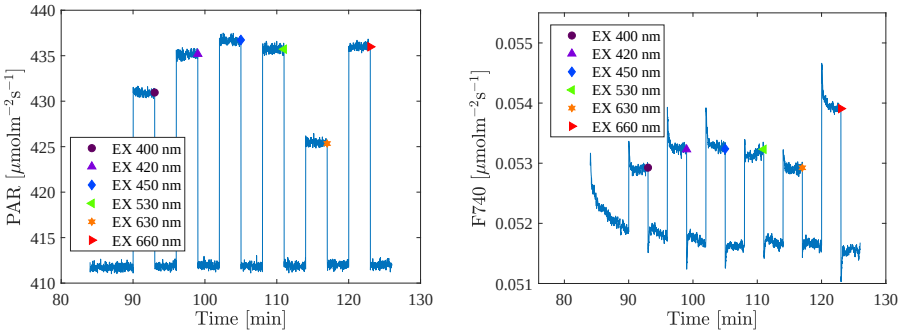

(**a**) Incident light intensity in the wavelength span 350–700 nm

(**b**) Fluorescence light intensity in the wavelength span 735–745 nm

Figure 3: Measurements on lettuce, holding each intensity level at three minutes. (**a**) Incident and (**b**) fluorescence light intensity (µmol m^{-2} s^{-1}) vs. time for one background light level (background intensity 500 µmol m^{-2} s^{-1}and spectrum having 85% red light). An excitation step pulse is sequentially added by each LED colour, one at a time. Note that the intensity level measured during the experiment was only about 412 and not 500 µmol m^{-2} s^{-1}. This is because when the light level was determined, no plants were present in the experimental unit and another type of spectrometer was used.

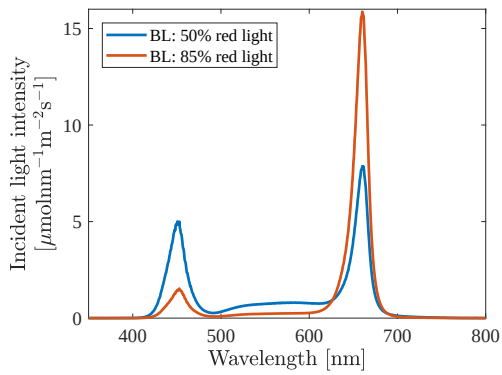

Figure 4: Spectra of background light. Intensity level 500 µmol m^{-2} s^{-1} and spectrum distribution 50% and 85% red light respectively.

Figure 3 shows the incident light (a) and fluorescence signal (b) for one (out of five) background spectrum at background intensity 500 µmol m^{-2} s^{-1}. Notice that the measured background intensity level shown in the figure is about 412 µmol m^{-2} s^{-1}. The reason is that the background light levels were determined using another spectrometer. In addition, the light was measured in an empty room, but when inserting the plants (for the experiments) the light environment is changed even though the lamp settings are constant. In Appendix 4 additional Figures 13 and 14 for other setups are presented. In one setup, the scheme in Figure 3a was repeated five times, once for each background spectrum, starting with 50% red light and finishing with only red light. In some setups the wavelength order was reversed, i.e., starting with background light spectrum with only red light and then decreasing the amount, and also starting the excitation with LEDs of longest wavelengths and continue in shorter wavelength order (that is reading Figure 3a from right to left). All details of the different settings are summarized in Table 1. In set A, the light was held constant at each light level for three minutes (six minutes at the first background light step when changing to a new background spectrum), while in set B an additional setup, staying at each light level only 20 s (60 s at the first BL), was also used. Another change from set A to set B was that an additional step of background light was added after the last excitation. This was done in order to more accurately capture any trend in the fluorescence that does not depend on the excitation step.

3 Results and Discussion

This section is divided into four subsections. In the first one, Section 3.1, the normalized absolute values of fluorescence (F740) and photosynthetic rate (PN) from set A are presented, which demonstrates a clear positive correlation between F740 measured at canopy level and PN measured at leaf level in the presence of various background light. In Section 3.2 the results of the F740 gains are presented, as a function of background light spectra and as a function of background light intensity. The mutual relation of the F740 gains do not change significantly with background light spectra. However, changes were noticed when light intensity increased up to a certain point. In Section 3.2 we discuss the fact that LED 660 is likely overestimated in our analysis. In Section 3.3 the results from the infrared gas analyzer are presented. Here we found that the light saturation level in the light curves, coincides with the light intensity where the mutual relation of the F740 gains do not change any more. Furthermore, the PN gains are presented and shown to correlate with

the F740 gains. Finally in Section 3.4, we discuss our results of the F740 gains and PN gains, compared to data from McCree and our dualex measurements.

3.1 Absolute Values of Fluorescence vs. Photosynthetic Rate

The normalized absolute value of fluorescence as a function of the normalized absolute value of the photosynthetic rate (i.e., all values is divided by the maximum measured value to a normalized value being one or less), is shown in Figure 5 for (a) cucumber and (b) lettuce. The background light intensity is $160\,\mu mol\,m^{-2}\,s^{-1}$, and background spectra ranging from 50% to 100% red light (i.e., set A). The black stars in the plot correspond to these background light levels, clustered in five groups. It corresponds to the five different spectral distribution of the background light, with higher amounts of red light resulting in both higher fluorescence and higher photosynthetic rate. The coloured dots correspond to the measurements when an excitation step (of about $20\,\mu mol\,m^{-2}\,s^{-1}$) is added by one of the six available LED colours.

The measurements clearly show a strong positive correlation between fluorescence (F740) measured at canopy level and photosynthetic rate (PN) measured at leaf level in the presence of various background light. For cucumber (Figure 5a), one reasonable approximation is to view the relation as two different linear regressions, one for the lower background intensity level (black stars, PAR 160 $\mu mol\,m^{-2}\,s^{-1}$) and one for the slightly higher (coloured dots, PAR 180 $\mu mol\,m^{-2}\,s^{-1}$). This indicates that the relation between F740 and PN is close to, but not exactly linear, changing slightly with the intensity. However, for the purpose of optimizing the spectrum for short term photosynthesis only a positive correlation between F740 and PN is required (it does not have to be linear). It should be noted that the time at each light level (three minutes) was enough to get a useful signal of the fluorescence, but hardly enough for the photosynthetic rate signal due to the relatively high noise magnitude. Furthermore, the variation in the strength of the correlation ($R^2 = 0.87$ and 0.96 for cucumber and lettuce respectively) could be attributed to mainly the variation in the photosynthetic rate signal. At this stage no conclusions about differences due to crop species can be drawn.

In set B, the background light consists of light from white LEDs (among others), which produce light also in the region where the fluorescence signal is measured. The white LEDs are held constant at each background light level, but the higher the intensity levels and the less red light in the spectrum, the more light is emitted from the white LEDs. That is why no data of the absolute value of the fluorescence in set B can be presented here.

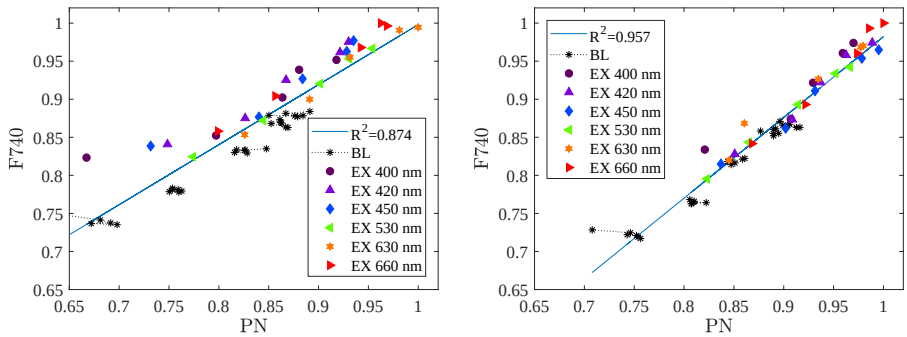

(**a**) Cucumber (**b**) Lettuce

Figure 5: Normalized fluorescence at 740 nm versus normalized photosynthetic rate. The black stars correspond to measurements at background light, i.e., intensity 160 µmol m^{-2} s^{-1} and the five clusters corresponds to five different spectral distribution from 50% up to 100% red light. The coloured dots correspond to measurements with additional excitation light with one LED at a time.

3.2 Fluorescence Gains, dF740/dq

The fluorescence gains (defined by Equation (C.2)), i.e., the change in fluorescence (integrated over 735–745 nm) divided by the change in incident light caused by an (small) excitation of one specific LED colour, were studied for excitations of every LED colour at different light qualities (50–100% red light) and quantities (160–1000 µmol m^{-2} s^{-1}).

dF740/dq vs. Incident Light Quality

Figure 6 shows the fluorescence gains vs. the proportion of red light in the background spectra for intensities 160 µmol m^{-2} s^{-1} (first row, from set A) and 500 µmol m^{-2} s^{-1} (second row, from set B). The figures are representative also for the other intensity levels tested. In set A the experiments were only repeated once (giving two measurements per level). The results presented are the mean values of these two measurements. In set B, at 500 µmol m^{-2} s^{-1}, the fluorescence gains were measured three times for lettuce and five times for cucumber. The error bars (in the second row) indicate the spread (one standard deviation) of the measurements at each point. As the background light approaches only red light, a small decrease in fluorescence gain for LED 660 was noticed for both cucumber and lettuce, at background intensity 160 µmol m^{-2} s^{-1}. However, this was not observed for higher light intensities. Considering the one standard deviation error bars, no significant

change in fluorescence gain as a function of background spectrum can be concluded.

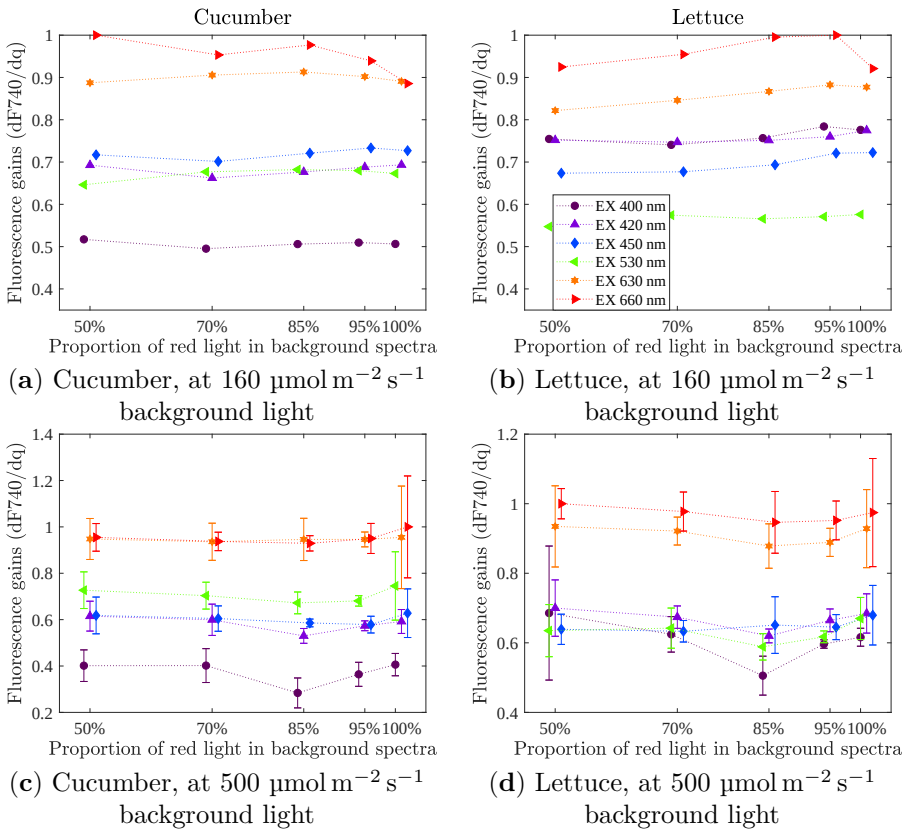

(**a**) Cucumber, at 160 µmol m^{-2} s^{-1} background light

(**b**) Lettuce, at 160 µmol m^{-2} s^{-1} background light

(**c**) Cucumber, at 500 µmol m^{-2} s^{-1} background light

(**d**) Lettuce, at 500 µmol m^{-2} s^{-1} background light

Figure 6: Fluorescence gains for each of the six LED colours when background light quality varies from 50 to 100% red light. The upper row is data from set A, and the lower row is for parts of set B. Left column is measurements on cucumber and right column is on lettuce. The bars in the lower plots represent ±one standard deviation calculated from the measurements at the current light setting.

The fluorescence gain is always highest for an excitation in red light (highest for LED 660 followed by LED 630). For the others it differs slightly depending on species and intensity level. LED 400 gives the lowest gain for cucumber, whereas all three blue LEDs (400, 420 and 450 nm) are about equal for lettuce. LED 530 gives a relatively higher gain for cucumber than for lettuce.

Our experiments do not indicate that the steady-state fluorescence gains (or

the short term photosynthetic rate gain, since they correlate) would change significantly with background light quality. That means, for a given incident intensity there is no need for an online controller to work continuously to find the optimal spectrum. On the other hand, due to the strong correlation between photosynthetic rate and fluorescence, and the fact that the relative fluorescence gains are consistent at each incident intensity level, the fluorescence gains could be an interesting signal to monitor, for example daily through the growth cycle, in order to detect if something unpredicted happens. If the input signal is the current to the lamp, instead of the measured incident light quanta, it would be possible to detect if any of the LED colours have degraded more than the others, and in such case reconsider the power distribution over the different LEDs.

dF740/dq vs. Incident Light Quantity

The difference in relative fluorescence gain as a function of incident light intensity was studied. In Figure 7 the mean values of the fluorescence gains of each LED colour at each intensity level are plotted with one standard error of the mean (according to Equation (C.4)). A couple of statistically significant changes can be noted as the intensity increases. The difference in gain between LED 660 and LED 630 decreases. Also, the gain of LED 530 increases relative to the gains of the blue LEDs. The starting point though, differs for the two species. For cucumber, the gain of LED 530 is about equal to the gain of LED 420 and LED 450 at $200\,\mu\mathrm{mol\,m^{-2}\,s^{-1}}$, while LED 530 has a higher gain than the blue LEDs at higher intensities. For lettuce on the other hand, the gain of the green LED is lower than the blues' at $200\,\mu\mathrm{mol\,m^{-2}\,s^{-1}}$, while they are in the same region for higher intensities.

For cucumber an additionally high intensity level was included in the experiments, at $1000\,\mu\mathrm{mol\,m^{-2}\,s^{-1}}$. As the intensity increases from 500 to $1000\,\mu\mathrm{mol\,m^{-2}\,s^{-1}}$, no change in relative fluorescence gain could be observed. One possible reason for this is that the light curve has reached saturation (as can be seen in Figure 8 in the next section), which means that even though more light is added, the photosynthesis rate cannot increase further.

Overestimated Fluorescence Gain from LED 660

The white LED has a significant illumination power in the fluorescence region (i.e. 735–745 nm), which can clearly be seen by observing its spectrum (see Figure 1a). For all other LEDs, a potential overlap is very hard to detect since it is very small or even zero. At the time when the experiments were conducted it was assumed that none of the LEDs in the excitation lamp had

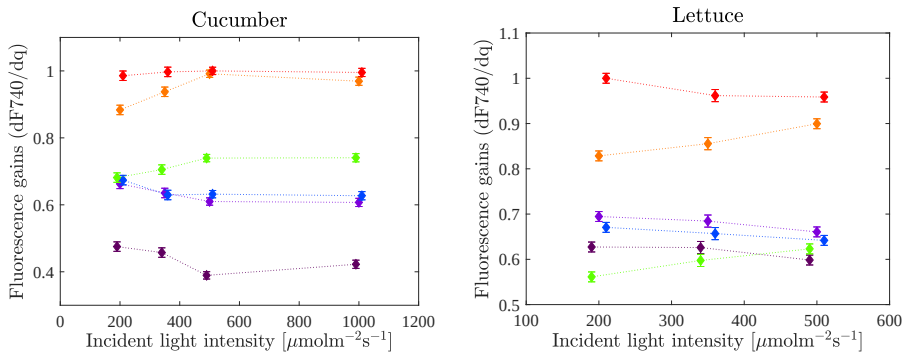

(**a**) Cucumber (**b**) Lettuce

Figure 7: Mean values (and standard errors of the mean) of the fluorescence gains at each intensity level, independent of the background spectra, for (**a**) cucumber and (**b**) lettuce.

any significant overlap with the fluorescence at 740 nm, based on observations of their spectra (see Figure 1b). However, even a very small overlap can have a relatively large impact since, (i) a large proportion of the light at 740 nm will be reflected and (ii) the fluorescence signal is weak compared to the incident light.

When integrating the incident light in the range 735–745 nm, and time-averaging the noisy signal, a slight increase can be observed when adding an excitation with LED 660, compared to when only illuminating with the background light or adding an excitation with any other LED colour. This indicates that the signal $\Delta F740 = F740_{EX} - F740_{BL}$ (see Equation (C.2)) that is measured with the spectrometer facing the plants, contains both fluorescence and reflectance when adding an excitation with LED 660, but not when adding an excitation with LED 400, 420, 450, 530 or 630. Since in all reported results, this signal is assumed to only consist of fluorescence, and no reflectance, the fluorescence gain for LED 660 is likely overestimated.

Several attempts were made to estimate the reflectance to estimate the errors caused by the reflected light from LED 660. However, we have not been able to get an estimate with a reasonable confidence interval, and thereby we are not able to report a reasonable estimate of how much the reflectance affect the measurements. This is partly, or fully, attributed to the low signal to noise ratio in the incident light spectrometer measurements in this waveband (signal level similar to noise level). Measurements with longer integration time to increase the signal level, or a spectrometer with a lower noise level, e.g., with a cooled detector, seems to be necessary for doing this estimation.

If indeed LED 660 has a significant overlap with the chlorophyll fluorescence waveband it may be possible to mitigate it by moving the waveband towards longer wavelengths, or compensate for the overlap, or more drastically, using optical filters in the lamp to block light in the fluorescence region.

3.3 Photosynthetic Rate

Light Curve

The light curve, i.e., the photosynthetic rate as a function of incident light intensity, was measured for four different cucumber leaves using an infrared gas analyzer (IRGA), see Figure 8. One time the external LED lamp was used as the light source (starting with high intensity and stepwise decreasing), and the other three times the internal LED lamp in the IRGA-machine was used, once with increasing light intensity and twice with decreasing intensity. The black dots in the figure are from the three different background intensity levels of the experiments in set B. At low light the relation between

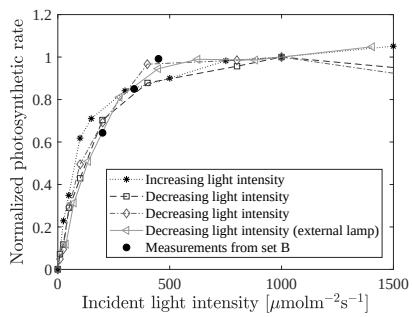

Figure 8: Normalized light curve for cucumber, i.e., the photosynthetic rate vs. light intensity.

incident light and photosynthetic rate is almost linear, but the dependency of the rate on the light intensity decreases, and for intensities higher than about $500\,\mu\text{mol}\,\text{m}^{-2}\,\text{s}^{-1}$, there is almost no increase in photosynthetic rate. This saturation phenomena is not seen for the absolute value of the steady-state fluorescence, which continues to increase with increasing light intensity (data not shown). On the other hand, the mutual relation of the fluorescence gains seems to be unchanged after reaching light saturation, as was discussed in the previous section (see Figure 7a). Hence, one possible application of fluorescence gain measurements is to identify where light saturation occurs. This could, for example, be of interest in stress detection due to light inhibition, as an alternative to the method presented in [26].

Photosynthetic Rate Gains, dPN/dq

Figure 9 shows the photosynthetic rate gains as a function of incident light quality (50–100% red light) when the incident intensity was 160 µmol m^{-2} s^{-1} (set A). The measurements were repeated on four different leaves (for each species), of which we show their mean value. The variability was notably larger than in the fluorescence data because of the nature of the method, but shows similar behavior to the fluorescence gains, compare with Figure 6 upper row (in Appendix 4 Figure 15, a scatter plot of PN gain vs. F740 gain are shown). The red light gave the highest gains. For cucumber LED 630 had a slightly higher gain than LED 660, which was not the case for the fluorescence gain. However, the fluorescence gain for LED 660 was most likely overestimated (see Section 3.2). Further, LED 530 gave the lowest gain for lettuce whilst LED 400 gives the lowest gain for cucumber. No significant change in photosynthetic rate gain as a function of background spectrum could be proven.

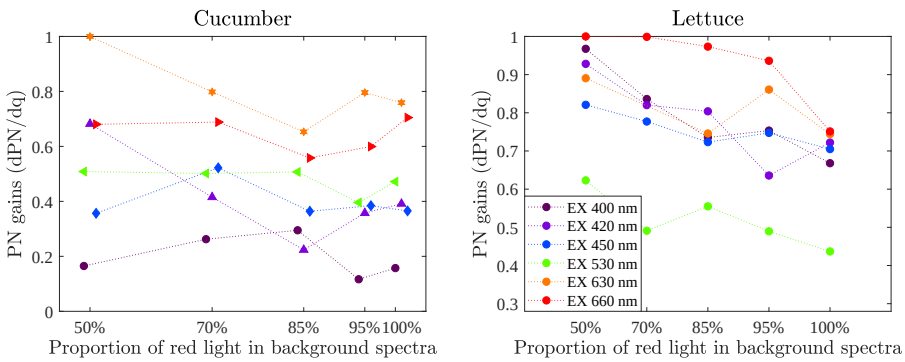

(**a**) Cucumber (**b**) Lettuce

Figure 9: Photosynthetic rate gains for each of the six LED colours when the background light quality varies from 50–100% red light, for (**a**) cucumber and (**b**) lettuce, normalized to the highest gain. Background intensity level was 160 µmol m^{-2} s^{-1} (set A). The plot shows the mean value of measurements on 4 different leaves.

In set B, the IRGA was used in three experiments on cucumber, once at each intensity level: 200, 350 and 500 µmol m^{-2} s^{-1} and with spectra of 50–100% red light. In Figure 10 the mean values of the PN gains at different intensity levels are plotted with the standard error of the mean (according to Equation (C.4)). The general picture is the same as for the cucumber in set A (recall set A had PAR 160 µmol m^{-2} s^{-1}, see Figure 9a), i.e., the gain was highest for red LEDs, followed by green and lowest for blue LEDs. Only in

one out of the three intensity levels the PN gain of LED 400 was significantly lower than the other blue, which was the case for all sets of the fluorescence gains (see Figure 7a). The PN gain of LED 660 was lower (or equal) to that of LED 630, which is not the case for the fluorescence gains at lower light intensities (recall again though, that the fluorescence gain for LED 660 was most likely overestimated). However in this setup, measurements were only conducted on one leaf per intensity level. To draw any conclusion about differences in relative PN gains as a function of light intensity level, more repetitions would be needed and also on different leaves.

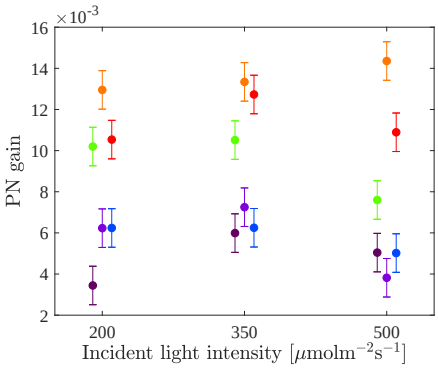

Figure 10: Photosynthetic rate gains vs. incident light intensity for cucumber (set B). Mean values of PN gains and one standard error of the mean are depicted. Note that different leaves have been used for the different intensity levels.

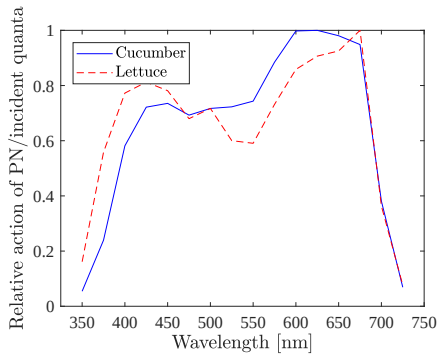

Figure 11: Relative action spectra, i.e., CO_2 uptake per incident quanta, derived from the experimental data given by McCree [7].

3.4 Comparisons

Comparison with McCree Data

Among many other species, McCree [7] measured the quantum yield (CO_2 uptake per absorbed photon) and absorbance rate for different wavelengths, for both cucumber and lettuce. Figure 11 shows the relative action spectra for these two (CO_2 uptake per incident photon), derived from data from McCree. Multiplying this action spectra and with the spectra of each individual LED colour from the excitation lamp (Heliospectra RX lamp, see spectra in

Figure 1b), and calculating the integral, one gets the PN gain for each LED colour that would have been expected based on McCree's experiments. The outcome is shown in Figure 12a. Comparing these with the PN gains that we measured (Figures 9 and 10), they do match very well, despite of all the different settings. For cucumber, McCree also found a slightly higher gain for LED 630, compared to LED 660, and also the lowest gain for LED 400. For lettuce on the other hand, LED 660 were slightly higher than LED 630, the blue LEDs were all close to each other, and LED 530 had the lowest gain. Also this is in complete agreement with our experimental results of the PN gains.

Figure 12b, is our experimentally measured fluorescence gains at the lowest background light that was used in this setup (160 µmol m^{-2} s^{-1}), i.e., the mean values of the gain for each colour in Figure 6a,b. It is remarkable how well these remotely measured steady-state fluorescence gains, caused by excitation of different colours, fit with the old photosynthetic rate data from McCree. This comparison also supports the assumption that the fluorescence gain for LED 660 is overestimated (see Section 3.2).

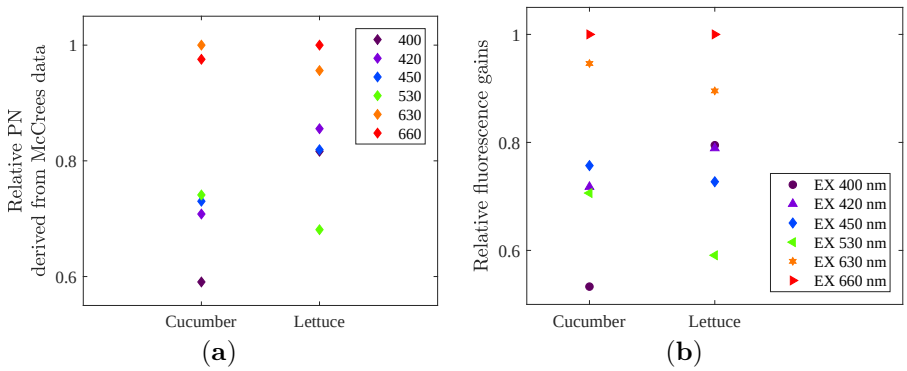

Figure 12: (**a**) Relative PN gain of each LED colour for cucumber and lettuce, calculated from data from McCree. (**b**) Experimentally derived fluorescence gains at background light intensity 160 µmol m^{-2} s^{-1} (set A).

Comparison with Dualex Measurements

The estimations of chlorophyll and flavonoid content, using Dualex Scientific's Chl and Flv indices (relative measurement), showed that cucumber has a significantly higher concentrations of both pigments compared to lettuce; twice higher chlorophyll content (35.0 ± 7.0 vs. 16.5 ± 4.2) and three times higher flavonoid content (1.04 ± 0.24 vs. 0.36 ± 0.08). Notice, the instrument has not been calibrated, hence only relative values are reported.

Flavonoids are concentrated on the surface structures and tissues of plants (cuticle and epidermis) and exerts some of its protection functions by screening incoming light in the UV but also the blue-violet part of the spectrum [27] the expected effect of a higher flavonoid content is a lower photosynthesis efficiency [28]. The effect is likely most distinct for the wavelengths where the flavonoids have the highest absorbance [27], it is expected to be highest for LED 400 and 420 in our experiment. Hence, the higher flavonoid content in cucumber could partly explain the lower fluorescence gains for LED 400 and somewhat also for LED 420, compared to the gains for lettuce.

A high photosynthetic rate for LED 630 and a low for LED 400 for cucumber (Figure 9a), could be a indicator of the relation between the content of chlorophyll *a* and *b*, in favor for chlorophyll *b*. The absorbtion spectrum for chlorophyll *b* in solvent has two peaks, at approximately 450 nm and 640 nm [29]. The absorbtion peaks for chlorophyll *a* on the other hand are slightly shifted, to around 430 nm and 660 nm. The blue peak for chlorophyll *a* is also essentially broader towards lower wavelengths, which means that chlorophyll *a* absorbs a considerably higher amount of light from LED 400, in comparison to chlorophyll *b*. Hence, a low photosynthetic rate gain for LED 400 together with a higher gain for LED 630 compared to LED 660, indicate that cucumber has a high content of chlorophyll *b* compared to chlorophyll *a*. However, it must be noted that the absorption in vivo and in a solvent differs [15], partly due to vibrational energy and the fact that the pigments are tightly packed and orbitals of the molecules overlaps.

4 Conclusions

A series of experiments have been conducted in order to evaluate whether fluorescence gains (see Equation (C.2)) could be used as feedback signals for energy optimising the spectrum of a LED lamp. The experiments did show a strong correlation between photosynthesis rate and steady state fluorescence even in the presence of background light, which entails the possibility of using the fluorescence gain as an indication of the strength of the photosynthetic rate. The advantage is that the fluorescence is measured remotely, on canopy level, fast and without moving the plants. However, the conducted experiments did not indicate that the mutual relation of the fluorescence gains would change depending on the background light quality. That means, in contrast to our working hypothesis, there is no need for an online controller to work continuously to find the optimal spectrum for a given incident intensity. On the other hand, the experiments showed that for increasing light

intensities, the mutual relation of the fluorescence gains do slightly change. However, as the intensity increases from 500 to 1000 µmol m^{-2} s^{-1} for cucumber, no further changes are obtained in the mutual relation of the fluorescence gains.

Due to the strong correlation between photosynthetic rate and fluorescence, and the fact that the mutual relation of the fluorescence gains are consistent at each incident intensity level, the fluorescence gains could be an interesting signal to monitor throughout the growth cycle. One possible application is to identify the light saturation level for photosynthesis, since the changes in the mutual relation of the fluorescence gains saturates at about the same intensity level as where light saturation for photosynthesis occurs. Another application, which is the aim of our further research, is to evaluate if changes in mutual relation of the fluorescence gains might be indication of an induced stress in the plant. Yet another application, is to use the current to the lamp as the input signal (instead of measured incident light quanta), and thereby detect if any specific LED group have degraded more than the others, and in such case reconsider the power distribution over the different LEDs.

Appendix

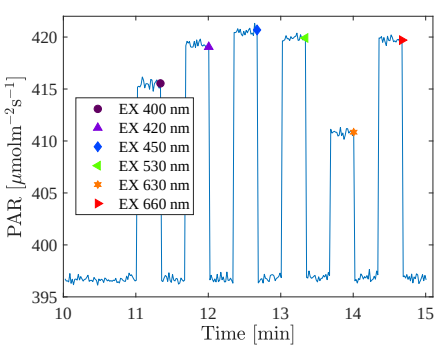

(**a**) Incident light intensity in the wavelength span 350–700 nm

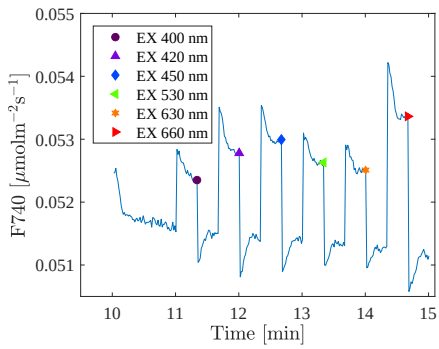

(**b**) Fluorescence light intensity in the wavelength span 735–745 nm

Figure 13: Measurements on lettuce, holding each intensity level at 20 s. (**a**) Incident and (**b**) fluorescence light intensity (µmol m^{-2} s^{-1}) vs. time for one background light level, i.e., background intensity 500 µmol m^{-2} s^{-1}and spectrum having 85% red light. An excitation step is sequentially added by each LED colour. Note that the intensity level measured during the experiment was only about 397 and not 500 µmol m^{-2} s^{-1}. This is because when the light level was determined, no plants were present in the experimental unit and another type of spectrometer was used.

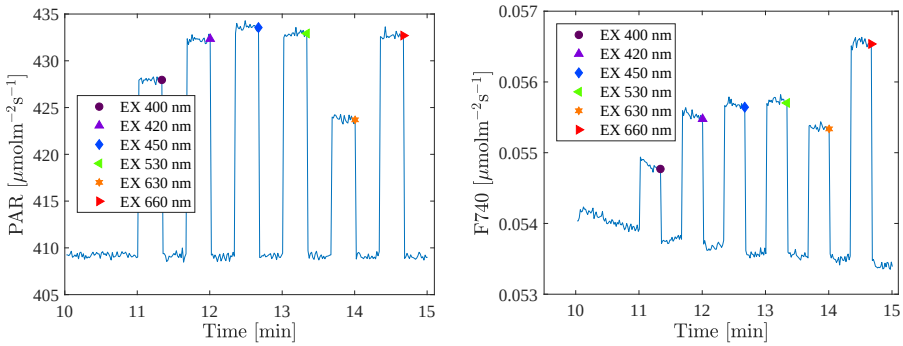

(**a**) Incident light intensity in the wavelength span 350–700 nm

(**b**) Fluorescence light intensity in the wavelength span 735–745 nm

Figure 14: Measurements on cucumber, holding each intensity level at 20 s. (**a**) Incident and (**b**) fluorescence light intensity ($\mu mol\,m^{-2}\,s^{-1}$) vs. time for one background light level, i.e., background intensity 500 $\mu mol\,m^{-2}\,s^{-1}$and spectrum having 85% red light. An excitation step is sequentially added by each LED colour. Note that the intensity level measured during the experiment was only about 409 and not 500 $\mu mol\,m^{-2}\,s^{-1}$. This is because when the light level was determined, no plants were present in the experimental unit and another type of spectrometer was used.

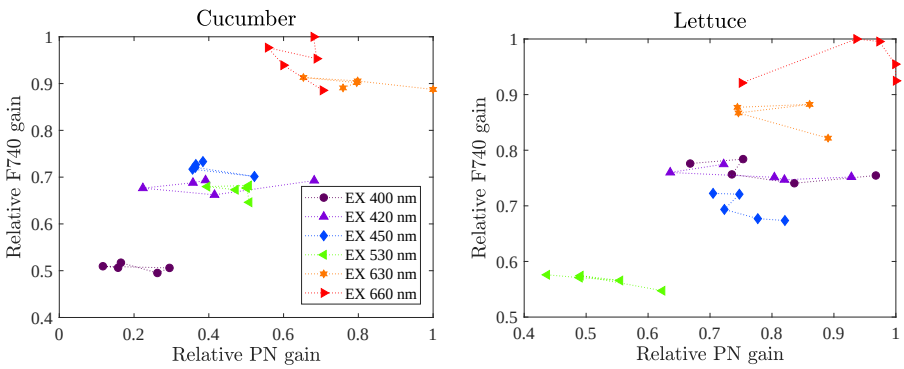

(**a**) Cucumber

(**b**) Lettuce

Figure 15: Fluorescence gain vs. photosynthetic rate gain for background light 160 $\mu mol\,m^{-2}\,s^{-1}$ (set A), i.e., combining Figures 6 and 9. The five points of each colour correspond to the five different background spectra (50-100% red light), and the colour indicates the colour of the added excitation light. The variability in the PN data is higher than in the F740 data.

References

[1] R. R. Shamshiri, F. Kalantari, K. C. Ting, K. R. Thorp, H. I. A., C. Weltzien, D. Ahmad, and Z. M. Shad, "Advances in greenhouse automation and controlled environment agriculture: A transition to plant factories and urban agriculture", *International Journal of Agricultural and Biological Engineering*, vol. 11, no. 1, pp. 1–22, 2018.

[2] E. F. Durner, *Principles of Horticultural Physiology*. CABI Publishing, 2013.

[3] M. Olle and A. Viršile, "The effects of light-emitting diode lighting on greenhouse plant growth and quality", *Agricultural and Food Science*, vol. 22, no. 2, 2013.

[4] T. Ouzounis, E. Rosenqvist, and C.-O. Ottosen, "Spectral effects of artificial light on plant physiology and secondary metabolism: A review", *HortScience*, vol. 50, no. 8, pp. 1128–1135, 2015.

[5] M. C. Snowden, K. R. Cope, and B. Bugbee, "Sensitivity of seven diverse species to blue and green light: Interactions with photon flux", *PLOS ONE*, vol. 11, no. 10, pp. 1–32, 2016.

[6] W. Hoover, "The dependence of carbon dioxide assimilation in a higher plant on wavelength of radiation", *Smithson. Inst., Misc.Coll.*, vol. 95, no. 21, pp. 1–13, 1937.

[7] K. J. McCree, "Action spectrum, absorptance and quantum yield of photosynthesis in crop plants", *Agricultural Meteorology*, vol. 9, pp. 191–216, 1972.

[8] K. Inada, "Action spectra for photosynthesis in higher plants", *Plant and Cell Physiology*, vol. 17, no. 2, pp. 355–365, 1976.

[9] R. Emerson, "Dependence of yield of photosynthesis in long-wave red on wavelength and intensity of supplementary light", *Science (American Association for the Advancement of Science)*, vol. 125, p. 746, 3251 1957.

[10] T. Wik, A. Carstensen, and T. Pocock, *Spectrum optimization for artificial illumination*, WO Patent App. PCT/EP2013/069,820, 2014.

[11] U. Schreiber, "Pulse-amplitude-modulation (pam) fluorometry and saturation pulse method: An overview", in *Chlorophyll a Fluorescence: A Signature of Photosynthesis*, G. C. Papageorgiou and Govindjee, Eds. Dordrecht: Springer Netherlands, 2004, pp. 279–319.

[12] R. Strasser, M. Tsimilli-Michael, and A. Srivastava, "Analysis of the chlorophyll a fluorescence transient", English, in *Chlorophyll a Fluorescence*, ser. Advances in Photosynthesis and Respiration, G. Papageorgiou and Govindjee, Eds., vol. 19, Springer Netherlands, 2004, pp. 321–362.

[13] G. Kirchhoff, "Ueber das verhältniss zwischen dem emissionsvermögen und dem absorptionsvermögen der körper für wärme und licht", *Annalen der Physik*, vol. 185, pp. 275–301, 1860.

[14] I. Moya, L. Camenen, S. Evain, Y. Goulas, Z. Cerovic, G. Latouche, J. Flexas, and A. Ounis, "A new instrument for passive remote sensing1. Measurements of sunlight-induced chlorophyll fluorescence", *Remote Sensing of Environment*, vol. 91, no. 2, pp. 186–197, 2004.

[15] A. Porcar-Castell, E. Tyystjarvi, J. Atherton, C. van der Tol, J. Flexas, E. E. Pfundel, J. Moreno, C. Frankenberg, and J. A. Berry, "Linking chlorophyll a fluorescence to photosynthesis for remote sensing applications: Mechanisms and challenges", *Journal of Experimental Botany*, vol. 65, no. 15, pp. 4065–4095, 2014.

[16] L. Ahlman, D. Bånkestad, and T. Wik, "Using chlorophyll a fluorescence gains to optimize led light spectrum for short term photosynthesis", *Computers and Electronics in Agriculture*, vol. 142, no. Part A, pp. 224–234, 2017.

[17] ——, "Led spectrum optimisation using steady-state fluorescence gains", *Acta Horticulturae*, vol. 1134, pp. 367–374, 2016.

[18] J. Flexas, J. M. Escalona, S. Evain, J. Gulías, I. Moya, C. B. Osmond, and H. Medrano, "Steady-state chlorophyll fluorescence (Fs) measurements as a tool to follow variations of net CO_2 assimilation and stomatal conductance during water-stress in C_3 plants", *Physiologia Plantarum*, vol. 114, pp. 231–240, 2002.

[19] L. Guanter, Y. Zhang, M. Jung, J. Joiner, M. Voigt, J. A. Berry, C. Frankenberg, A. R. Huete, P. Zarco-Tejada, J.-E. Lee, M. S. Moran, G. Ponce-Campos, C. Beer, G. Camps-Valls, N. Buchmann, D. Gianelle, K. Klumpp, A. Cescatti, J. M. Baker, and T. J. Griffis, "Reply to magnani et al.: Linking large-scale chlorophyll fluorescence observations with cropland gross primary production", *Proceedings of the National Academy of Sciences*, vol. 111, no. 25, E2511, 2014.

[20] K. Maxwell and G. N. Johnson, "Chlorophyll fluorescence - a practical guide", *Journal of Experimental Botany*, vol. 51, no. 345, pp. 659–668, 2000.

[21] C. van der Tol, W. Verhoef, and A. Rosema, "A model for chlorophyll fluorescence and photosynthesis at leaf scale", *Agricultural and Forest Meteorology*, vol. 149, no. 1, pp. 96–105, 2009.

[22] C. Van Der Tol, J. A. Berry, P. K. E. Campbell, and U. Rascher, "Models of fluorescence and photosynthesis for interpreting measurements of solar-induced chlorophyll fluorescence", vol. 119, no. 12, pp. 2312–2327, 2014.

[23] Y. Goulas, Z. G. Cerovic, A. Cartelat, and I. Moya, "Dualex: A new instrument for field measurements of epidermal ultraviolet absorbance by chlorophyll fluorescence", *Appl. Opt.*, vol. 43, no. 23, pp. 4488–4496, 2004.

[24] N. Tremblay, Z. Wang, and Z. G. Cerovic, "Sensing crop nitrogen status with fluorescence indicators. a review", *Agron. Sustain. Dev.*, vol. 32, no. 2, pp. 451–464, 2012.

[25] G. E. Box, H. W. G., and H. J. Stuart, *Statistics for Experimenters*, Wiley, Ed. 1978.

[26] A.-M. Carstensen, T. Pocock, D. Bånkestad, and T. Wik, "Remote detection of light tolerance in basil through frequency and transient analysis of light induced fluorescence", *Computers and Electronics in Agriculture*, vol. 127, pp. 289–301, 2016.

[27] A. Gitelson, O. Chivkunova, T. Zhigalova, and A. Solovchenko, "In situ optical properties of foliar flavonoids: Implication for non-destructive estimation of flavonoid content", *J. Plant Physiol.*, vol. 218, pp. 258–264, 2017.

[28] F. Morales-Flores, K. S. Olivares-Palomares, M. I. Aguilar-Laurents, J. F. Rivero-Cruz, B. Lotina-Hennsen, and B. King-Díaz, "Flavonoids affect the light reaction of photosynthesis in vitro and in vivo as well as the growth of plants", *J. Agric. Food Chem.*, vol. 63, no. 37, pp. 8106–8115, 2015.

[29] D. W. Lawlor, *Photosynthesis*, Third, B. S. P. Limited, Ed. Garland Science, 2001.

PAPER D

Stress detection using proximal sensing of chlorophyll fluorescence on canopy level

Linnéa Ahlman, Daniel Bånkestad, Sammar Khalil,
Karl-Johan Bergstrand, Torsten Wik

AgriEngineering,
vol. 3, pp. 648–668, 2021

The layout has been revised.

Abstract

Chlorophyll fluorescence is interesting for phenotyping applications as it is rich in biological information and can be measured remotely and non-destructively. There are several techniques for measuring and analyzing this signal. However, standard methods available use rather extreme conditions, e.g. saturating light and dark adaption, which are difficult to accommodate in the field or in a greenhouse and, hence, limit their use for high-throughput phenotyping. In this article we use a different approach, extracting plant health information from the dynamics of the chlorophyll fluorescence induced by a weak light excitation and no dark adaption, to classify plants as healthy or unhealthy. To evaluate the method, we scanned over a number of species (lettuce, lemon balm, tomato, basil, and strawberries) exposed to either abiotic stress (drought and salt) or biotic stress factors (root infection using *Pythium ultimum*and leaf infection using Powdery mildew *Podosphaera aphanis*). Our conclusions are that, for abiotic stress, the proposed method was very successful, while, for powdery mildew, a method with spatial resolution would be desirable due to the nature of the infection, i.e., point-wise spread. *Pythium* infection on the roots is not visually detectable in the same way as powdery mildew; however, it affects the whole plant, making the method an interesting option for *Pythium* detection. However, further research is necessary to determine the limit of infection needed to detect the stress with the proposed method.
Keywords: abiotic stress; biotic stress; classification; fluorescence dynamics; lettuce; lemon balm; tomato; basil; strawberries

1 Introduction

Modern advanced greenhouses are increasingly equipped with control functionalities. The temperature, humidity, CO_2-concentration, and light intensity can be controlled to optimal values, and irrigation and fertilization can be automated [1]. An interesting development for automated and efficient precision agriculture is the detection and diagnosis of plant stress. Standard

methods for stress detection are often destructive or disruptive [2] and, hence, not an option for on-line detection.

However, much research has been carried out in the area of optical sensors [3] for measuring the reflected and fluorescent light from the canopy as a mean for non-distruptive remote sensing of stress. Even though many methods have been suggested, sensor-based phenotyping is still at an early stage of development and not yet commonly applied in the field [3], [4]. Thus, there is still a need of more research to develop reliable and cost-effective sensors for stress detection [2].

The light energy absorbed by the plants is used for photosynthesis, reemitted as heat, or reemitted as fluorescence. This has made fluorescence an indispensable tool for studying photosynthesis in a wide range of applications [5], [6]. In particular, if stress factors influence the plants in a way such that the photosynthesis is affected one would expect an influence on the fluorescence response as well.

Fluorescence is classically measured and analyzed using a pulse amplitude modulation fluorometer (PAM) and requires measurements from both fully dark adapted plants and plants at fully saturating light [7]. In practice, this restricts its use to mainly on-leaf measurements. Another, completely different, fluorescence based method is sensing of solar induced fluorescence (SIF) [8], [9]. This is a passive method, done remotely on an airborne scale, measuring the fluorescence of a whole field, for example.

In between remotely sensed and on-leaf level sensed fluorescence, there is proximal sensing [10]. One method using proximal sensing of fluorescence is the laser induced fluorescence transient (LIFT) technique [11]. A blue laser projects a collimated beam onto the leaves, in flashlets of 1.6 µs and in excitation protocols with up to 7500 flashlets [12]. The emitted fluorescence at 690 nm is collected and then used to determine photosynthetic properties. The LIFT device can be used both in labs and in the field, at distances up to 50 m [13]. Another innovation in the field of proximal sensing and fluorescence measurements, was presented by Urschel and Pocock [14]. It uses a chlorophyll *a* fluorometer, developed to capture canopy level red and far-red fluorescence (i.e., the peaks around 685 and 740 nm), induced by saturating light pulses. The instrument, however, is mainly developed to monitor growth.

There is a lot of ongoing research on advanced optical sensors for stress detection (see review articles [2], [4], [15]). A wide range of spectral and spatial resolutions on the sensors are used; fluorescence spectroscopy [16], [17] and multicolour fluorescence imaging [18] as well as hyperspectral imaging [19]–[22]. Such equipment generates large amounts of data and one way of handling that is to use machine learning algorithms for feature selection [21]

as well as for classification. For a review of classification of biotic stress using machine learning [23].

Not only different types of sensors are under investigation, also many different types of light protocols are used when gathering data. In addition to referring to the reviews, we highlight a few recent and, from our point of view, particularly interesting studies: Sun *et al.* [24] investigated three different mutants of *Arabidopsis* and their resistance to drought stress. Kinetic chlorophyll fluorescence imaging data was collected at a distance between the sample and the lens of about 20 cm. The plants were subjected to dark adaption for 15 min, followed by a measurement sequence of 200 s, where the light protocol consisted of several saturating light pulses in a dark background or in a constant actinic background light. Deep learning methods were applied to extract features, which were then used as inputs to a machine learning classification algorithm.

Blumenthal *et al.* [25] used video imaging data from a prototype set-up (GrowScanner, GrowTech Inc). Their process starts with dark adaption, followed by light excitation and measurements of the fluorescence intensity on one point of the leaf during 15 s. The smoothed intensity signal, as well as its derivative, are used as inputs to an unsupervised machine learning algorithm (Hidden Markov Models), to cluster plants with respect to type of stress and stress level.

Römer *et al.* [17] used a compact fiber-optic fluorescence spectrometer with a laser as excitation source, placed a few millimeters from the leaf and measuring the spectrum with a resolution of 2 nm in the range 370-800 nm. To reduce the numbers of features piecewise polynomials were fitted to the data and a (Support Vector Machine) classifier could then, with a high accuracy, distinguish between healthy and unhealthy wheat leaves.

All though showing promising results, all the methods above rely on saturating light and/or dark adaption, which are difficult to accomodate in the field or in a greenhouse. The measurements used for stress detection in this study are based on the dynamic fluorescence response (DFR), i.e., dynamic characteristics of the fluorescence response to weak and long light excitation pulse, without prior dark adaption. A spectrometer was used to measure fluorescence on canopy level, i.e., through proximal sensing of fluorescence.

We have previously shown correlation to photosynthesis [26]–[28] and used it for growth tracking [29] and for light stress detection [30]–[32]. In the latter work, the variations in the DFR originating from a weak excitation from a blue LED light was used for light stress detection. The dynamics in the response in the fluorescence signal on minute-scale could be used to distinguish between different light stress levels.

We hypothesized that it is possible to distinguish between healthy and various kinds of abiotically or biotically stressed plants, by analysing the information in the fluorescence signal. We investigated this by using a method similar to the DFR-method and extracted features from the dynamic responses, to be used in a machine learning classification context.

Several stress factors were scanned: drought (lettuce) and salt stress (lettuce and lemon balm), root infection with the fungal pathogen *Pythium ultimum* (basil, tomato, and lettuce) and infection with the fungal pathogen for Powdery mildew, *Podosphaera aphanis* (strawberries). The strengths of this method is that the measurements are done on-line, remotely on canopy level, and that the plants neither need to be dark adapted nor exposed to saturating light.

Furthermore, market available LED lamps were used in the experiments, and the blue channel was used to construct the weak excitation signal in the form of a positive step change. For this study, a spectrometer was used but a simpler, cheaper type of photodiode with a bandpass optical filter could be applicable. In such case, it could be economically justified to distribute sensors over entire greenhouses.

2 Materials and methods

A variety of different plant species and stress factors have been investigated in this screening study where proximal fluorescence step response measurements were made on one or multiple plants at a time.

2.1 Plant materials and Cultivation conditions

The abiotic stress experiments were conducted at Heliospectra PlantLab in Gothenburg, while the biotic stress experiments were conducted at the Swedish University of Agricultural Sciences (SLU), Alnarp, Sweden. All experimental setups include both healthy reference plants and plants exposed to stress factors.

Abiotic stress

The abiotic stress factors investigated were salt and drought stress. All these tests were performed in an indoor growing facility where light, temperature and humidity were controlled (200 $\pm$ 20 µmol m^{-2} s^{-1}, 22/16 °C day/night temperature, RH 60%). Two cultivars of lettuce (*Lactuca sativa* cv. Great lakes 118, referred to as lettuce 'a', and another cultivar from a commercial

grower in Sweden, referred to as lettuce 'b') were used for measurements for both stress factors. The measurements were conducted around 4 weeks after sowing.

For salt stress, additional measurements were made on a third cultivar of lettuce (*Batavia lettuce* cv. Othilie^{RZ}, referred to as lettuce 'c') and lemon balm (from a commercial grower in Sweden). Those measurements were conducted 4–6 weeks after sowing. The plants were grown in a mix of 2 parts of soil and 1 part of vermiculite. Sample sizes were, 7 pots of each lettuce 'a' and 'b' (2 salted, 2 dried, 3 reference), 20 pots of lettuce 'c' (9 salted, 11 reference) and 14 pots of lemon balm (8 salted, 6 reference). The total number of measurements conducted were; 23 for lettuce 'a' (15/4/4 on ref/salt/dry), 31 for lettuce 'b' (15/8/8 for ref/salt/dry), 27 for lettuce 'c' (15/12 for ref/salt) and 26 for lemon balm (16/10 on ref/salt).

The plants in the reference group were watered every morning. For the salt stressed group, the daily watering was replaced by watering with salty water (200 mM NaCl), starting the day before the first measurement. Hence, they were assumed to become increasingly stressed over time. The plants in the drought stress group received no water one day before the first measurement and were further on only occasionally watered with a lower amount of water. This was to avoid wilting within the week that the measurements were collected. The moisture content in the soil was monitored as a reference of the drought level.

Biotic stress

Root infection with Pythium ultimum
Six pots of each species; basil (*Ocimum basilicum* cv. Basilikum), tomato (*Solanum lycopersicum* cv. Picolino), lettuce 'a' and 'b' (see section 2.1) were planted for the experiment with the root pathogen *Pythium ultimum*. Unfortunately, one tomato did not grow, hence, one sample less of that species was available. The plants were grown in a greenhouse in Alnarp, Sweden, during sunny days in June 2020. No supplemental light was used and RH was 80%. The temperature varied over the day and peaked above 30 °C.

An inoculum of *Pythium* was prepared as described by Hultberg *et al.* [33]. Briefly, mycelium from *Pythium* grown on PDA (Difco 213400) were transferred to and grown on water agar plates for two days. Small pieces (1 cm × 1 cm) were then cut from the periphery of the colony and transferred to a Petri dish with 15 mL of cleared fruit juice broth (11.5 g of rolled oats boiled with 125 mL of V8 fruit juice (Friggs, Sweden) and 500 mL water). The suspension was centrifuged for 15 min at 500 g (Avanti J-20, Beckman Coulter,

CA, USA).

The supernatant was diluted with water to 625 mL, 0.94 g of $CaCO_2$ was added, and the broth was autoclaved. The Petri dishes were incubated in darkness for three days at 25 °C. The mycelium was washed twice in an autoclaved mineral solution (0.145 g $Ca(NO_3)_2$, 0.012 g $MgSO_4$, 0.099 g KH_2PO_4 and 0.016 g $FeCl_3$, L^{-1}) and once in autoclaved distilled water.

The mycelium was then transferred to Petri dishes with 15 mL of autoclaved distilled water, incubated at 40 °C for 30 min and then transferred to room temperature. The zoospores were released after about 1 h. The zoospore suspension was carefully collected in sterile vessels, and zoospores were counted in a haemocytometer.

The fungus was grown for 3 weeks at 22 °C in 20 mL of Schmitthenner's medium. The mycelium was briefly homogenized in a blender and diluted with NaCl to 3×103 CFU mL^{-1} (Colony forming unit) as enumerated on PDA (Potato Dextrose Agar) media containing 200 mg L^{-1} kanamycin. The *Pythium* suspension was added to the sowing soil/substrate three times: at 3, 4, and 5 weeks after sowing. Every week, two to five measurements were conducted on each plant species and each group (ref/infected).

Leaf infection with Podosphaera aphanis

For the experiment with the leaf pathogen of Powdery mildew, *Podosphaera aphanis*, strawberry cuttings were planted in pots and grown in the greenhouse. Out of the 90 plants, 1/3 were moved to another room in the greenhouse where they were infected with powdery mildew. The infection was done with help of other heavily infected plants that were placed among the plants to be infected and with a brush the spores were moved to those plants. This was done daily throughout the whole experiment.

Four days after infection, all plants were moved into a growth chamber, with one room for the infected plants and one identical room for the reference plants. This is referred to as day 1 (week 1) of the experiment, from which the measurements started and continued for one month. The light intensity was 300 $\mu mol\, m^{-2}\, s^{-1}$ (8:00 a.m.–10:00 p.m.) and the temperature 22 °C. RH was initially 60%; however, from day 3, it was increased to 70% (and 85% at 2:00 p.m.–6:00 p.m.). The increased humidity was to enhance the spread of pathogen.

The experimental unit, in which the fluorescence step response measurements were conducted, was placed in the room of the infected plants. To reduce the risk of spread of pathogen into the room with healthy plants, no plants were moved back there. Thus, the healthy plants were consumed as reference once they had been subjected to measurements, this being the reason for starting with 2/3 of the plants in the healthy group.

2.2 Experimental setup

Here we present information about the experimental unit, i.e. the box mounted with lamps and spectrometers to which the plants were moved for measurements, as well as the light scheme used to extract information in the fluorescence signal. The data preparation of the fluorescence signal and the used reference measurements are also described.

Experimental unit

As the abiotic and biotic stress experiments were conducted at different locations (Gothenburg and Alnarp, Sweden), two different experimental units were used. The only thing that differed between them was the dimensions of the units, 2 × 1 × 1 m (H × W × D) in Gothenburg and 2 × 1 × 0.8 m in Alnarp. The units consist of aluminum profiles that hold white, highly diffusive, and reflective walls in place. At the top, three Heliospectra LX lamps are mounted; two for background light and one for excitation light, all placed about 1.5 m above the plants.

A spectrometer (STS, Ocean Insight, Orlando, FL, USA) was placed on canopy level, facing the lamps, to measure incident light with an integration time of 0.1–0.2 s, depending on the light intensity. A second spectrometer (QE65000, Ocean Insight, Orlando, FL, USA) was equipped with a 600 µm optical fiber, placed in between the lamps, and pointing downwards, thus, measuring the reflected and fluorescent light from the plants. As the fluorescence signal is relatively weak, the integration time was long (normally 0.8 s, in a few abiotic stress experiments even 1–2 s), to get a stable signal. The lamps and the spectrometers were controlled with a scheme programmed in Matlab (Mathworks Inc., Natick, MA, USA).

Light scheme

The plants were moved one at a time (two at a time for strawberries) to the experimental unit for the fluorescence step response measurements without any dark adaption. The lamps first hold the (lowest) background light for a few minutes for the plants to adapt to the new light level. When the light scheme starts it keeps the background light level for another 4–5 min, whereafter a blue constant excitation light (30–70 $\mu mol\, m^{-2}\, s^{-1}$) is added over 3 min. This is sequentially repeated for several background light levels. An example is shown in Figure 1, where (a) is the incident light within the PAR region (400–700 nm), and (b) is the fluorescence, integrated over wavelengths 720–760 nm.

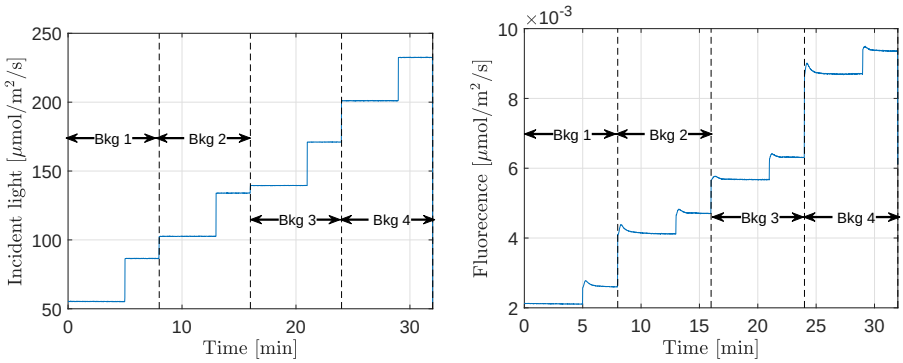

(a) Incident light.

(b) Fluorescence signal.

Figure 1: (a) Incident light (background and excitation) within PAR, repeated for four different background light levels. (b) Fluorescence signal (integrated over wavelengths 720-760 nm).

An overview of all settings for the different experiments are presented in Table 1. The light levels presented are the ones measured during the experiments. The variation in excitation light intensity were not intended and were only a result of different setups. Regarding the light intensity levels, we were initially interested in scanning a very wide range of intensities. However, based on the results from the salt stress experiments, slightly lower light intensities were used for the remaining abiotic stress experiments.

In the *Pythium* setup, higher light intensities were chosen for basil and tomato, compared to for lettuce, as they were expected to handle high light better. The powdery mildew setup started with a very small pilot study, were four different light levels were included (110, 215, 275 and 400 µmol m^{-2} s^{-1}), whereof the two lower ones looked the most promising and were thus chosen for the main setup.

Data preparation

The light in the region 400-700 nm is considered as the photosynthetically active radiation (PAR), and therefore the incident light detected by the spectrometer was integrated over this wavelength interval. This was considered as the input signal to the system. The output signal was the chlorophyll *a* fluorescence, *ChlF*, integrated over the wavelength span 720–760 nm. The ChlF has two peaks; one at 685 nm and one at 740 nm. However, earlier research has shown a stronger correlation between photosynthesis and the fluorescence signal in the 740 nm region (compared to the 685 nm region) [27], hence the

Table 1: The settings for all experimental sets.

	Abiotic Stress		**Biotic Stress**	
Stressor	**Salt & drought**	**Salt**	**Pythium**	**Powdery mildew**
Crop species	Lettuce 'a', Lettuce 'b'	Lettuce 'c', Lemon balm	(*i*) Lettuce 'a', Lettuce 'b', (*ii*) Basil, Tomato	Strawberries
Growing environment	Closed	Closed	Greenhouse	Closed*
Bkg light	5 min	4 min	5 min	5 min
µmol m^{-2} s^{-1}	55, 110, 135, 200	85, 215, 465, 760	(*i*) 110, 215, 275 (*ii*) 215, 275, 405	110, 110, 215, 215
Excitation light	3 min	3 min	3 min	3 min
µmol m^{-2} s^{-1}	30	45	70	70

* The strawberries were grown in a greenhouse, prior to the experiment.

peak choice in this setup.

To enable comparisons between sets with different background light, the data was normalized. The ChlF curves for each background light level were first shifted to an intensity equal to zero just before the excitation step started and then normalized such that the response signal was (approximately) equal to one at the end of the excitation, according to

$$y_{normalized} = (\text{raw data } - y_{zero})/y_{one}, \tag{D.1}$$

where

y_{zero} = mean value of ChlF the last 1 min of the background light level, and
y_{one} = mean value of ChlF the last 1 min of the excitation.

Two parameters that we paid extra attention to were the maximal fluorescence value during the excitation, referred to as the peak value, and the peak time, which is the time from the start of the excitation to the time the peak value occurs (Figure 2). These values were extracted from smoothed data (window width 5 samples) to decrease the impact of noise.

When interested in how dispersed measurements in a sample are, we use

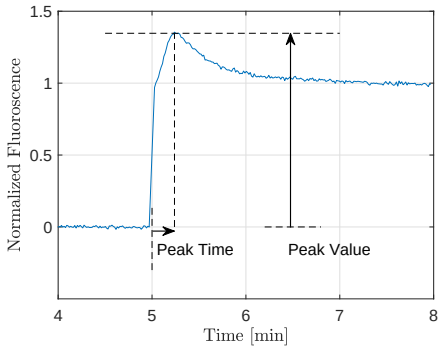

Figure 2: Arrows showing the Peak Time and the Peak Value. Peak value is the maximal value of the normalized fluorescence. Peak time is the time evolved from the time the excitation light is added until the peak value is reached.

the standard deviation (std), defined as

$$std = \sqrt{\frac{1}{n-1}\sum_{i=1}^{n}(y_i - \overline{y})^2}, \tag{D.2}$$

where n is the number of samples, y_i is measurement i and $\overline{y}$ is the mean value of the measurements. When interested in how close the sampled mean and the true population mean are to each other, the standard error of the mean, defined as

$$sem = \frac{std}{\sqrt{n}}, \tag{D.3}$$

was considered instead.

To verify whether two parameters statistically differ from each other, for example whether the mean value μ (of the peak time, or the peak value) differs between the healthy and the stressed group, a two sampled t-test was used [34]. Then the null hypothesis (H_0) and the alternative hypothesis (H_1) were formulated according to

$$\begin{aligned} H_0 &: \mu_{\text{healthy}} = \mu_{\text{stressed}} \\ H_1 &: \mu_{\text{healthy}} \neq \mu_{\text{stressed}} \end{aligned} \tag{D.4}$$

where μ was the mean value of each group.

Reference measurements

Abiotic stress
In the drought stress experiment the volumetric water content in the soil was measured with an EC-5 (METER Group Inc., Pullman, WA, USA).

In the salt stress experiment, the plants continued to get salty water throughout the experiment, with a consequent accumulation of the total amount of salt added. Hence, days after experimental start is a measure assumed to correlate with stress level. No other explicit measure of stress level was used.

Biotic stress
Three weeks after *Pythium* inoculation, the plants were harvested and separated into two parts: the root part and the part with the leaves together with the stems. These parts were subjected to dry weight measurements. The method for estimating the amount of *Pythium* on the roots is described in [35].

About 20 g of fresh weight roots was first macerated in a mortar for 2 min after the addition of 50 mL of detergent solution (0.1% peptone and 0.2% sodium hexametaphosphate). The mixture was then shaken at 200 rpm for 20 min at room temperature. An amount of 1 mL of the mixture was serially diluted in 9 mL NaCl, and 100 µL volumes of the serial dilution were spread, in triplicates, on PDA-plates containing 200 mg L^{-1} of kanamycin after incubation of the plates in 25 °C for 24 hours. Based on colony counting, the CFU g^{-1} DW root was calculated.

The maximum photosynthesis (A_{max}) was measured at a light intensity of 1000 µmol m^{-2} s^{-1} using an infra-red gas analyser photosynthesis instrument (LCPro+, ADC Bioscientific, Hoddesdon, UK). The light was supplied using the internal LED-array with red and blue LEDs. Measured values were allowed to stabilize for 20 min before readings. The measurements were conducted on experimental day 11 (on tomato, basil, and lettuce 'a') and again on day 19 (on tomato and basil).

The strawberries in the powdery mildew experiment were visually inspected throughout the experiment to get an idea of how the mildew spread. Figure 3 shows an example of different degrees of powdery mildew infection.

3 Results

3.1 Abiotic stress

The fluorescence step response was measured on lettuce 'a' and 'b', on healthy, dry, and salt stressed plants. Figure 4 shows all the fluorescence responses

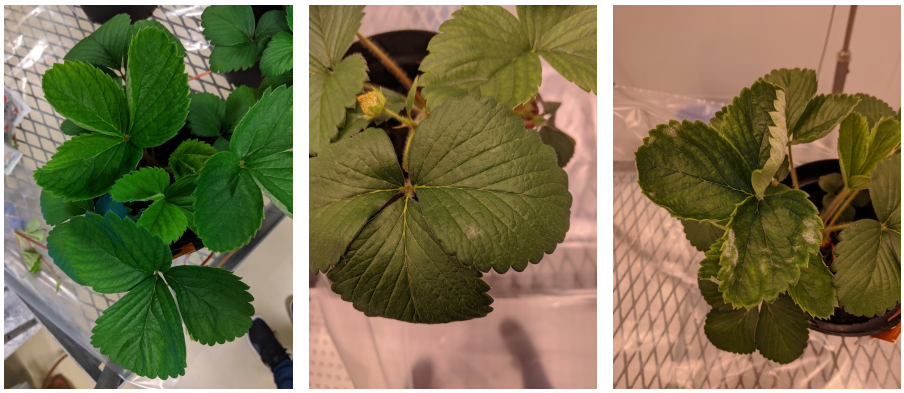

Figure 3: Powdery mildew infected plants; left—reference plant without visual symptom, middle—infected level 1, and right—infected level 2.

(normalized according to Eq. D.1) for lettuce 'a' at the lowest background light level. Green dotted lines correspond to reference plants, solid orange lines are the salt stressed plants, and the red dashed lines are the dry ones. As can be seen, the initial dynamics after the step excitation differ between the plants depending on their conditions.

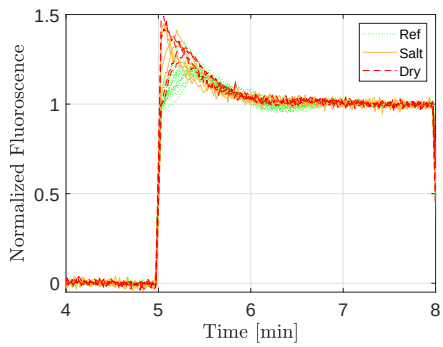

Figure 4: The fluorescence response of the first excitation for all biotic stress experiments on lettuce 'a'. Green dotted lines: healthy reference plants. Orange solid lines: salt stressed plants. Red dashed lines: drought stressed plants.

For each of the four different background light levels (ranging from 55 to 200 µmol m^{-2} s^{-1}), the peak time and the peak value (for definition see Figure 2) of the responses were extracted. The results for lettuce 'a' are presented in Figure 5 and for lettuce 'b' in Figure 6. The stressed plants generally had

a shorter peak time and a higher peak value. In Appendix (Table 6), a summary of the data is presented, where the time axis is ignored, and the data is divided into groups of healthy, salt and drought stressed.

A two sampled t-test was used to evaluate whether the mean peak time and/or the mean peak value are significantly different between stressed and healthy plants. For all groups (lettuce 'a' and 'b', salt and drought stressed, peak time and peak values), the differences were significant at a confidence level of at least 0.95 for the first and second background light level, and for most combinations also at the third and fourth background light level. Furthermore, one can notice a trend in the figures, that the higher the background light level is, the lower the mean peak time.

The peak time also decreased for the salt stressed plants as time evolves (Figure 6(a), Bkg 1), a result that could be seen as a sign that the plants are getting more and more stressed the longer they were watered with salty water. The moisture content in the soil were measured in 14 of the experiments. Figure 7 shows how the peak time and peak value (for the lowest background light) vary with the moisture content. The results show that the measured moisture content were indeed lower in the dried pots and that the moisture content is positively correlated with peak time and negatively correlated with peak value.

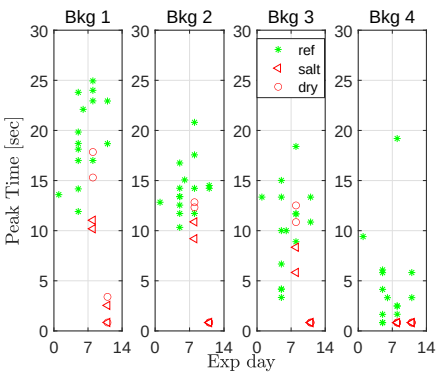

(a) Lettuce 'a'. Peak time.

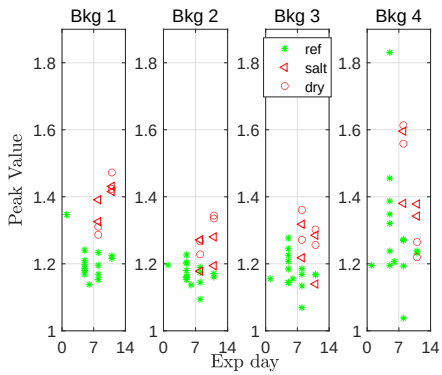

(b) Lettuce 'a'. Peak Value.

Figure 5: Peak time (a) and peak value (b) of the responses at all four background light levels for healthy (ref) as well as salt and drought stressed lettuce 'a'.

In an additional setup, lettuce 'c' and lemon balm were evaluated for salt stress. Higher background light levels were included in this setup (85–760 $\mu mol\,m^{-2}\,s^{-1}$). For the two lower light levels (85 and 215 $\mu mol\,m^{-2}\,s^{-1}$), the

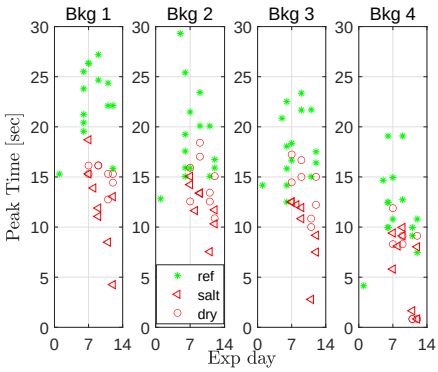

(a) Lettuce 'b'. Peak time.

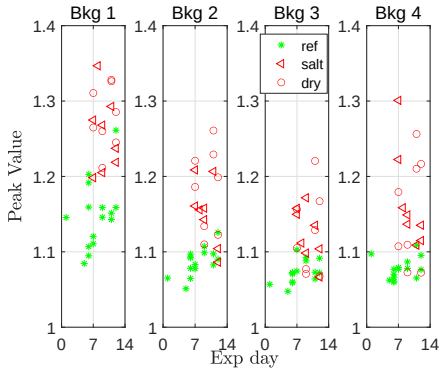

(b) Lettuce 'b'. Peak Value.

Figure 6: Peak time (a) and peak value (b) of the fluorescence step response for measurements on lettuce 'b'; healthy (green star), as well as salt (red triangle) and dry (red circle) stressed. First subplot (on a and b) corresponds to the lowest background light level (Bkg 1).

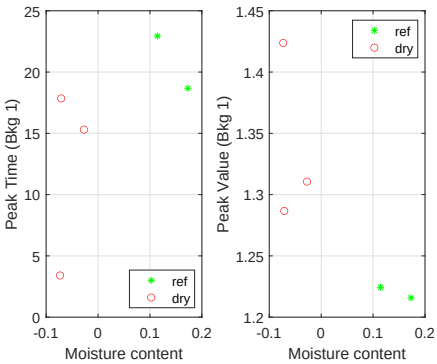

(a) Lettuce 'a'.

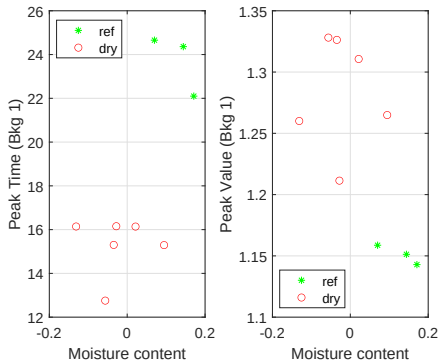

(b) Lettuce 'b'.

Figure 7: Peak time and peak value at the lowest background light level vs. relative moisture content (higher value more irrigated) for (a) lettuce 'a' and (b) lettuce 'b'.

results were in line with the previous findings. The fluorescence step response can indeed also here be used to distinguish between healthy and stressed plants both for lettuce 'c' and for lemon balm, with shorter peak time and higher peak value for stressed plants. The distinction was even more clear for the lemon balm case.

In Table 2, the peak times and peak values for the lowest background light level are summarized. This shows the mean value and the standard deviation of the mean for each group: healthy and salt stressed (for each measurement day). The differences of the mean values were significant (with a confidence of at least 95%), even when comparing the healthy group with only the "least" stressed group, i.e., salt treated (day 1).

Table 2: Peak time and peak values (mean values and standard error of the mean, SEM) of responses at the lowest background light level, for healthy and salt stressed lemon balm and lettuce 'c'.

		Peak Time		**Peak Value**	
Lettuce 'c'	Sample size	Mean	SEM	Mean	SEM
Healthy	14	26.31	2.06	1.107	0.007
Salt treated (day 1)	4	17.75	0.48	1.142	0.015
Salt treated (day 2)	4	17.00	0.82	1.215	0.030
Salt treated (day 4)	4	13.50	0.50	1.278	0.017
Lemon balm					
Healthy	16	15.69	0.66	1.145	0.015
Salt treated (day 1)	5	5.60	1.47	1.247	0.045
Salt treated (day 3)	5	3.40	0.24	1.270	0.027

For increasing background light levels, there were less but faster dynamics in the fluorescence step responses. As a consequence, the peak value occurred within the first or second sample for all measurements at the two highest background light levels (465 and 760 µmol m^{-2} s^{-1}), and for the salt stressed plants also at the 215 µmol m^{-2} s^{-1} light level. Furthermore, the steady-state level of the fluorescence was not reached within the 4 min the light was held constant, in contrast to the two lower light levels, where either steady-state was reached or the remaining transients were very small. This also complicates the automation of the data treatment.

To conclude, these experiments shows that it is indeed possible to detect salt and drought stress with proximal measured fluorescence dynamics on canopy level and it is preferable to then have a background light of 200 µmol m^{-2} s^{-1}

or less.

3.2 Pythium ultimum

Fluorescence step responses were measured once a week for three weeks, starting the week the pathogens were added (except for lettuce 'b', where only measurements from the last two weeks are available). Figure 8 shows the peak time as well as the corresponding peak value of the responses of lettuce 'b' for the three different background light intensities.

For each week, the peak time is lower in the infected group compared to the reference group, at the lowest background light level (Bkg 1). The difference was significant at a confidence level of 0.95 for week 3 but not week 2 (but at a confidence level of 0.90 it is). At higher background light, the majority of the registered peak times are at the first sample, making comparisons meaningless. All values are available in Appendix (Table 7). The peak value, on the other hand, showed no distinction between the healthy and infected groups. Note that the sample size is small (four measures week 2 and six measures week 3); therefore, more data is needed to confirm differences with a high level of significance.

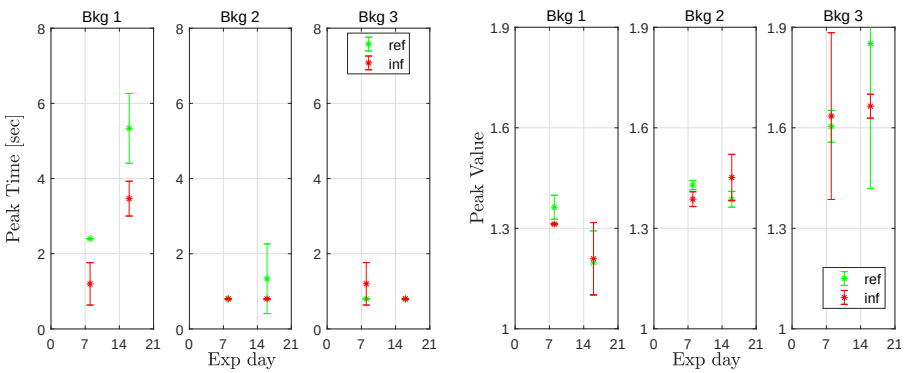

(a) Lettuce 'b'. Peak time.

(b) Lettuce 'b'. Peak value.

Figure 8: The fluorescence step response peak time (a) and peak value (b) for lettuce 'b' at three different background light levels. Mean value and std for 2–5 measurements each week and for each group (reference and infected with *Pythium ultimum*).

For lettuce 'a', basil, and tomato, it was not possible to distinguish between healthy and infected plants when inspecting the fluorescence step responses (Figures 9 and 10). However, the response parameters changed over time such that the peak time decreased and the peak value increased over the three

weeks. Comparing the peak times from all measurements week 1 with week 2 or 3, they significantly (at a confidence level of 0.95) differs for lettuce 'a', basil, and tomato, at all background light levels. The peak values significantly differs when comparing measurements week 1 with week 3, for all species and at all background light levels. Data available in Appendix (Table 8).

At the end of the experiment, the lettuce and basil had passed the appropriate harvest day, and the tomato would have needed transplanting for optimal development. The measurement were made in a sunny period when it was warm in the greenhouse. On day 1, the temperature varied from 19 °C at night up to 28.5 °C at noon. On day 4, the range had increased to 20-31 °C. Unfortunately, further temperature measurements were lost; however, but the authors believe the increasing indication of stress (shorter peak time and higher peak value) with time is a heat stress response.

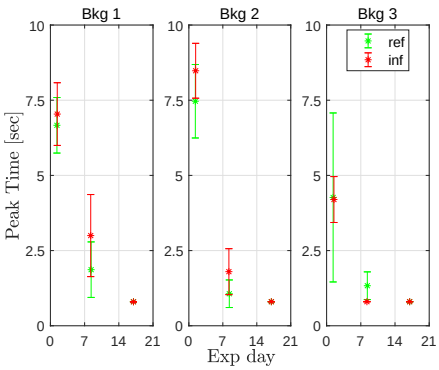

(a) Lettuce 'a'. Peak time.

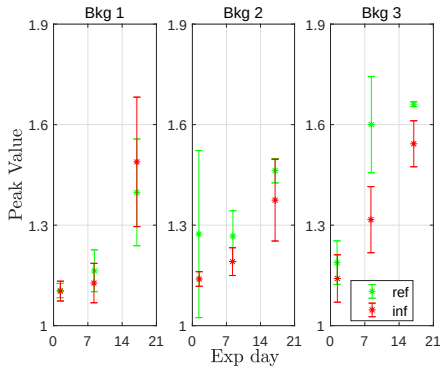

(b) Lettuce 'a'. Peak value.

Figure 9: The fluorescence step response peak time (a) and peak value (b) for lettuce 'a' at three different background light levels. Mean value and std for 2-5 measurements each week and for each group (reference and infected with *Pythium ultimum*).

The reference measurements are summarized in Table 3; dry weight (DW; of leaves, stems and roots), the amount of pathogen on the roots (per dry weight roots) and the maximal photosynthetic rate. Each set contains 3 measurements and the mean values and the standard deviations (according to Eq. D.2) are presented in the table. All plant species (except lettuce 'a') had a lower dry weight in the infected group. However, the differences were small and not significant, indicating that the infection did not have a large impact on the photosynthesis of the whole plant. The amount of pathogens on the roots differed significantly between the different plant species. The highest

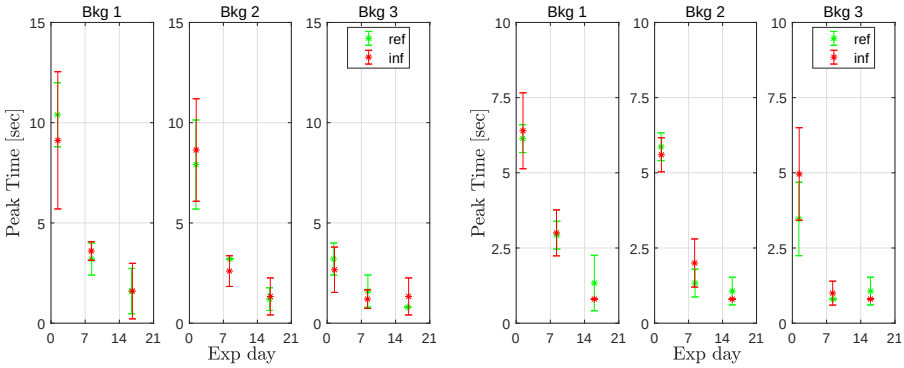

(a) Tomato. Peak time.

(b) Basil. Peak time.

Figure 10: The fluorescence step response peak time for tomato (a) and basil (b) at three different background light levels. Mean value and std for 2-5 measurements each week and for each group (reference and infected with *Pythium ultimum*).

Table 3: Reference measurements in the *Pythium ultimum* experiment. Mean values with standard deviations within parenthesis, of three measurements in each set.

	DW	**Pathogen**	**Maximal Photosynthetic rate**	
			Day 11	**Day 19**
	g	CFU g^{-1}DW root	µmol CO_2 m^{-2} s^{-1}	
Tomato				
Healthy	10.13 (2.65)		10.9 (1.80)	8.8 (0.65)
Infected	5.94 (5.23)	6.822 (0.009)	9.0 (0.99)	5.4 (3.73)
Basil				
Healthy	8.00 (0.31)		14.7 (3.59)	6.6 (0.64)
Infected	7.30 (1.50)	5.599 (0.019)	12.7 (2.69)	8.1 (1.25)
Lettuce 'a'				
Healthy	15.07 (1.31)		8.5 (2.53)	
Infected	16.54 (0.96)	6.543 (0.077)	3.6 (2.28)	
Lettuce 'b'				
Healthy	8.53 (1.30)			
Infected	7.65 (0.72)	7.538 (0.069)		

amount was found in lettuce 'b', whereas the lowest amount was found in basil.

This is in line with that it was only for lettuce 'b' where a statistically significant difference in the peak time was detected between healthy and *Pythium* infected plants. The maximal photosynthetic rate was measured on basil, tomato, and lettuce 'a' on day 11, and again on tomato and basil on day 19.

In line with the expectations that was concluded from the dry weight measurements, the photosynthetic rate measurements only indicated a slightly lower photosynthetic rate for the infected plants (and only in 4 out of 5 groups, where a group refers to one species and one measurement day), and the differences were not significant. However, there was a significant decrease in photosynthesis between day 11 and day 19. Hence the maximal photosynthetic rate seem to decrease more over time than as a consequence of the *Pythium* infection in this experiment.

3.3 Powdery mildew, Podospaera aphanis

In this setup, over 150 measurements were conducted in order to collect enough data to be used in a supervised machine learning classification algorithm. Unfortunately, the spread of powdery mildew was slower and more uneven than expected, thus, making it difficult to correctly label the data collected in the middle of the experiment.

For the first group of plants that were exposed to the infection—group w0—the infection started four days before the experiment started, i.e., week 0. They were placed in another (slightly warmer) room in the greenhouse, and, when the experiment started, all strawberries were moved to one out of two identical room in a closed environment. The intention was to infect more plants over the course of the experiment by moving them into the "infected room" after being subjected to fluorescence step response measurements.

In the same way, group w1 refers to the group that were infected during week 1, after being measured as reference. However, the infection did not evolve as anticipated. Table 4 shows the number of plants that visually showed signs of infection during the experiment. Inf 1 corresponds to very light symptoms and Inf 2 slightly more (Figure 3). A few plants were harvested every week, hence the decreasing total numbers of plants (the harvested leaves were frozen, as a backup for possible PCR-measurements to quantify the infection level). As a consequence of the low degree of infection, group w1 was excluded from the presentation of the data.

Figure 11 shows the peak value and peak time for the fluorescence step response after the first excitation at the lowest background light level (110

Table 4: Powdery mildew experiment. Numbers of plants that visually show signs of infection (Inf 1: very light symptom, Inf 2: slightly more). Total amount of plants decreases over time, as plants are harvested.

Day	**10**	**15**	**17**	**22**	**30**
Group w0					
No sign	26	12	6	2	0
Inf 1	3	12	18	14	3
Inf 2	0	2	2	6	13
% infected	10%	54%	77%	91%	100%
Group w1					
No sign	18	13	13	11	5
Inf 1	1	3	3	2	1
Inf 2	0	0	0	0	0
% infected	6%	19%	19%	15%	17%

$\mu\text{mol}\,\text{m}^{-2}\,\text{s}^{-1}$). The results are similar for the second excitation (same background light level). For the third and fourth excitation (both at light level 215 $\mu\text{mol}\,\text{m}^{-2}\,\text{s}^{-1}$) the mean value of the peak time is slightly lower and the mean value of the peak value is slightly higher.

Four groups are included in the presented figure: the reference group (green stars), infected week 0 (red triangles), and infected week 3/4 (blue circles/triangles). Hence, the plants of the blue marks had only been in the infected room for one week and had no visible symptoms yet, in contrast to group w0 in these weeks, and would thereby be expected to behave more similar to the healthy group than the infected group. However, there was no clear distinction between the healthy and infected groups, as shown in Figure 11.

The peak time for most of the measurements were around 10 s, which is relatively high, indicating that the plants appeared to be healthy. The only significant change is in week 5, when the peak time has decreased to around 5 s. This could be an indication of higher stress than the previous weeks and this occurs for plants in both groups. Looking at the mean of the peak value, there was only a distinction between the two groups during week 1 and week 5 (Table 5). The peak value was then higher for the infected plants.

During week 5, there were visible symptoms of powdery mildew in the infected group (and not in the reference group). Hence, it cannot be excluded that it was the powdery mildew infection that caused the differences in peak values. However, as the differences in peak values between the infected/healty is not consistent throughout the whole experiment, it is not likely that the

difference in week 1 is due to the infection.

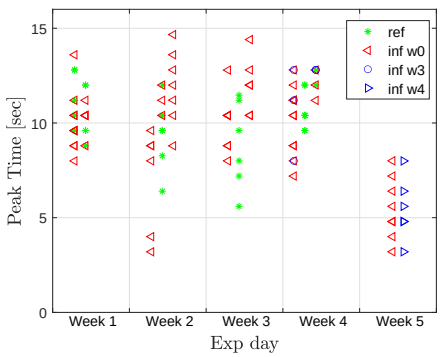

(a) Strawberries. Peak time.

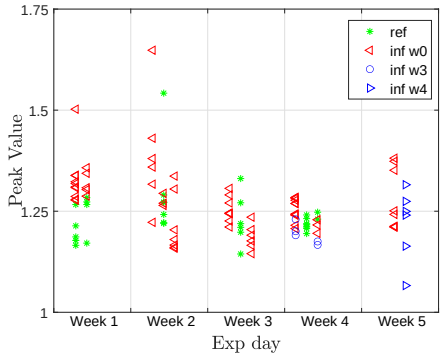

(a) Strawberries. Peak value.

Figure 11: Fluorescence step response (a) peak time and (b) peak value for powdery mildew infected strawberries at the lowest background light level. ref: healthy plants, inf w0: infected week 0, i.e., 4 days prior to first measurement, inf w3/4: measured as reference week 3/4, after that placed in the infected unit, having no visual symptoms yet.

Table 5: Powdery mildew experiment. Peak values at the first background light level, for ref and infected plants, week 1 and week 5.

		Peak Value		
Week	Group	**Mean**	**Std**	**Sem**
1	ref	1.223	0.049	0.016
1	inf w0	1.326	0.055	0.014
5	inf w3/4	1.218	0.090	0.037
5	inf w0	1.279	0.076	0.027

4 Discussion

The aim with this study was to test the hypothesis that it is possible to distinguish between healthy and stressed plants from variations in the dynamic fluorescence response (DFR). The DFR method applied here to detect stress is a modification of the method proposed in Carstensen *et al.* to analyze level of light stress [31]. In that work, transfer function responses were fitted to the step responses, and then the transfer functions were analyzed in the frequency domain using Bode plots. When applying this to the data presented here, an

autotomized fitting was difficult to achieve, and therefore, the time responses were analyzed instead—more specifically, the peak time and the normalized peak value.

These two features alone were sufficient to distinguish between healthy and abiotically stressed plants (drought and salt stress investigated), where faster dynamics (shorter peak time) and a higher normalized peak value were found to be indicators of stress. This stress response is also in agreement with the light stress experiments by Carstensen *et al.* [30], [31]. Hence, we concluded that abiotic stress (salt and drought) can be distinguished from healthy plants using DFR.

The experiments with biotic stress unfortunately have some deficiencies. In particular, this is the case in the set with *Pythium ultimum* infection; the sample size is small, a few reference measurements are lacking, and the plants were grown in a warm greenhouse, which likely led to heat stress. Generally, no significant difference could be detected between healthy and *Pythium* infected plants, with the applied DFR-method. Hence, we could not confirm the hypothesis for this stressor. It was only for lettuce 'b' the mean value of the peak time varied as a function of plant status; however, due to small sample size, it is hard to confirm differences on a high level of significance.

However, the measurements of pathogens on the roots showed that these were the plants with the highest occurrence of pathogens. Therefore, and due to the nature of the infection, i.e., a root infection that is difficult to visually detect, we suggest more research to determine if there is a critical level of infection required, in order for the method to work for detection of *Pythium* infection. Furthermore, in a stress detection setting where several step responses are measured (for example, several step responses every night), it is easier to detect differences compared to only singular measurements as was done in this study.

The plants in the *Pythium* setup were grown in a warm greenhouse, and we detected a significantly higher stress the third week compared to the first week, for all species included. It was likely heat stress that was detected, even though it cannot be excluded that it could be something else, such as malnutrition. Unfortunately, there is no data to neither confirm nor reject that. It was warm in the greenhouse during the *Pythium* experiments: day one it was 28.5/19 °C day/night temperature and day four it was 31/20 °C. Unfortunately, subsequent temperature data was lost but the outdoor weather continued to be warm and sunny, and this was the case also in the greenhouse.

The measurements of maximal photosynthetic rate (data for 5 out of 8 plant species and days were available), indicated a slight decrease as a consequence

of *Pythium* infection in most of the measurements; however, the decrease was larger when comparing measurements from day 19 and with the ones from day 11 (Table 3). The fact that the photosynthetic apparatus was only slightly affected by the infection but more affected over time can (at least partly) explain the fact that the proposed fluorescence detection method captured a difference over time (increased heat stress) but could not distinguish between healthy and infected samples.

For powdery mildew on strawberries, a pilot study with heavily infected plants indicated that the peak time and the peak value could be used to separate healthy and infected plants. However, in the main experiment the plants were never infected to the same degree, and it was also not possible to distinguish between the two groups, except from the peak value measurements during week 1 and week 5 (Table 5). Potentially, this is due to the infection in week 5; however, as the difference was not detected throughout the whole experiment, there is likely another explanation of the difference in week 1.

To start the infection, group w0 had to be moved to another room in the greenhouse (to ensure no infection of the reference group), in which the temperature was about 5 °C higher. This was done four days prior to the start of the experiment when all plants were moved to the controlled, indoor environment. The difference in fluorescence step response in the two groups during week 1 may, therefore, be because they reacted differently to the movement from the greenhouse to the indoor environment, either due to the powdery mildew or to the different temperatures they were exposed to in the greenhouse.

The method proposed here only measures the mean value of the fluorescence response over the entire canopy (two plants for the powdery mildew setup). Consequently, to be detected, a considerable part of the canopy must be affected. This is beyond the limit of acceptance for a detection method for powdery mildew. As this infection starts with a local infection, it would likely be more efficient to use a sensor with higher spatial resolution, e.g., a fluorescence camera. Possibly one could then detect specific areas of the plant that have a deviating step response signatures due to the infection.

The intention of using a machine learning algorithm to extract the most important features for classification of healthy/infected strawberry plants was unfortunately not possible. The infection did not spread at the rate that we expected, which led to uncertain annotation of the plants. However, it may still work to use the dynamic fluorescence response to generate input features to a classification algorithm. In such an algorithm, additional features can be added to increase the performance and to solve the problem of finding a general threshold value of, for example, the peak time or peak value, to classify

plants as healthy or not. Candidate features to investigate could be ambient conditions (temperature, humidity etc.), plant status (age, development state, species etc.) or other features from the fluorescence dynamics.

In the presented method, we measure the transient behavior of chlorophyll fluorescence. However, this is slightly different from standard methods, in the sense that we did not included dark adaption. A dark-adapted leaf that is illuminated with continuous (or modulated) excitation shows a characteristic change in chlorophyll *a* fluorescence intensity over time [36]. This is called the fluorescence transient, or the Kautsky effect, named after Hans Kautsky, who first reported this phenomenon in 1931 [37].

The fast part of this transient occurs within the first second of illumination and is called the OJIP transient curve; the fluorescence level at origin (O), followed by two intermediates (I, J) and finally the peak (P). The following, slower dynamics, SMT (semi-steady state, maximum, and terminal steady-state), occurs on the time scale of minutes [38].

Due to the current sample rate we use, normally 0.8 s, we cannot capture the behaviour of the fast transient (OJIP). Instead, the peak that we follow is likely something that is similar to the second maximum, M. A previous study on bean leaves [39] reported that the time of the M-peak decreased for an increased heat stress on the leaves. This is clearly in line with our results, in that a short peak time indicated plant stress.

Another finding from the conducted experiments, was that the distinction between healthy and stressed plants was easier to detect at low background light intensities. The higher the background light level, the faster the dynamics in the fluorescence step response for all plants, no matter of stress status, thus, making it difficult to distinguish between them, at least with the current sampling rate. This can be seen in Figures 6, 8–10, comparing the peak time at the first background light level with the latter ones.

Previous research on dark adapted pea leaves, showed that the shape of the fluorescence transient curve was very different depending on the excitation light level [40]. The excitation light from a LED with peak wavelength at 650 nm, at approximately 30, 300, and 3000 µmol m^{-2} s^{-1} were investigated. For the highest light, the slope from P to T was smooth, whereas, in the case of the lowest light, the semi-steady state S and second maximum M were pronounced. In our setup, we did not elaborate on the excitation light (it was always within 30–70 µmol m^{-2} s^{-1}); however, in addition to the excitation light, we also had different background light levels. Our finding—that the dynamics became faster at higher background light levels—might actually be the transition from a fluorescence curve where the M-peak is pronounced (low light) to the case where there is a smooth decrease from the P-peak to the

terminal steady state, T. Hence, at the higher background light, there is no "M-peak" to detect and, instead, the maximal value occurs in the "P-peak", which is within our first measured sample.

5 Conclusions

A method for plant stress detection is presented where the measurements can be done on-line, remotely on the canopy level, and the plants neither need to be dark adapted, nor exposed to saturating light. Furthermore, the equipment can be relatively simple. For this research a spectrometer was used; however, a simpler, cheaper type of photodiode with a bandpass optical filter could be applicable, and, in such case, could be distributed over a large greenhouse. Furthermore, ordinary (controllable) LED growth lights, already in place in many advanced greenhouses, were used to supply the (relatively weak) blue light used to excite a fluorescence response.

The results from this research show that the abiotic stress by drought and salt (and probably heat), can efficiently be detected by the suggested method. The examined biotic stress from powdery mildew *Podosphaera aphanis* (on strawberries) and the root infection *Pythium ultimum* (on two types of lettuce, basil, and tomato) could not be significantly distinguished from healthy plants.

However, the results indicate that, for a severe infection, the stress appeared to be detectable. For the root infection case, the disease is difficult to detect visually, and hence this is an interesting option. More experiments are then needed to determine if there is a critical level of infection for detection and, then, to decide whether it is an acceptable limitation or not.

Powdery mildew, on the other hand, does not affect the whole plant at start—instead, it spreads point-wise. Due to that nature, it will likely be more efficient to have a sensor with higher spatial resolution as it is desired to detect the mildew already at a stage when it is only visible on very small spots on single leaves.

Appendix

Data presented in Tables 6, 7, and 8, is from a two sampled t-test. If $\mathbf{h} = 1$, the null hypothesis (that the mean value of the two groups are equal, jf. Eq D.4) was rejected at significance level α (here $\alpha = 0.05$). **df**: degree of freedom of the test. **tstat**: value of the test statistic. **sd**: pooled estimate of the population standard deviation. **p**: the probability of observing a test statistic under the hull hypothesis (small values of **p** cast doubt on the validity

of the null hypothesis). **h**: hypothesis test result.

Table 6: Two way ANOVA table, comparing peak times and peak values in abiotic stress experiments. A, B, and C: lettuce 'a', reference, salt, and drought stressed plants. D, E, and F: lettuce 'b', reference, salt, and drought stressed plants.

Comparison		**Bkg light**	**df**	**tstat**	**sd**	**p**	**h**
group	parameter						
A and B	peak time	1	17	5.42	4.31	$4.6E^{-5}$	1
A and B	peak time	2	17	4.78	3.27	$1.8E^{-4}$	1
A and B	peak time	3	17	2.69	4.21	0.016	1
A and B	peak time	4	16	1.62	4.32	0.126	0
A and B	peak value	1	17	-6.85	0.05	$2.8E^{-6}$	1
A and B	peak value	2	17	-2.95	0.04	0.009	1
A and B	peak value	3	17	-2.06	0.06	0.056	0
A and B	peak value	4	16	-2.85	0.10	0.012	1
A and C	peak time	1	17	3.44	5.15	0.003	1
A and C	peak time	2	17	3.60	3.71	0.002	1
A and C	peak time	3	17	1.53	4.72	0.144	0
A and C	peak time	4	16	1.61	4.32	0.126	0
A and C	peak value	1	17	-5.20	0.06	$7.3E^{-5}$	1
A and C	peak value	2	17	-5.86	0.04	$1.9E^{-5}$	1
A and C	peak value	3	17	-4.42	0.05	$3.8E^{-4}$	1
A and C	peak value	4	16	-2.21	0.13	0.042	1
D and E	peak time	1	21	5.95	4.19	$6.7E^{-6}$	1
D and E	peak time	2	21	3.95	3.91	$7.3E^{-4}$	1
D and E	peak time	3	21	5.36	3.40	$2.6E^{-5}$	1
D and E	peak time	4	21	3.10	3.85	0.005	1
D and E	peak value	1	21	-5.15	0.05	$4.2E^{-5}$	1
D and E	peak value	2	21	-5.18	0.03	$4.0E^{-5}$	1
D and E	peak value	3	21	-4.92	0.02	$7.2E^{-5}$	1
D and E	peak value	4	21	-5.15	0.04	$4.2E^{-5}$	1
D and F	peak time	1	21	5.22	3.41	$3.5E^{-5}$	1
D and F	peak time	2	21	2.58	3.94	0.018	1
D and F	peak time	3	21	2.87	3.17	0.009	1
D and F	peak time	4	21	3.11	4.18	0.005	1
D and F	peak value	1	21	-6.74	0.04	$1.2E^{-6}$	1
D and F	peak value	2	21	-6.21	0.04	$3.6E^{-6}$	1
D and F	peak value	3	21	-3.45	0.03	0.002	1
D and F	peak value	4	21	-4.03	0.04	$6.0E^{-4}$	1

Table 7: Two way ANOVA table, comparing peak times and peak values for healthy (Ref) or *Pythium ultimum* infected (Inf) lettuce'b'. G: Ref week 2 (w 2), H: Inf w 2, I: Ref w 3, J: Inf w 3.

Comparison		**Bkg light**	**df**	**tstat**	**sd**	**p**	**h**
group	parameter						
G and H	peak time	1	2	3.01	0.40	0.095	0
G and H	peak time	2	2	-1.57	0.00	0.256	0
G and H	peak time	3	2	-1.00	0.40	0.421	0
G and H	peak value	1	2	1.98	0.03	0.186	0
G and H	peak value	2	2	2.28	0.02	0.150	0
G and H	peak value	3	2	-0.17	0.18	0.880	0
I and J	peak time	1	4	3.12	0.73	0.036	1
I and J	peak time	2	4	1.00	0.66	0.374	0
I and J	peak time	3	4	0.48	0.00	0.656	0
I and J	peak value	1	4	-0.15	0.10	0.889	0
I and J	peak value	2	4	-1.54	0.05	0.198	0
I and J	peak value	3	4	0.74	0.31	0.498	0

Table 8: Two way ANOVA table, comparing peak times and peak values for week (w) 1, 2, and 3, for plant in the *Pythium ultimum* setup. Plants are divided into groups independent of if being infected or not. Stress is detected over time, authors belief that heat stress is detected. K: tomato, week 1 (w 1), L: tomato, w 2, M: tomato, w 3. N: basil, w 1, O: basil, w 2, P: basil, w 3. Q: lettuce 'a', w 1, R: lettuce 'a', w 2, S: lettuce 'a', w 3.

Comparison		**Bkg light**	**df**	**tstat**	**sd**	**p**	**h**
group	parameter						
K and L	peak time	1	13	5.68	2.10	$7.5E^{-5}$	1
K and L	peak time	2	13	6.12	1.74	$3.7E^{-5}$	1
K and L	peak time	3	12	3.53	0.81	0.004	1
K and L	peak value	1	13	-3.61	0.10	0.003	1
K and L	peak value	2	13	-3.79	0.10	0.002	1
K and L	peak value	3	12	-3.12	0.23	0.009	1
K and M	peak time	1	11	6.00	2.34	$8.9E^{-5}$	1
K and M	peak time	2	11	6.60	1.88	$3.9E^{-5}$	1
K and M	peak time	3	10	3.46	0.87	0.006	1
K and M	peak value	1	11	-7.67	0.10	$9.7E^{-6}$	1
K and M	peak value	2	11	-5.92	0.11	$1.0E^{-4}$	1
K and M	peak value	3	10	-4.89	0.13	$6.3E^{-4}$	1
N and O	peak time	1	13	7.68	0.84	$3.5E^{-6}$	1
N and O	peak time	2	13	12.47	0.62	$1.3E^{-8}$	1
N and O	peak time	3	13	5.86	1.15	$5.6E^{-5}$	1
N and O	peak value	1	13	-0.36	0.17	0.724	0
N and O	peak value	2	13	-3.06	0.08	0.009	1
N and O	peak value	3	13	-1.55	0.24	0.146	0
N and P	peak time	1	12	11.14	0.87	$1.1E^{-7}$	1
N and P	peak time	2	12	19.83	0.44	$1.5E^{-10}$	1
N and P	peak time	3	12	5.36	1.20	$1.7E^{-4}$	1
N and P	peak value	1	12	-1.07	0.19	0.306	1
N and P	peak value	2	12	-4.40	0.10	$8.7E^{-4}$	1
N and P	peak value	3	12	-1.45	0.22	0.172	1

continuing on next page

Comparison group	parameter	Bkg light	df	tstat	sd	p	h
Q and R	peak time	1	13	7.68	1.10	$3.5E^{-6}$	1
Q and R	peak time	2	13	13.69	0.93	$4.2E^{-9}$	1
Q and R	peak time	3	12	4.83	1.24	$4.1E^{-4}$	1
Q and R	peak value	1	13	-1.72	0.04	0.108	0
Q and R	peak value	2	13	-0.55	0.12	0.590	0
Q and R	peak value	3	12	-3.60	0.13	0.004	1
Q and S	peak time	1	12	15.57	0.73	$2.5E^{-9}$	1
Q and S	peak time	2	12	16.31	0.83	$1.5E^{-9}$	1
Q and S	peak time	3	11	4.88	1.26	$4.9E^{-4}$	1
Q and S	peak value	1	12	-5.77	0.11	$8.8E^{-5}$	1
Q and S	peak value	2	12	-3.25	0.13	0.007	1
Q and S	peak value	3	11	-12.55	0.06	$7.3E^{-8}$	1

References

[1] R. R. Shamshiri, F. Kalantari, K. C. Ting, K. R. Thorp, H. I. A., C. Weltzien, D. Ahmad, and Z. M. Shad, "Advances in greenhouse automation and controlled environment agriculture: A transition to plant factories and urban agriculture", *International Journal of Agricultural and Biological Engineering*, vol. 11, no. 1, pp. 1–22, 2018.

[2] S. Sankaran, A. Mishra, R. Ehsani, and C. Davis, "A review of advanced techniques for detecting plant diseases", *Computers and Electronics in Agriculture*, vol. 72, no. 1, pp. 1–13, 2010.

[3] I. Simko, R. J. Hayes, and R. T. Furbank, "Non-destructive phenotyping of lettuce plants in early stages of development with optical sensors", English, *Frontiers in Plant Science*, vol. 7, 2019.

[4] A. Galieni, N. D'Ascenzo, F. Stagnari, G. Pagnani, Q. Xie, and M. Pisante, "Past and future of plant stress detection: An overview from remote sensing to positron emission tomography", *Frontiers in Plant Science*, vol. 11, p. 1975, 2021.

[5] A. Porcar-Castell, E. Tyystjarvi, J. Atherton, C. van der Tol, J. Flexas, E. E. Pfundel, J. Moreno, C. Frankenberg, and J. A. Berry, "Linking chlorophyll a fluorescence to photosynthesis for remote sensing applications: Mechanisms and challenges", *Journal of Experimental Botany*, vol. 65, no. 15, pp. 4065–4095, 2014.

[6] E. H. Murchie and T. Lawson, "Chlorophyll fluorescence analysis: a guide to good practice and understanding some new applications.", *Journal of experimental botany*, vol. 64, no. 13, pp. 3983–3998, 2013.

[7] U. Schreiber, "Pulse-amplitude-modulation (pam) fluorometry and saturation pulse method: An overview", in *Chlorophyll a Fluorescence: A Signature of Photosynthesis*, G. C. Papageorgiou and Govindjee, Eds. Dordrecht: Springer Netherlands, 2004, pp. 279–319.

[8] M. Meroni, M. Rossini, L. Guanter, L. Alonso, U. Rascher, R. Colombo, and J. Moreno, "Remote sensing of solar-induced chlorophyll fluorescence: Review of methods and applications", *Remote Sensing of Environment*, vol. 113, no. 10, pp. 2037–2051, 2009.

[9] H. Aasen, S. Van Wittenberghe, N. Sabater Medina, A. Damm, Y. Goulas, S. Wieneke, A. Hueni, Z. Malenovský, L. Alonso, J. Pacheco-Labrador, M. P. Cendrero-Mateo, E. Tomelleri, A. Burkart, S. Cogliati, U. Rascher, and A. Mac Arthur, "Sun-induced chlorophyll fluorescence ii: Review of passive measurement setups, protocols, and their application at the leaf to canopy level", *Remote Sensing*, vol. 11, no. 8, 2019.

[10] E.-C. Oerke, A.-K. Mahlein, and U. Steiner, "Proximal sensing of plant diseases", in *Detection and Diagnostics of Plant Pathogens*, M. L. Gullino and P. J. M. Bonants, Eds. Dordrecht: Springer Netherlands, 2014, pp. 55–68.

[11] Z. Kolber, D. Klimov, G. Ananyev, U. Rascher, J. Berry, and B. Osmond, "Measuring photosynthetic parameters at a distance: Laser induced fluorescence transient (lift) method for remote measurements of photosynthesis in terrestrial vegetation", *Photosynthesis Research*, vol. 84, pp. 121–129, 2005.

[12] B. Keller, I. Vass, S. Matsubara, K. Paul, C. Jedmowski, R. Pieruschka, L. Nedbal, U. Rascher, and O. Muller, "Maximum fluorescence and electron transport kinetics determined by light-induced fluorescence transients (lift) for photosynthesis phenotyping", *Photosynthesis Research*, vol. 140, pp. 221–233, 2019.

[13] A. R. Raesch, O. Muller, R. Pieruschka, and U. Rascher, "Field observations with laser-induced fluorescence transient (lift) method in barley and sugar beet", *Agriculture*, vol. 4, no. 2, pp. 159–169, 2014.

[14] M. R. Urschel and T. Pocock, "Remote Detection of Growth Dynamics in Red Lettuce Using a Novel Chlorophyll a Fluorometer", *Agronomy-Basel*, vol. 8, no. 10, 2018.

[15] J. Zhang, Y. Huang, R. Pu, P. Gonzalez-Moreno, L. Yuan, K. Wu, and W. Huang, "Monitoring plant diseases and pests through remote sensing technology: A review", *Computers and Electronics in Agriculture*, vol. 165, p. 104 943, 2019.

[16] Á. Polonio, M. Pineda, R. Bautista, J. Martínez-Cruz, M. L. Pérez-Bueno, M. Barón, and A. Pérez-García, "Rna-seq analysis and fluorescence imaging of melon powdery mildew disease reveal an orchestrated reprogramming of host physiology", *Scientific Reports*, vol. 9, no. 7978, 2019.

[17] C. Römer, K. Bürling, M. Hunsche, T. Rumpf, G. Noga, and L. Plümer, "Robust fitting of fluorescence spectra for pre-symptomatic wheat leaf rust detection with support vector machines", *Computers and Electronics in Agriculture*, vol. 79, no. 2, pp. 180–188, 2011.

[18] M. Pineda, M. L. Pérez-Bueno, V. Paredes, and M. Barón, "Use of multicolour fluorescence imaging for diagnosis of bacterial and fungal infection on zucchini by implementing machine learning", *Functional Plant Biology*, vol. 44, no. 6, pp. 563–572, 2017.

[19] M. T. Kuska and A.-K. Mahlein, "Aiming at decision making in plant disease protection and phenotyping by the use of optical sensors", *European Journal of Plant Pathology*, vol. 152, no. 4, pp. 987–992, 2018.

[20] M. S. Mohd Asaari, P. Mishra, S. Mertens, S. Dhondt, D. Inzé, N. Wuyts, and P. Scheunders, "Close-range hyperspectral image analysis for the early detection of stress responses in individual plants in a high-throughput phenotyping platform", *ISPRS Journal of Photogrammetry and Remote Sensing*, vol. 138, pp. 121–138, 2018.

[21] A. Moghimi, C. Yang, and P. M. Marchetto, "Ensemble feature selection for plant phenotyping: A journey from hyperspectral to multispectral imaging", *IEEE Access*, vol. 6, pp. 56 870–56 884, 2018.

[22] J. Behmann, D. Bohnenkamp, S. Paulus, and A.-K. Mahlein, "Spatial Referencing of Hyperspectral Images for Tracing of Plant Disease Symptoms", English, *Journal of Imaging*, vol. 4, no. 12, 2018.

[23] J. Behmann, A.-K. Mahlein, T. Rumpf, C. Roemer, and L. Pluemer, "A review of advanced machine learning methods for the detection of biotic stress in precision crop protection", English, *Precision Agriculture*, vol. 16, no. 3, 239–260, 2015.

[24] D. Sun, Y. Zhu, H. Xu, Y. He, and H. Cen, "Time-Series Chlorophyll Fluorescence Imaging Reveals Dynamic Photosynthetic Fingerprints of sos Mutants to Drought Stress", *Sensors*, vol. 19, no. 12, 2019.

[25] J. Blumenthal, D. B. Megherbi, and R. Lussier, "Unsupervised machine learning via hidden markov models for accurate clustering of plant stress levels based on imaged chlorophyll fluorescence profiles & their rate of change in time", *Computers and Electronics in Agriculture*, vol. 174, p. 105 064, 2020.

[26] L. Ahlman, D. Bånkestad, and T. Wik, "Led spectrum optimisation using steady-state fluorescence gains", *Acta Horticulturae*, vol. 1134, pp. 367–374, 2016.

[27] ——, "Using chlorophyll a fluorescence gains to optimize led light spectrum for short term photosynthesis", *Computers and Electronics in Agriculture*, vol. 142, no. Part A, pp. 224–234, 2017.

[28] L. Ahlman, D. Bånkestad, and T. Wik, "Relation between changes in photosynthetic rate and changes in canopy level chlorophyll fluorescence generated by light excitation of different led colours in various background light", *Remote Sensing*, vol. 11, no. 4, 2019.

[29] D. Bånkestad and T. Wik, "Growth tracking of basil by proximal remote sensing of chlorophyll fluorescence in growth chamber and greenhouse environments", *Computers and Electronics in Agriculture*, vol. 128, pp. 77–86, 2016.

[30] A.-M. Carstensen, T. Pocock, D. Bånkestad, and T. Wik, "Remote detection of light tolerance in basil through frequency and transient analysis of light induced fluorescence", *Computers and Electronics in Agriculture*, vol. 127, pp. 289–301, 2016.

[31] A.-M. Carstensen, T. Wik, D. Bånkestad, and T. Pocock, "Exploring the dynamics of remotely detected fluorescence transients from basil as a potential feedback for lighting control in greenhouses", *Acta Horticulturae*, vol. 1134, pp. 375–384, 2016.

[32] J. Lindqvist, D. Bånkestad, A.-M. Carstensen, B. Lundin, and T. Wik, "Complexity of chlorophyll fluorescence dynamic response as an indicator of excessive light intensity", *IFAC-PapersOnLine*, vol. 49, no. 16, pp. 392–397, 2016.

[33] M. Hultberg, B. Alsanius, and P. Sundin, "In vivo and in vitro interactions between pseudomonas fluorescens and pythium ultimum in the suppression of damping-off in tomato seedlings", *Biological Control*, vol. 19, no. 1, pp. 1–8, 2000.

[34] D. Montgomery, *Design and Analysis of Experiments*, 7th, ser. Student solutions manual. John Wiley & Sons, 2009.

[35] S. Khalil and W. A. Beatrix, "Effect of growing medium water content on the biological control of root pathogens in a closed soilless system", *The Journal of Horticultural Science and Biotechnology*, vol. 86, no. 3, pp. 298–304, 2011.

[36] G. C. Papageorgiou and Govindjee, Eds., *Chlorophyll a Fluorescence A Signature of Photosynthesis*. Springer, 2004, vol. 19.

[37] H. Kautsky and A. Hirsch, "Neue versuche zur kohlensäureassimilation", *Naturwissenschaften*, vol. 19, p. 964, 1931.

[38] A. Stirbet and Govindjee, "On the relation between the kautsky effect (chlorophyll a fluorescence induction) and photosystem ii: Basics and applications of the ojip fluorescence transient", *Journal of Photochemistry and Photobiology B: Biology*, vol. 104, no. 1, pp. 236–257, 2011, Special Issue on Recent Progress in the Studies of Structure and Function of Photosystem II.

[39] I. P. Levykina and V. A. Karavaev, "Fluorescence induction changes in bean leaves after heat treatment", *Biophysics and Medical Physics*, vol. 71, no. 1, pp. 128–134, 2016.

[40] R. J. Strasser, A. Srivastava, and Govindjee, "Polyphasic chlorophyll a fluorescent transient in plants and cyanobacteria", *Photochemistry and Photobiology*, vol. 61, no. 1, pp. 32–42, 1995.

PAPER E

Tracking optimal plant illumination using proximal sensed chlorophyll fluorescence gain

Linnéa Ahlman, Daniel Bånkestad, Torsten Wik

Manuscript,
2021

The layout has been revised.

Abstract

In a plant factory, the lighting system stands for a large proportion of the energy consumed. Determining the level of illumination that optimally balances energy costs and photosynthetic rate could allow for a substantially reduced energy demand and/or improved crop yield. However, finding the optimal illumination is a complex problem. Here, we use the light response curve (rate of CO_2 consumption vs. light intensity) as a measure of efficiency. First, we present results from experiments on lettuce, basil, and sunflower. An infrared gas analyzer was used to measure the photosynthetic rate for different light intensity levels to find the light intensity where the light response curve starts to saturate. Simultaneously, we measured the chlorophyll fluorescence gain (ChlF gain) with a spectrometer. The ChlF gain is here defined as the amplitude of the fluorescence signal when a weak, blue LED excitation lamp is pulsed at a frequency of approximately 1 Hz. The observed ChlF gain was found to be a concave function of light intensity, i.e., it has a maximum for a certain light intensity. Furthermore, we found that the maximal ChlF gain coincides with a point where the light response curve starts to saturate. Based on this, we propose a way to optimally and automatically adjust the light intensity. In simulation, we then show how an extremum seeking controller can be effectively used for the proposed task.

1 Introduction

Light emitting diodes, LEDs, are becoming common for plant growth; both as complementary light in greenhouses and as the only light source in a closed environment. Since a decade ago there has been commercially available LED lamps where both the light intensity and light spectrum can be adjusted. However, high installation costs have led to undersized systems where the installed lamps are generally used at maximal power. The development is towards higher efficiency of each LED and lower cost for lamp installation, and we are hence approaching the point when controlling and varying the intensity of the light will be economically justified. The light intensity can then be adapted to the potentially varying amount of light that the plants

need or can handle at each time instance. However, to control the light in such a way a measure of the current plant status is needed.

The chlorophyll *a* fluorescence, ChlF, signal is a potential candidate to be used as a remote, on-line measure of plant status. Two of the most common tools for measuring and analyzing chlorophyll fluorescence are the pulse amplitude modulation (PAM) fluorometry developed by Schreiber [1], and the photosynthetic efficiency plant analyser (PEA) developed by Strasser *et al.* [2]. However, these methods require a precise measurement of the fluorescence from fully dark-adapted plants, which is compared with the fluorescence at fully saturating light, and it is normally done on leaf level. Hence, these techniques are not suitable for the online task aimed for in this work. Another fluorescence based method that possibly could be used is the laser induced fluorescence transient (LIFT) technique [3]. This method has been developed to be used both in laboratory environment and in field at distances up to 50 m from the canopy level [4]. In this technique a blue laser projects a collimated beam onto the leaves, in flashlets of 1.6 µs, in excitation protocols with up to 7500 flashes [5]. However, the high light projected to a single point of a leaf makes it less suitable for on-line use in a control loop than an aggregated measure of a larger area illuminated by the lamp.

There are previous works where researchers attempt to use fluorescence measurements as a biological feedback to control the light. Iersel *et al.* [6]utilized the night for dark adaption, and a MINI-PAM (a fluorometer leaf clip-instrument) for a feedback loop to control the photosynthetic photon flux density (PPFD) to a set electron transport rate (ETR) in Photosystem II (a protein complex that is part of the photosynthesis). In contrast to our aim, this system controls the light to a predefined ETR-level and the biofeedback is only from the point where the fluorometer is attached to the leaf. Another interesting system, FUSSY, developed by Urschel and Pocock [7], is based on ChlF measurements in the far red area (740 nm). In addition to a photodiode module it consists of blue LEDs providing excitation pulses of 2000 $\mu\text{mol}\,\text{m}^{-2}\,\text{s}^{-1}$ with an adjustable frequency (200 Hz in the presented experiment). The system is, in fact, described as a remote ChlF detection system for real-time tracking of plant growth parameters.

The goal of the work presented here, however, is not only to find a remote, non-invasive measure of plant growth on canopy level, but also to find a way that enables self-regulation to the optimal light intensity. Determining the level of illumination that optimally balances energy costs and photosynthetic rate is complex. Here, we will assume that it is economically justified to increase the light until the light response curve starts to saturate, i.e., when more light does not lead to a substantial increase in the amount of CO_2 the

plant can convert to energy.

In our previous research we noticed that the steady-state ChlF gain, measured as change in fluorescence intensity when a weak excitation light is turned on or off, depended on the background light intensity with a peak occurring close to the expected production light intensity [8]. This is also in line with the results presented by Flexas *et al.* [9] where they observed a peak in the fluorescence (F_s/F_o, i.e., steady state ChlF normalized by dark adapted basal rate) when viewed as a function of light intensity. The peak shifted depending on whether the plant was healthy, or drought/water stressed. In addition, the slope of the light response curve of net CO_2 assimilation also changed such that the peak in F_s/F_o occurred at a light level close to the region where the net CO_2 assimilation shows signs of saturation.

In two master thesis works within our research group ChlF measurements were made at various background light levels with an excitation lamp that was switched on and off with a frequency of 1 Hz [10], [11]. The difference in ChlF when the excitation light was turned on and off, i.e., a fast ChlF gain measure, was noticed to also have a maximum, similar to the steady-state ChlF gain. Based on this, we have examined the possibility of having a feedback control of the light intensity aiming to find the point where the ChlF gain has its maximal value.

Here we present two parts of this research. First, we present measurements conducted on lettuce, basil, and sunflower. The fast ChlF gain at canopy level was determined for increasing background light intensities at the same time as the net CO_2 assimilation was measured on one leaf. For all species we found that the maximum ChlF gain correlated well to the light level where the photosynthetic rate was high but had started to saturate. The second part is a simulation study. Dynamical models of the plant's fluorescence emission as a function of light intensity were created from the measurements in the experimental part. These models were used to illustrate a novel idea of how the light intensity automatically can be controlled using an extremum seeking control algorithm pushing the light to the point where maximal ChlF gain is reached. The simulations show that such a control solution can be a feasible way to track the light optimum, and also how to efficiently analyze tuning trade-offs and effects of noise and disturbances.

2 Experimental part

2.1 Materials and methods

Lettuce, basil, and sunflower, all grown in greenhouse in Alnarp, Sweden, were included in the study. To force different light responses, measurements were done on plants with different soil moisture, even to the point where some of them were drought stressed. The volumetric water content in the soil was measured with a WET-2 Sensor (and the readout unit HH2 Moisture Meter), prior and after each experiment, see Figure 1(a). In total, 9, 4, and 5 measurements were conducted on lettuce, basil, and sunflower, respectively.

(a) WET Sensor (b) Li-cor

Figure 1: (a) The greenhouse where the plants were grown. A WET Sensor was used to measure the water content in the soil. (b) The experimental unit. A Li-cor portable photosynthesis system, to measure the photosynthetic rate, and an STS spectrometer to measure incident light.

Experimental unit

To perform the measurements, one plant at a time was moved from the greenhouse to a controlled indoor environment in a unit ($l \times w \times h = 1 \times 0.8 \times 2$ m) having white, highly diffusive and reflective walls. At the top of the unit, three Heliospectra LX lamps were mounted, of which two were used for background light and one for excitation light. One spectrometer (STS, Ocean Insight, Orlando, FL, USA) was placed on canopy level, facing the lamps and measuring incident light (Figure 1(b)). The second spectrometer (QE65000, Ocean Insight, Orlando, FL, USA) was equipped with a 600 µm optical fiber, placed between the lamps and pointing downwards, thus measuring the reflected and fluorescent light from the plants at a distance of about 1.5 m above canopy level.

Light scheme and fluorescence measurements

The background light came from a combination of white, red, and blue LEDs and was held constant for about 15 min at each level. Starting at a low level the background light was increased in 5–7 steps within the range 100–800 µmol m^{-2} s^{-1}. In addition to the background light, blue excitation light (peak wavelength 450 nm) was pulsed at a rate of approximately 0.4 Hz (1.2–1.4 sec on, and 1.2–1.4 sec off) and an intensity of 10 µmol m^{-2} s^{-1}.

The chlorophyll fluorescence gain, ChlF gain, is here defined as

$$\begin{aligned} ChlF\,gain &= \int_{\lambda_1}^{\lambda_2} Fluo_{ex,on} d\lambda - \int_{\lambda_1}^{\lambda_2} Fluo_{ex,off} d\lambda \\ &= F_{ex,on} - F_{ex,off}, \end{aligned} \tag{E.1}$$

where $Fluo_{ex,on}$ and $Fluo_{ex,off}$ are the fluxes of photons for each wavelength, detected by the spectrometer pointing towards the plant when the excitation lamp is on and off, respectively. The wavelengths λ_1 and λ_2 are chosen to cover the 740 nm-peak of the chlorophyll fluorescence. Normally $\lambda_1 = 730$ and $\lambda_2 = 800$ nm, but for sunflower some combinations of high background light and long integration time caused saturation of the detected photons within this region, due to overlap of the red 660 nm LED in the fluorescence region. To avoid saturation effects λ_1 was then increased to 763 nm. To allow comparisons this was done for all sunflower measurements. At each background light level the ChlF gain was sampled 360 times.

Rate of photosynthesis

At the same time as the fluorescence gain was measured, a Li-Cor 6800 infrared gas analyzer (Li-Cor 6800, Li-Cor Inc.) was used to measure the photosynthetic rate at each background light level. The instrument was equipped with the Multiphase Flash Fluorometer (6800-01A), which is a combined chamber (3×3 cm) and light source. The light is controlled by tracking the ambient light, which is measured with the built-in LI-190R quantum sensor. The internal light source is then giving the same amount of light (within PAR) to the leaf in the chamber, as detected from the ambient light. The spectrum of the internal light is 90% red and 10% blue.

All leaf CO_2-exchange measurements were conducted at 400 ppm CO_2 and with an air flow of 600 µmol s^{-1} through the chamber. The leaf temperature was allowed to vary, and therefore the leaf temperature increased throughout the experiment, as the light intensity increased. The ratio $T_{\mathrm{air}}/T_{\mathrm{leaf}}$, however, remained the same throughout each experiment. The autolog function saved

data with a sampling time of 1–2 min.

2.2 Experimental results

Raw data fluorescence gain

Different wavelength spans were investigated, to get a stable signal of the ChlF gain. Increasing the wavelength span from $\lambda_2 = 760$ to $\lambda_2 = 800$ nm, decreased the variance in the data by 20%. Increasing it further, to $\lambda_2 = 850$ nm, did not decrease the variance further, due to the low photon flux at high wavelengths. Hence, λ_2 was set to 800 nm. Figure 2(a) shows the measured fluorescence gain (measured over wavelengths 730–800 nm) throughout one experiment. The different colors indicate when background light is changed, and the dashed black lines indicate the mean value of the last 50% of the dataset at each background light level. Figure 2(b) shows the mean value of the fluorescence gain along the y-axis and the background light level along the x-axis, when including different parts of the measurements at each background light level. The fluorescence gain is higher in the beginning, and therefore the mean value of the first 5 measurements (red circles) gives higher absolute values compared to the other sets. Furthermore, using the last 50% or the last 10% of the data (green/blue stars) apparently gives the same results here. As we are only interested in the shape of the curve of fluorescence gain vs incident light, and not the absolute values, the conclusion is that for our purpose it is not necessary to await a steady state. The first few measurements after a large change in incident light, should be thrown away though, since these values can be very high compared to the steady state value. Otherwise, it is generally good to include many measurements to reduce the variance of the mean. From here on the last 50% of each dataset is included when presenting the mean values of the fluorescence gain. The data is also normalized from 0 to 1 for each dataset.

Raw data photosynthetic rate

Raw data measured with the infrared gas analyser from one experiment are shown in Figure 3(a), photosyntetic rate on the left y-axis and incident light on the right y-axis. The mean value of the last 50% of the data at each background light level was used to calculate the mean value at that level (data highlighted by black diamonds). The incident light detected by the IRGA was always higher, compared to the light detected by the STS spectrometer (Figure 3(b)). The difference is consistent throughout all experiments and the relation is linear, as can be seen in the figure. The differences could be due to

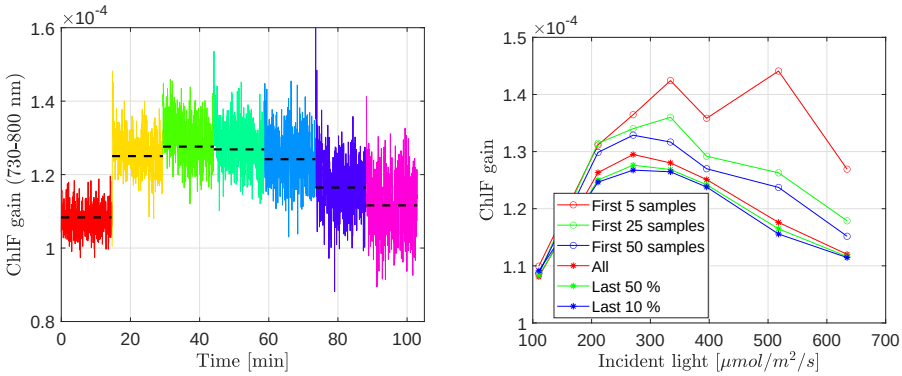

(a) Raw data (b) Fluorescence gain vs incident light

Figure 2: (a) Fluorescence gain throughout one experiment. Different colors indicate different background light levels. (b) Fluorescence gain vs incident light using different parts of the data set to calculate the mean fluorescence gain at each background light level.

calibration or placement in the experimental unit. From here on, the incident light presented will be the one measured with the STS spectrometer.

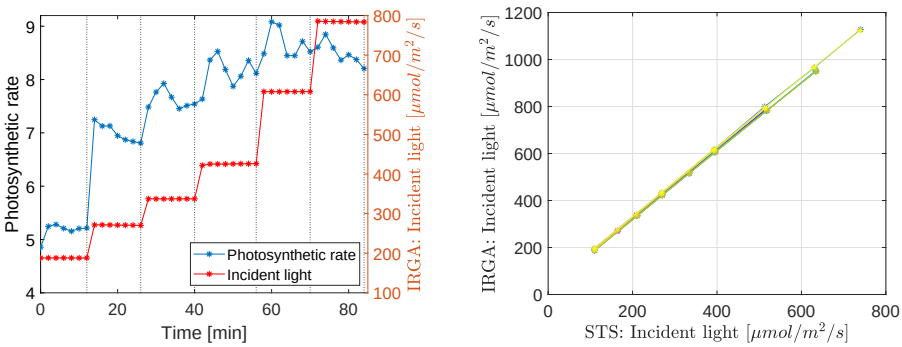

(a) Raw data from IRGA (b) Incident light

Figure 3: (a) Raw data, left axis: photosynthetic rate, right axis: incident light. (b) Incident light measured by (x-axis) STS-spectrometer and (y-axis) build in spectrometer in IRGA.

Fluorescence gain and photosynthetic rate vs incident light

The results of the fluorescence gain and photosynthetic rate vs incident light are presented in Figure 4, one row for each species. The mean water content (wc) in the soil, measured before and after each experiment, is displayed in the legends.

The first row in Figure 4 shows the results for sunflower. In this set, the correlation between fluorescence gain peak and the start of saturation in the photosynthetic rate is very clear. Two sets (Exp S1 and S4) had an early fluorescence gain peak (at 300 µmol m^{-2} s^{-1}) and the corresponding photosynthetic rate curves also start to saturate at that level. For the three other experiments (Exp S2, S3 and S5) the fluorescence gain peak occurs at 600 µmol m^{-2} s^{-1}, and the photosynthetic rate curve also continuous to increase up to this level. The water content in the soil correlates well to where light saturation occurs. For the two sets with high water content in the soil (Exp S3 and S5) the plants could cater light to a high level. For two other sets (Exp S1 and S4) a low water content in the soil meant that the plant could cater only a low amount of light. However, in the fifth case (Exp S2) there was a dry plant that could cater light to a high level, something that could also be seen in the fluorescence gain curve. For this study, the important result is however that the fluorescence gain curve can be used as a representation of the photosynthetic rate curve and not as a sign of irrigation level.

The second row of Figure 4 shows the results for lettuce. In six out of the nine sets the fluorescence gain peak was at a background light of 270 µmol m^{-2} s^{-1}(solid lines in Figure 4(d)), in two sets the peak was reached at the previous background light (210 µmol m^{-2} s^{-1}, Exp L3 and L6, dashed lines) and in one set the peak was reached at the next background light level (for that experiment about 400 µmol m^{-2} s^{-1}, Exp L9, dashed line). In the light response curves the corresponding peaks in fluorescence gain are indicated by a filled diamond. Only looking at these points, the light levels seem to be at approximately the level where saturation starts (for Exp L1, L8 and L9) or at a point were more light can be added for a substantial increase of photosynthetic rate (Exp L2, L3, L4, L5, L6, L7). In addition, all filled circles correspond to light levels where the relative fluorescence gain is above 0.8. If pushing towards these points, the highest light level where the relative fluorescence gain is above 0.8, then it corresponds well to where most of the curves has started to reach light saturation. For the lettuce experiments we find no clear correlation between water content and when the photosynthetic rate curve saturates.

The third row of Figure 4 shows the results for basil. Exp B3 and B4 is

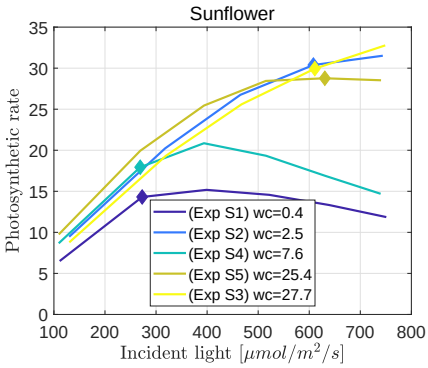

(a) Sunflower, photosynthesis.

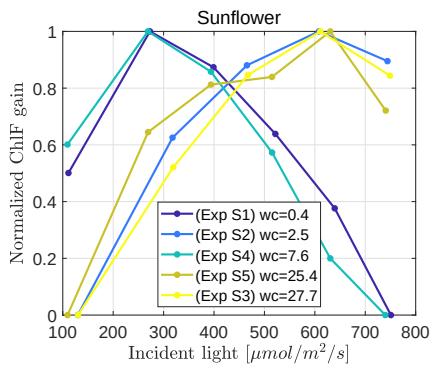

(b) Sunflower, fluorescence gain.

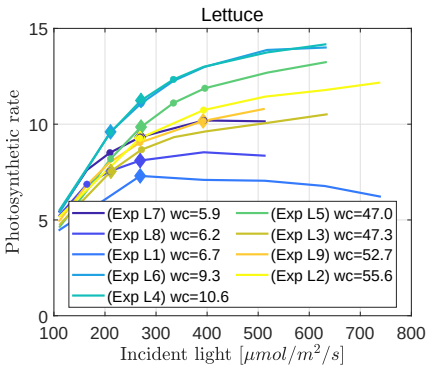

(c) Lettuce, photosynthesis.

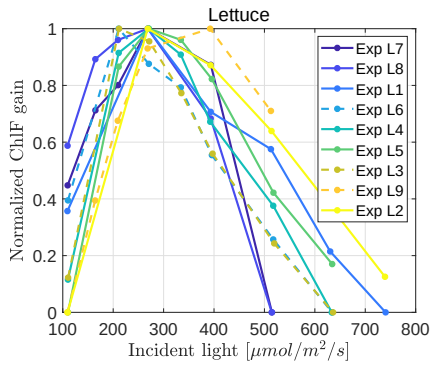

(d) Lettuce, fluorescence gain. Legend, see (c).

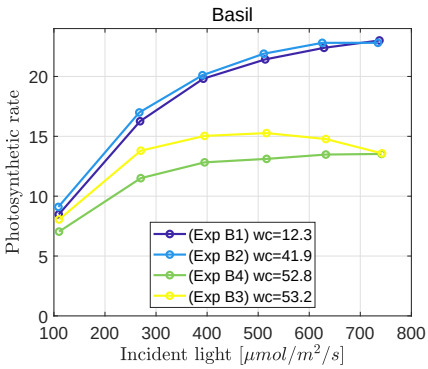

(e) Basil, photosynthesis.

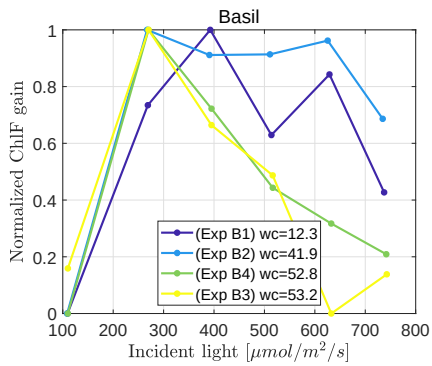

(f) Basil, fluorescence gain.

Figure 4: Left column, photosynthesis versus incident light. Right column, normalized fluorescence gain versus incident light. Each row; Sunflower, Lettuce, and Basil. The water content (wc) for each experiment is found in the legend. The filled diamonds indicates the light level where the fluorescence gain has its maximum.

measured on the same plant, but on different days, whereas Exp B1 and B2 were measures on two different plants. For Exp B3 and B4, the fluorescence gain (plot (b)) has a peak for light just below 300 µmol m^{-2} s^{-1} after which the fluorescence gain decreases significantly. This coincides with the intensity where the photosynthetic rate starts to saturate (plot (a)). For experiment B1 and B2 the saturation of the photosynthetic rate curve occurs much later. These experiments do not have as clear peak in the fluorescence gain as the other two measures. The relative value of the fluorescence gain is high even for lights up to 600 µmol m^{-2} s^{-1}. However, the illumination level where the fluorescence gain drops significantly coincides with the start of saturation in the photosynthetic rate curves. The fluorescence gain measure of Exp B1 stands out as noisy. Dividing the 360 measurements into four groups and calculating the ChlF gain for each of them, the shape of the fluorescence gain curve is almost the same no matter which set is used for Exp B2–B4 (Figure 16, in Appendix) but that is not the case for Exp B1. Hence, the measurements in this set are, for a currently unknown reason, far more noisy than the others.

3 Simulation part

In this part, we propose the concept of controlling the light intensity from a LED lamp, towards the point where the fluorescence gain is maximized. This is motivated by the experimental part (Section 2) which indicated that the light intensity level where the fluorescence gain peaks, coincides or strongly correlates with the light intensity where the light response curve starts to saturate, i.e., a point where the photosynthesis has reached a high level but increasing the light intensity even further will only slightly increase the photosynthesis.

3.1 Simulation setup

For the simulation study, a model was built in the Simulink environment in MATLAB (MathWorks, Inc., Natick, MA, USA). A schematic overview of the system is presented in Figure 5. It consists of three main parts: First, a *Plant Model*, which for a given incident light, u, simulate the fluorescence signal, F. Second, a *ChlF gain calculation* part, where the chlorophyll fluorescence gain, y, is calculated from the noisy measurements of the fluorescence signal, F. Finally, the *Controller*, which determines the background light intensity level, u_{bkg}, based on the ChlF gain signal, y.

The incident light to the plants, u, is the sum of the background light (i.e.,

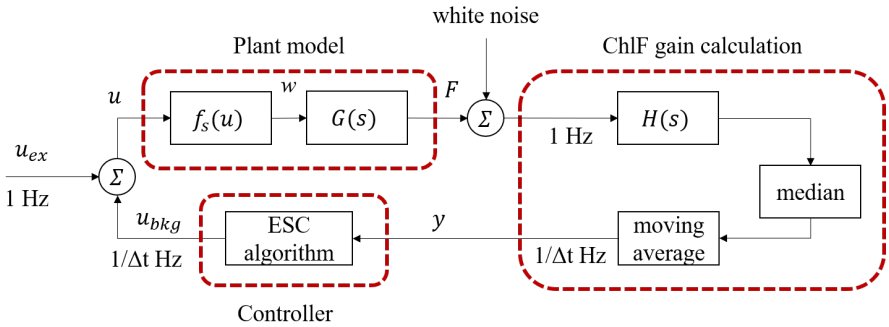

Figure 5: Block scheme of the feedback system.

the control signal) u_{bkg}, which updates at a frequency of $1/\Delta$t Hz, and the excitation lamp, which has a frequency of 1 Hz. Further, the plant model is simulated as continuous (in time) while the fluorescence signal is sampled with 1 Hz. The noisy ChlF gain is filtered through a median and a moving average filter, then sent to the controller at a frequency of $1/\Delta$t Hz.

Plant model

Data from Section 2 was used to derive a model of the plant i.e., how the fluorescence dynamically depends on the incident light. A Hammerstein model [12] was used to describe the nonlinear system. The input signal (sum of control signal and excitation light) first passes through a static nonlinear function $f_s(u)$ and then the signal is filtered through a linear time-invariant transfer function $G(s)$. Data from the experiments with lettuce was used for the simulation study. First, a second order polynomial was fitted to the data of steady-state fluorescence gain, y_{ss}, as a function of incident light, as illustrated in Figure 6.

A second order polynomial, defined as

$$y_{ss}(u) = p_1 \cdot u^2 + p_2 \cdot u + p_3, \tag{E.2}$$

is smooth, concave (for negative p_1) and therefore has no local extrema. The factor p_1 defines the curvature of the polynomial; the larger p_1 the sharper the curvature, and the easier for the controller to find the optimum. Two models were included in the simulation study, corresponding to the one with the smallest (further on referred to as Static Model 1, SM 1) and the largest (SM 2) value of p_1. Parameter values are presented in Appendix (Table 1).

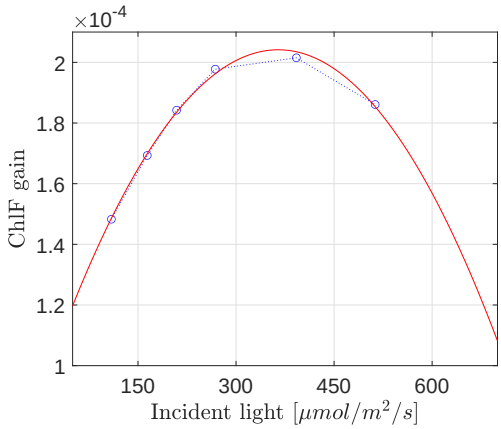

Figure 6: Fluorescence gain versus incident light. Measurements data (Exp L9) and 2nd order polynomial fit, according to Eq. E.2.

The filter $G(s)$ was normalized to have unit stationary gain, which implies that in steady state $F_{ss} = w = f_s(u)$, and the derivative of the output with respect to incoming light is

$$\frac{df_s(u)}{du} \approx \frac{\Delta f_s(u)}{\Delta u} = \frac{F_{ex,on} - F_{ex,off}}{\Delta ex}|_{ss} = \frac{1}{\Delta ex} y_{ss}, \tag{E.3}$$

where $F_{ex,on}$ is the fluorescence signal when the excitation lamp is turned on, $F_{ex,off}$ when it is off, and Δex is the light intensity amplitude of the excitation light. By integration of this equation the static model $f_s(u)$ can be extracted

$$f_s(u) \approx \frac{1}{\Delta ex} \int y_{ss}(u)du = \frac{1}{\Delta ex}(\frac{p_1}{3}u^3 + \frac{p_2}{2}u^2 + p_3 u). \tag{E.4}$$

Hence, the static nonlinear function $f_s(u)$ is modelled as a third order polynomial.

The dynamic transfer function $G(s)$ was identified using System Identification Toolbox (Mathworks Inc.), where the input data was modelled as a unit step and the output was the fluorescence measurements when increasing the background light from one level to the next. One example of this raw data is shown in Figure 7(a). The last 1/3 of the data (marked with yellow/red) was used for linear detrending, and the data was furthermore normalized to be 0 at the end of the first light level and to 1 at the end of the second light level, to get unit gain of $G(s)$. An output error model was found to give the best

fit to data, that is

$$y(t) = \frac{B(q)}{F(q)} \cdot w(t) + e(t), \tag{E.5}$$

where y is the output, w is the input, e is white noise and q is the shift operator. A third order model was needed to get a good fit for all sets, i.e.,

$$\begin{aligned} B(q) =& b_1 + b_2 \cdot q^{-1} + b_3 \cdot q^{-2} \\ F(q) =& 1 + f_1 \cdot q^{-1} + f_2 \cdot q^{-2} + f_3 \cdot q^{-3}. \end{aligned} \tag{E.6}$$

Transfer functions were generated for each light level change in all lettuce data sets. As the data was sampled a discrete model was fitted to the data, which was then converted to a continuous-time model assuming zero-order hold of the inputs. Three models were chosen to be included in the simulation study (Figure 7(b)). Dynamic Model 1 (DM 1), since it had a slightly longer settling time, DM 2, since it had an undershoot and DM 3 since it had the highest peak. The other models were similar to the chosen ones or had less dynamics. The parameter values of the chosen models are given in Appendix (Table 1).

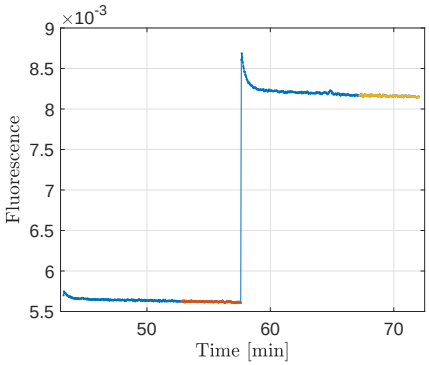

(a) Raw data, Dynamical Model 3.

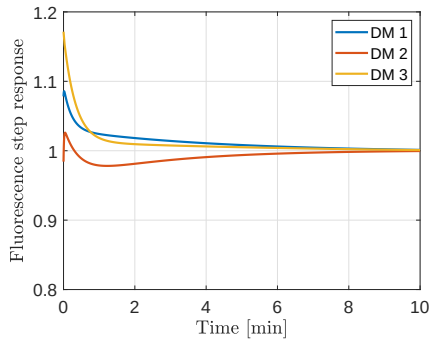

(b) Step response for chosen Dynamical Models.

Figure 7: (a) Raw data of the fluorescence signal. The last 1/3 of the data (marked yellow/red) is used for detrending. (b) The step responses for the chosen dynamical models; DM 1, DM 2 and DM 3.

ChlF gain calculation

The second part of the block scheme (Figure 5) is the extraction of the fluorescence gain signal, y, from the measured fluorescence, F. Comparing the

fluorescence signal when the excitation lamp is turned on and off, as in Eq. E.1, would correspond to filtering the fluorescence signal through $H = H_a$, where

$$H_a(q) = 1 - q, \tag{E.7}$$

and using every second output. That works fine, as long as the background light level is only increasing, as in the experimental part. However, there is a transient slope in the fluorescence signal due to the dynamics, having different sign depending on if the background light is increasing or decreasing, which leads to trouble when being in the region where the background light is alternated (e.g., around an optimum). Hence, the mean value of the ChlF gain when the excitation lamp is increased and decreased was used instead, which means that

$$H(q) = \frac{1}{2}(1 - 2q^{-1} + q^{-2}). \tag{E.8}$$

This helps reducing the impact of transients in the fluorescence signal caused by changes in the background light.

Furthermore, a median filter (block "median", with filter window 5) is used to remove outliers, caused by noisy measurements or from changes in the background light, because then F_{k-1} differs from F_k not only as a result of small changes in the excitation light but also because of the much larger changes in background light. Finally, a moving average filter is used to reduce the impact of the measurement noise. With a frequency of $1/\Delta$t the estimated ChlF gain, y, is eventually fed to the controller.

The measurements from Section 2 on lettuce were also used to get a realistic estimate of the measurement noise. The last 25% of the fluorescence measurements at each background light level (in total 6–7 steps per experiment) was included, the data were linearly detrended, and the standard deviation (σ) of the noise was calculated to be $5.59(\pm 2.26) \times 10^{-6}$. Further on, the spectrum was inspected, and it was concluded that the noise can be considered to be white. Hence, in simulation white, Gaussian noise,

$$\mathcal{N}(0, \sigma^2),$$

is added to the fluorescence signal, where σ was normally chosen to be 5×10^{-6}, but performance was also evaluated for 1×10^{-6} and 10×10^{-6}.

ESC algorithm

A control task where the goal is to track the maximum (or minimum) of an objective function belongs to the class of extremum seeking control (ESC)

[13]. This can be achieved without the need of a model of the plant. For the current setup, a model free setup is essential, since it is generally a complicated task to model the behavior of the fluorescence signal. In the previous section we tried to do exactly that, however, in reality a model would depend on many different parameters not included in the simulation. Though, rather than using a controller that relies on an inaccurate model, we propose an ESC which should track how the optimum changes, and tune it such that it is robust to large changes in the plant behavior.

Assume that the plant response from incident light to fluorescence gain can be described by

$$\begin{aligned} \dot{x} &= f(x, u) \\ y &= h(x), \end{aligned} \tag{E.9}$$

where $x \in \mathbb{R}^n$ is the vector of state variables, $u \in \mathbb{R}$ is the input or control signal, in our case the light intensity, and $y \in \mathbb{R}$ is the output, in our case the fluorescence gain, and f and h are continuous functions. Further, assume that

$$f(x, u) = 0 \text{ if and only if } x = l(u), \tag{E.10}$$

where l is a continuous map describing the steady-state map from input to states. Now, if we also assume the system is asymptotically stable for all such steady states, then the goal for the controller is to maximize the objective function

$$J(u) = h \circ l(u), \tag{E.11}$$

being the steady-state input-output map of the system.

First, the most traditional perturbation based extremum seeking scheme was considered, where a sinusoid perturbation signal, which must be slow in comparison to the plant dynamics, is added to the control signal [13], [14]. By comparing the dynamics of the input and output signal, i.e., if they are in phase or in antiphase, it can be concluded where on the objective function curve the current input, u, operates and, hence, decide the direction of the control action that will push the input signal to the optimal point $u = u^*$, where

$$\frac{dJ(u^*)}{du} = 0. \tag{E.12}$$

By construction this controller has the advantage that the step size is larger when being far from the optimum and decreases when getting close to the optimum. For such a controller there are five parameters that needs to be decided/tuned: the amplitude and the frequency of the perturbation signal,

the cut-off frequencies of one high-pass and one low-pass filter, and finally the gain of an integrator in the control loop. In addition to the design parameters the controller needs to be able to handle startups (as the lamp will be turned off every night), avoiding too much fluctuation or overshoot.

After extensive testing it was, however, decided that a simpler controller, the constant stepping method [15] would be used, since, for the proof of concept it is preferable to use an as simple model as possible, still managing the task. A scheme of this control strategy is presented in Figure 8. It starts with an initial guess of the control signal, u (light intensity), which is held constant during Δt seconds, whereupon the output, y (fluorescence gain), is measured and stored. The control signal is then shifted with Δu and the output is measured again. If the difference in control signal resulted in an increased performance (larger y), then the control signal shifts again, in the same direction as in the previous step. Contrary, if y decreased then the controller updates the control signal in the opposite direction.

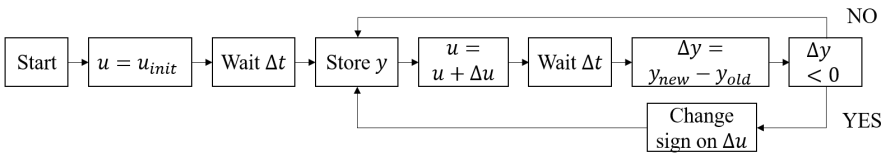

Figure 8: Control scheme for the stepping method.

3.2 Results from simulation

No noise added

When no noise is included, there is no need for the median and moving average filters. Hence, in all results presented in this section the filter windows are set to 1, and thus, the last measure of ChlF gain at each background light level is directly sent to the controller.

The simulations show that the controller works as intended, as long as the time, Δt, is sufficiently long. Figure 9 shows an example of the incident light, or the control signal (left column), and the difference in the ChlF gain (y) between two consecutive background light levels, Δy, (right column) for Δt = 8, 6 and 4 sec. It shows that if Δt is pushed towards too low values, an increased fluctuation occurs in the control signal, due to the dynamics in the fluorescence signal.

The fluctuation of u around the optimal light intensity can be used to

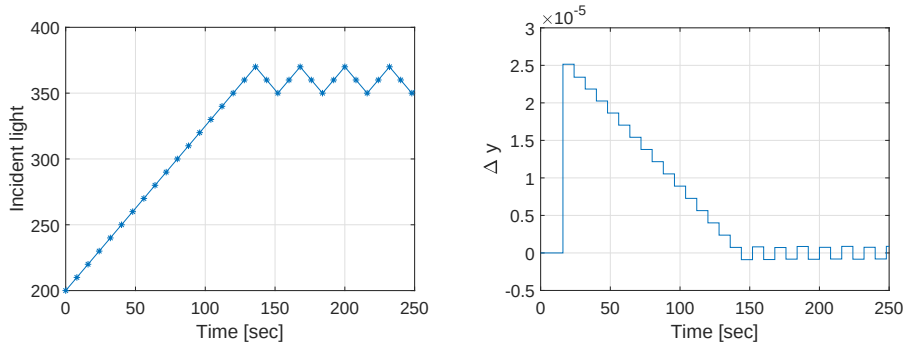

(a) Δt = 8 sec (b) Δt = 8 sec

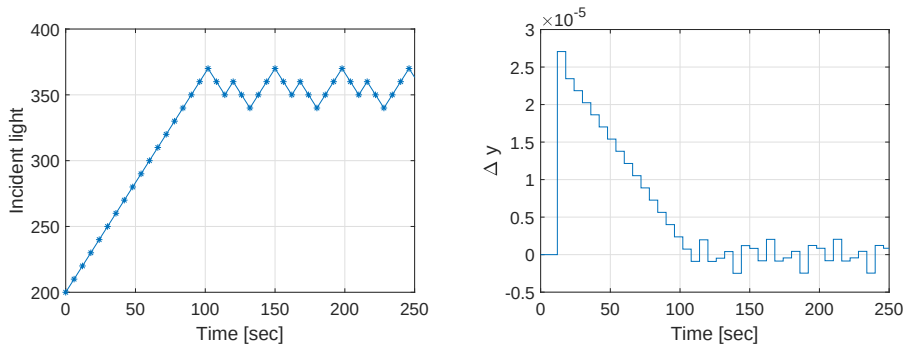

(c) Δt = 6 sec (d) Δt = 6 sec

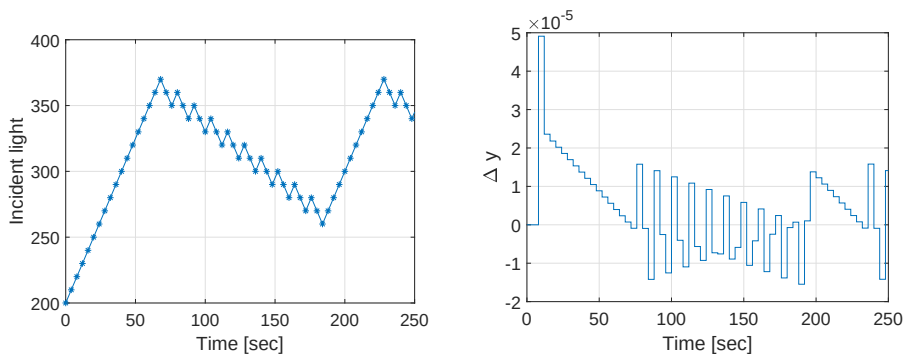

(e) Δt = 4 sec (f) Δt = 4 sec

Figure 9: ESC simulation results. Left column: control signal, u (incident light). Right column: $\Delta y = y_{new} - y_{old}$, where y is the ChlF gain measured in the end of each background light level. Settings: SM 2, DM 2, Δu = 10 µmol m^{-2} s^{-1}, Δt = 8, 6 and 4 sec.

evaluate of settings of the controller. Optimally, Δt is pushed as low as possible, without increasing the fluctuations. In Figure 10, the amplitude as a function of Δt is plotted, for the two different static models (SM 1 (a) and SM 2 (b)), the three different dynamical models (solid/dashed/dotted lines), and for Δu = 5/10/20 µmol m^{-2} s^{-1}. First of all, the figure clearly demonstrates that SM 1 is indeed harder to control than SM 2, which was expected due to the different curvature of the objective functions. To be sure not to fluctuate more than Δu, Δt must be at least 10, 8, or 6 sec, for SM 2, while it needs to be 90, 60, or 18 sec for SM 1 (for Δu equal to 5, 10, or 20 µmol m^{-2} s^{-1}, respectively). If allowing a fluctuation of 1.5×Δu, the time can be reduced to 9, 5, or 5 sec for SM 2, or 20, 8, or 7 sec for SM 1.

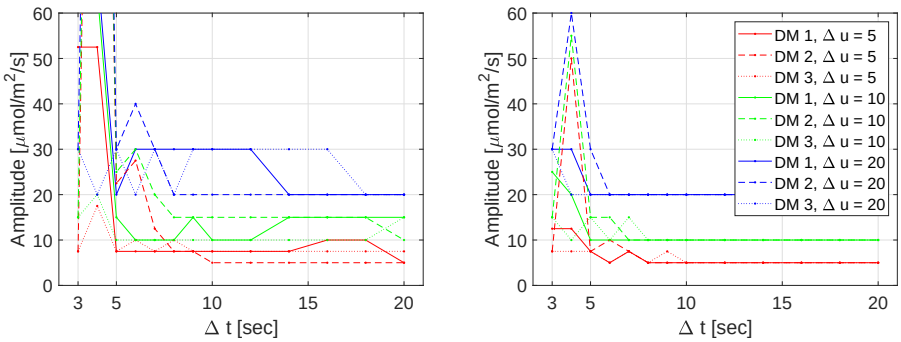

(a) SM 1 (b) SM 2

Figure 10: The amplitude around optimal PAR for various Δt. (a) SM 1 and (b) SM 2, red/green/blue for DM 1/2/3 and solid/dashed/dotted lines for Δu = 5/10/20 µmol m^{-2} s^{-1}.

Over all, increasing Δt to 6 or even 10 sec, will for most settings increase the performance significantly. Further increasing Δt will not decrease the fluctuations for SM 2, and for SM 1 it requires that Δt increases a lot to get a significant decrease in fluctuation. Hence, a suitable setting for a controller would be Δt = 10 sec, and the choice of Δu can be seen as a tradeoff between how large the fluctuations around the optimum is and how fast the controller should be able to change the light, i.e., Δu/Δt.

If the task is only to compensate for varying optimum, we assume that the speed would not be an issue. For example, recall Figure 4(e,f), the optimum light varied within 300–600 µmol m^{-2} s^{-1} for sunflower. If this change would happen within one day, the controller needs to handle a speed of

$$300\ \mu\text{mol}\,\text{m}^{-2}\,\text{s}^{-1}/(24\ \text{h} \times 60\ \text{min/h}) = 0.21\ \mu\text{mol}\,\text{m}^{-2}\,\text{s}^{-1}/\text{min},$$

hence very small steps, Δu, and/or long Δt compared to what was presented above, could handle that. However, the high speed is important if needed to compensate for varying background light.

Noisy measurements

To reduce the impact of measurement noise, the time at each light level, Δt, has to be increased as the variance of the mean decreases with the amount of data. The median filter length was set to 5, and the filter length of the moving average filter was set to Δt–4, after evaluating the performance of different filter lengths by simulation.

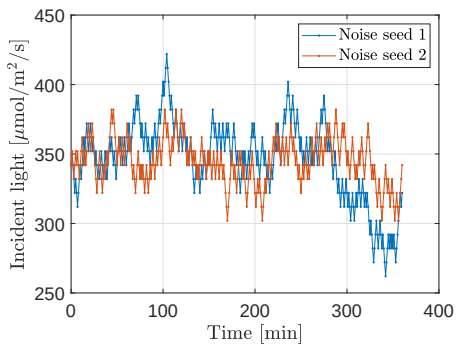

Figure 11: The evolution of the control signal (incident light) over time, for two different seeds of noise. Settings: SM 1, DM 1, Δu = 10 µmol m^{-2} s^{-1}, Δt = 1 min.

The performance of the controllers was evaluated by comparing the maximal amplitude of the fluctuations around the optimum after 6 h simulation, when initialized at optimum, for 20 different seeds of noise. Figure 11 shows an example of how the incident light varies when applying the control strategy with the noisy measurements, for two different seeds of noise (both with the same standard deviation, 5×10^{-6}). For the two examples the amplitude of the fluctuations were 40 and 80 µmol m^{-2} s^{-1}, respectively.

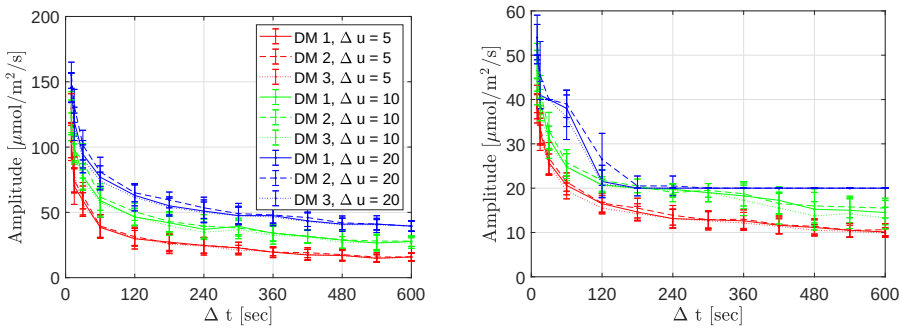

(a) SM 1 (b) SM 2

Figure 12: The amplitude of the control signal around the optimal value, for different Δt. (a) static model 1, (b) static model 2, red/green/blue lines corresponds to Δu=5/10/20 µmol m^{-2} s^{-1} and solid/dashed/dotted lines corresponds to dynamic model 1/2/3. The error bars shows one standard deviation, estimated from 20 measures.

Figure 12 shows the amplitude around the optimal value for all different settings, as a function of Δt. The error bars indicate one standard deviation, estimated from 20 different noise seeds. The difference among the three dynamical model (solid/dashed/dotted lines) is small, due to the relatively long time scales. There is a clear distinction between the two static models, though, where SM 1 is harder to control and consequently the amplitude is larger compared to SM 2. The largest impact in the performance in terms of amplitude around optimum, is reached when increasing Δt from 10 sec to 1 or 2 min. Further increasing Δt will not increase the performance at the same rate. Increasing the performance further could then be done by decreasing Δu instead.

Choosing suitable settings, Δu and Δt, could be seen as a tradeoff between how large amplitude that is acceptable and how fast the controller can change the light i.e., the rate Δu/Δt. This is illustrated in Figure 13 ((a) SM 1 and (b) SM 2), where settings with high speed and/or low amplitude is preferred. Comparable results can be achieved with different combinations of Δu and Δt, but in general, if low amplitude is essential (lower than 40 or 20 µmol m^{-2} s^{-1}, for SM 1 and SM 2 respectively) the same amplitude can be received at higher rate if choosing a lower Δu.

For the data presented so far, the standard deviation of the noise was 5×10^{-6}. For the case with higher noise, std 10×10^{-6}, the amplitude at optimum increased with approximately 20%. On the other hand, with a setup where the noise level is only 1×10^{-6}, the amplitude instead decreased by 40%. In such

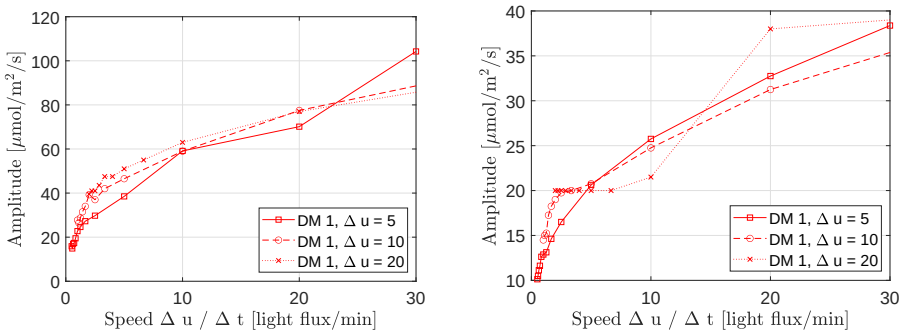

(a) SM 1 (b) SM 2

Figure 13: The trade off between fluctuation around optimum (y-axis) and the speed that the light can be changed (x-axis), for (a) SM 1 and (b) SM 2.

a case, the time at each background light level can be significantly shortened and still have the same performance. For example, the amplitude reached, having $\Delta t = 3$ min and noise level 5×10^{-6}, is reached for $\Delta t = 30$ ($\pm$ 12) sec (or 80 $\pm$ 15 sec for SM 1, Δu 5) if std of the noise is 1×10^{-6}.

Tracking changing optimum

If the optimum changes, the controller should follow and adapt to the new light level. A limitation of the constant stepping method, though, is that the controller can maximally change the light at a rate of $\Delta u/\Delta t$ light flux per time unit. This means that slowly varying set points can be followed but a faster change may not. We illustrate this by studying how the controller handle an additive and time varying light source. Ideally, the controller would decrease the light intensity with the same amount as the added light from other light sources increases, for the plants to get a constant (optimal) light.

Two sets of sunlight measurements were used (Figure 14). The first one is from a low light April day in Sweden (data from SMHI [16]). It is sampled once every hour and the intensity is linearly interpolated in between. The maximal increase in light intensity is between 8 and 9 a.m., when the light increases by $3\,\mu\text{mol}\,\text{m}^{-2}\,\text{s}^{-1}$/min. During the rest of the day the change is always lower than $2\,\mu\text{mol}\,\text{m}^{-2}\,\text{s}^{-1}$/min.

The second set is collected in September in Spain, during 8–10 a.m. This data is sampled much faster, from 9 a.m. it is sampled with a period of 2 s, and hence more fluctuations in the light was captured. During the first hour the rise is smooth, about $2\,\mu\text{mol}\,\text{m}^{-2}\,\text{s}^{-1}$/min, while in the second hour the rise is

on average 6.5 µmol m^{-2} s^{-1}/min, with fluctuations that are much larger, up to 150 µmol m^{-2} s^{-1}/min.

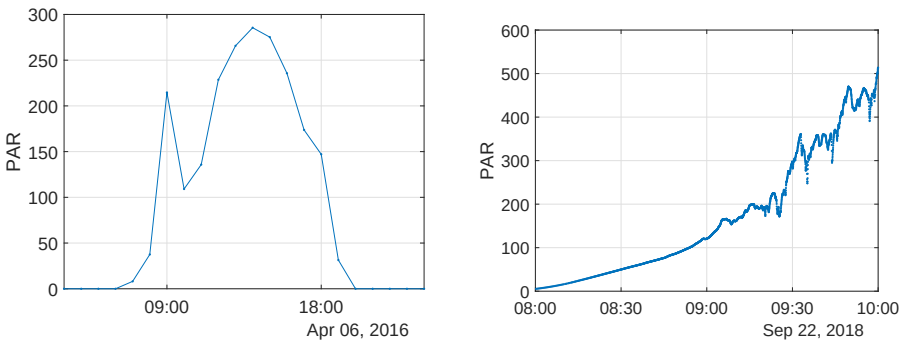

Figure 14: Ambient light in (a) Sweden a day in April with very low light and in (b) Spain two hours in the morning of a day in September.

Figure 15 shows the performance of the controller when ambient light disturbance is added. The solid blue/red lines are the control signals, the yellow line is the ambient light disturbance, and the dotted lines are the sum of them, thus the total light the plants receive. The settings of the controller were $\Delta u = 10$ µmol m^{-2} s^{-1} and $\Delta t = 1$ min (red lines) and 3 min (blue lines), yielding a rate $\Delta u/\Delta t$ of 10 and 3.3 µmol m^{-2} s^{-1}, respectively. In the case with slowly varying background light (Swedish April light) both controllers can handle the disturbance well, although the slower controller ($\Delta t = 3$ min) performance slightly worse when the light increases at the highest rate (at 8–9 a.m.), in the noise free case, however, it would have handle it even better. Notice the tradeoff; the faster controller fluctuates more, during the first 4 simulated hours (when no sunlight is added) delivering light with intensity 360 ± 25 µmol m^{-2} s^{-1}, while the slower controller is within 360 ± 20 µmol m^{-2} s^{-1}, to the price of not being able to compensate for the fastest changes.

In the case of September light in Spain, the controllers only handle it well in the first 60 and 80 min, respectively. Later, the fluctuation becomes too large, and the controllers get stuck. They take one step $+\Delta u$, conclude that the performance decreases hence take the next step $-\Delta u$. However, it still gets worse so the controller changes sign again and this continues as long as the ambient light increases too fast.

To be able to handle fluctuating ambient light the controller needs to be considerably faster. In the current case (simulated without noise) a controller with

$\Delta u = 10$ µmol m^{-2} s^{-1} and $\Delta t = 5$ sec, ($\Delta u/\Delta t = 120$ µmol m^{-2} s^{-1}/min) performs rather well. Decreasing the step time to $\Delta t = 3$ sec, however, results in instability. To have a robust controller in a real setup, though, it is not a good idea to push towards the limit that the simulations allow because of the uncertainties in the shape of the ChlF gain and the noise amplitude.

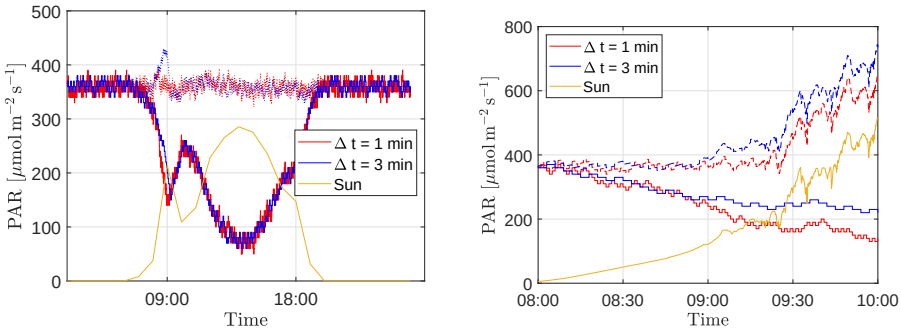

Figure 15: The control signal (solid blue/red lines) when added sunlight disturbance (yellow line) and the sum of them (dashed lines) which is the light the plants receive. Ambient light from (a) April in Sweden and (b) September in Spain.

4 Discussion and conclusions

In this paper we have studied a completely new method to automatically adjust the light intensity to track the current optimal illumination level. We have demonstrated indications that the fluorescence gain, calculated according to Eq. E.1, is concave with respect to the incident light, with a maximal fluorescence gain that coincides to a point where the photosynthetic rate starts to saturate.

The results were most clear for sunflower, though the measurements on basil and lettuce show promise as well. For the case of lettuce, it might be that the peak in the fluorescence gain occurs a little too early. However, this can be managed by manipulating the objective function. For one or two of the basil measurements (Figure 4(c)) the peak fluorescence gain was not as clear. If that means that there are multiple optima, this may be troublesome for the suggested control strategy.

From the data collected in the experiments we have constructed models of how the light intensity affects the fluorescence gain. There are, of course,

many other parameters that affect the fluorescence response, such as type of plant, development status, stress factors, light history etc., which has not been accounted for in this paper. Two static models of the ChlF gain, having different curvature, and three different models of the plant dynamics were chosen, and all combinations were included in the simulation study. We cannot know, which model that best fits a certain setup, but the simulated results can give us an indication of what kind of settings would be a good starting point for a real setup.

Simulations of the fluorescence, assuming noise-free measurements, show that holding the illumination level constant for 10 sec gives close-to optimal performance regardless of the model type, since the fluorescence gain has reached close enough to a steady state by then. Furthermore, there is a clear trade-off between how fast the controller can change the light (Δu/Δt, μmol m^{-2} s^{-1}/min), and performance, measured as fluctuations around the optimum. The optimal settings found was Δt $\approx$ 10 sec and then adjusting Δu depending on how important rate of change and performance is in the current setup.

Due to measurement noise, Δt needs to be longer to give an accurate ChlF gain, by averaging more measurements. For the evaluated models, the performance significantly increases when Δt increases to 1–2 min. To lower the amplitude of the fluctuations, one can decrease Δu, while if increased rate of change of the controller is essential Δu can instead be increased.

The maximal rate of change in the ambient light that the controller can compensate for is Δu/Δt. If measuring the incident light disturbance, however, a control setup with feed forward can be used to compensate for the ambient light, such that the ESC can handle any remaining rate of change.

Decreasing the noise level is a key improvement measure to increase the performance of the controller. For example, a low noise level (std 1×10^{-6}) and a Δt = 0.5 min corresponds to the same performance as a higher noise level (std 5×10^{-6}) and Δt = 3 min.

Another potential improvement of the control algorithm, is to let Δt and/or Δu vary. When far away from optimum, the rate of change is more important, but when being close to optimum, smaller step size Δu is desirable in order to decrease the oscillations. Up to this point we only used the sign of dy to determine the sign of Δu, but there is also information in the relative amplitude of dy, that could be used in a setup with varying Δu.

Appendix

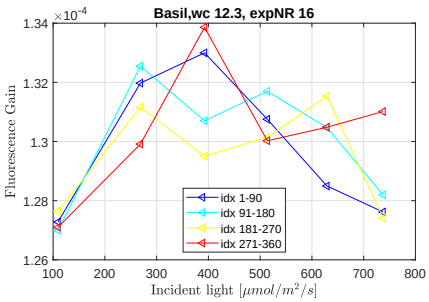

(a) Basil exp nr 16.

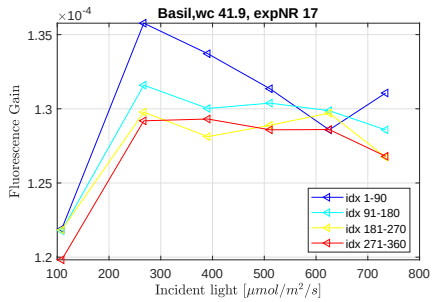

(b) Basil exp nr 17.

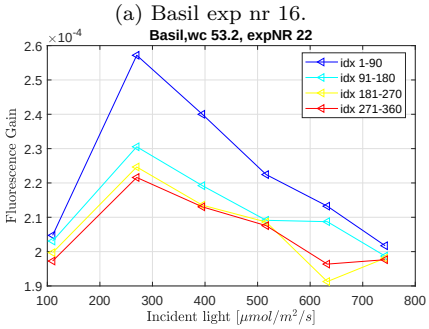

(c) Basil exp nr 22.

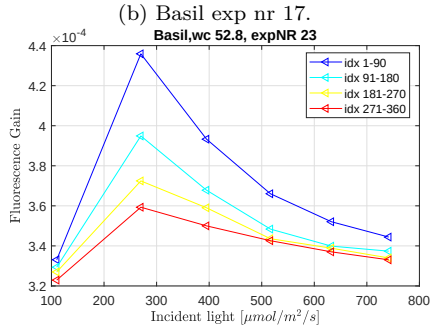

(d) Basil exp nr 23.

Figure 16: Fluorescence gain, when including different parts of the measurements. In total there are 360 measures at each light level, here divided into 4 groups.

Table 1: Parameters for the Statical and Dynamical models used in the simulations. See Eq. E.4,E.5,E.6 for description of the parameters.

Static Models		
	SM 1	SM 2
p_1	-6.5929e-11	-8.5316e-10
p_2	4.5693e-08	6.2200e-07
p_3	9.5418e-05	9.0783e-05

Dynamical Models			
	DM 1	DM 2	DM 3
b_1	1.0783	0.9843	1.1715
b_2	-1.9749	-1.8679	-2.2215
b_3	0.8982	0.8849	1.0505
f_1	-1.8346	-1.9401	-1.8771
f_2	0.8470	0.9847	0.8741
f_3	-0.0108	-0.0433	0.0036

References

[1] U. Schreiber, "Pulse-amplitude-modulation (pam) fluorometry and saturation pulse method: An overview", in *Chlorophyll a Fluorescence: A Signature of Photosynthesis*, G. C. Papageorgiou and Govindjee, Eds. Dordrecht: Springer Netherlands, 2004, pp. 279–319.

[2] R. Strasser, M. Tsimilli-Michael, and A. Srivastava, "Analysis of the chlorophyll a fluorescence transient", English, in *Chlorophyll a Fluorescence*, ser. Advances in Photosynthesis and Respiration, G. Papageorgiou and Govindjee, Eds., vol. 19, Springer Netherlands, 2004, pp. 321–362.

[3] Z. Kolber, D. Klimov, G. Ananyev, U. Rascher, J. Berry, and B. Osmond, "Measuring photosynthetic parameters at a distance: Laser induced fluorescence transient (lift) method for remote measurements of photosynthesis in terrestrial vegetation", *Photosynthesis Research*, vol. 84, pp. 121–129, 2005.

[4] A. R. Raesch, O. Muller, R. Pieruschka, and U. Rascher, "Field observations with laser-induced fluorescence transient (lift) method in barley and sugar beet", *Agriculture*, vol. 4, no. 2, pp. 159–169, 2014.

[5] B. Keller, I. Vass, S. Matsubara, K. Paul, C. Jedmowski, R. Pieruschka, L. Nedbal, U. Rascher, and O. Muller, "Maximum fluorescence and electron transport kinetics determined by light-induced fluorescence transients (lift) for photosynthesis phenotyping", *Photosynthesis Research*, vol. 140, pp. 221–233, 2019.

[6] M. W. van Iersel, G. Weaver, M. T. Martin, R. S. Ferrarezi, E. Mattos, and M. Haidekker, "A chlorophyll fluorescence-based biofeedback system to control photosynthetic lighting in controlled environment agriculture", *Journal of the American Society for Horticultural Science*, vol. 141, no. 2, pp. 169–176, 2016.

[7] M. R. Urschel and T. Pocock, "Remote Detection of Growth Dynamics in Red Lettuce Using a Novel Chlorophyll a Fluorometer", *Agronomy-Basel*, vol. 8, no. 10, 2018.

[8] L. Ahlman, D. Bånkestad, and T. Wik, "Using chlorophyll a fluorescence gains to optimize led light spectrum for short term photosynthesis", *Computers and Electronics in Agriculture*, vol. 142, no. Part A, pp. 224–234, 2017.

[9] J. Flexas, J. M. Escalona, S. Evain, J. Gulías, I. Moya, C. B. Osmond, and H. Medrano, "Steady-state chlorophyll fluorescence (Fs) measurements as a tool to follow variations of net CO_2 assimilation and stomatal conductance during water-stress in C_3 plants", *Physiologia Plantarum*, vol. 114, pp. 231–240, 2002.

[10] J. Tran Nguyen and S. Wiede, "Detect plant stress by measuring chlorophyll fluorescence gain from lamp pwm signal", Master's thesis, Chalmers tekniska högskola, 2019.

[11] F. Steimle, "Biofeedback control for optimizing light intensity on plants based on canopy level chlorophyll fluorescence gain", Master's thesis, Chalmers tekniska högskola, 2020.

[12] K. Narendra and P. Gallman, "An iterative method for the identification of nonlinear systems using a hammerstein model", *IEEE Transactions on Automatic Control*, vol. 11, no. 3, pp. 546–550, 1966.

[13] K. B. Ariyur and M. Krstić, "Siso scheme and linear analysis", in *Real-Time Optimization by Extremum-Seeking Control*. John Wiley & Sons, Ltd, 2003, ch. 1, pp. 1–20.

[14] C. Zhang and R. Ordóñez, "Design of extremum seeking control", in *Extremum-Seeking Control and Applications*. Springer-Verlag London, 2012, ch. 3, pp. 52–54.

[15] J. Sternby, *A Review of Extremum Control*, English, ser. Technical Reports TFRT-7161. Department of Automatic Control, Lund Institute of Technology (LTH), 1979.

[16] SMHI. (2021). Extracting strång data. T. Carlund, Ed. Data produced with support from the Swedish Radiation Protection Authority and the Swedish Environmental Agency., [Online]. Available: `http://strang.smhi.se/extraction/`.